CHARACTERIZATION OF INTERFERON REGULATORY FACTOR 4 (IRF4) TARGET GENES IN MELANOMA CELL LINES

by

Erdem Yılmaz

B.S., Molecular Biology and Genetics, Boğaziçi University, 2011

Submitted to the Institute for Graduate Studies in
Science and Engineering in partial fulfillment of
the requirements for the degree of
Master of Science

Graduate Program in Molecular Biology and Genetics
Boğaziçi University
2014

CHARACTERIZATION OF INTERFERON REGULATORY FACTOR 4 (IRF4) TARGET GENES IN MELANOMA CELL LINES

APPROVED BY:

Assist. Prof. Necla Birgül İyison .....
(Thesis Supervisor)

Assist. Prof. N.C. Tolga Emre .....

Assist. Prof. Cory Dunn .....

DATE OF APPROVAL: 23.07.2014

ACKNOWLEDGEMENTS

I would like to emphasize my strongest gratitude to my supervisor, Assist. Prof. Tolga Emre for his guidance and assistance along this thesis process. From the day he accepted me to his lab, his guidance during tough times, and scientific contributions not only made this thesis study possible but also improved me as a researcher.

I would like thank Assist. Prof. Necla Birgül İyison for awakening my curiosity towards science as a researcher and helping me in every way that she can.

I would also like to thank my third jury member Assist. Prof. Cory Dunn for sparing his valuable time to evaluate, criticize and improve this thesis.

My lab-mates Ekin Ece Erkan, Mustafa Can Ayhan, Ulduz Sobhiafshar, Cansu Yerinde, Ahmet Buğra Tufan and Nalan Yıldız are appreciated greatly for making the laboratory, a place to have fun and work at the same time. All of their practical contributions and moral support are cherished as well.

Last but not least, I would like to honor to my closest friends; Vahap Kapıkıran, Pelin Aksoy Kapıkıran, Uğur Kaplan, Güner Kaçmaz, Ayşegül Taşcı, Mehmet Ali Dalyan and Balkan Canher for their friendship and help whenever I needed them the most.

Güneş Tunçgenç has always been very affectionate. I am very happy to have her support which is a great source of motivation to me all the time.

This study was supported by grants from Framework Programme 7 (FP7) Marie Curie – Career Integration Grant (CIG), EMBO – Integration Grant (IG) and TUBITAK-1001-113Z103.

ABSTRACT

CHARACTERIZATION OF INTERFERON REGULATORY FACTOR 4 (IRF4) TARGET GENES IN MELANOMA CELL LINES

IRF4 is a critical transcription factor in the development and function of immune cells, and additionally, it is deregulated in certain myeloid and lymphoid malignancies. Until recently, IRF4 expression was thought to be restricted to immune cells; however, recent studies showed its expression in non-immune cells, such as melanocytes. We observed that certain human melanoma cell lines also have IRF4 expression and its expression appears critical for the viability of melanoma cells as in the case of B-cell origin malignancies. As there is a relative lack of understanding about IRF4 in melanoma we set out to identify its downstream transcriptional target genes using high-throughput sequencing in order to identify the pathways and biological processes IRF4 regulates in human melanoma cells. For this purpose, as a first step, we determined the optimal conditions for the expression profiling analysis. Then, we compared gene expression profiles of IRF4 knock down cells with control by high-throughput cDNA sequencing (RNA-seq). We analyzed the sequencing data via a bioinformatics pipeline to find the significantly differentially expressed genes upon IRF4 knock-down. We validated the results of RNA-seq by real-time semi-quantitative polymerase chain reaction for selected genes. Subsequently, we performed characterization of enriched functional classes of the differentially expressed genes by gene enrichment analysis of gene ontology terms. Our analysis indicates that IRF4 predominantly activates genes related to proliferation, and represses genes linked with lipid metabolism in human melanoma cell lines. Additionally, following leads from the results of RNA-seq analysis we showed the role of IRF4 on the transcriptional regulation of a prominent melanocyte master regulator and a key survival pathway in certain melanoma cell lines.

ÖZET

INTERFERON REGULATORY FACTOR 4 (IRF4) HEDEF GENLERİNİN MELANOMA HÜCRE HATLARINDA BELİRLENMESİ

IRF4, bağışıklık hücrelerinin gelişiminde ve işlevlerinde öneme sahip bir transkripsiyon faktörüdür. IRF4 regülasyonunun çeşitli miyeloid ve lenfoid malignansilerde bozulduğu bilinmektedir. IRF4 anlatımının sadece bağışıklık hücreleri ile sınırlı olduğu sanılmaktayken, yakın zamandaki çalışmalar, IRF4 anlatımının melanosit hücreleri gibi, bağışıklık hücresi olmayan hücrelerde de gerçekleştiğini göstermiştir. Önceki çalışmalarımızda, belirli melanoma hücre hatlarında IRF4 anlatımının olduğu ve bu anlatımın B-hücrelerinde olduğu gibi, melanoma hücrelerinin de canlılığı için önemli olduğu gözlemlenmiştir. Melanomada IRF4'un rolü ile ilgili bilgi eksikliği olduğu için, IRF4'un transkripsiyonel hedef genlerini tespit etmek amacıyla yeni nesil dizileme yaptık. Hedef genleri belirlemek, IRF4'un hangi yolaklarda yer aldığını ve hangi biyolojik süreçleri düzenlediğini anlamamıza yardımcı olacaktır. Bunun için ilk adım olarak, analiz için en uygun koşulları belirledik. Sonra, IRF4'u susturulmuş hücreler ile kontrol hücrelerin gen anlatım profillerini yeni nesil cDNA dizilemesi (RNA-seq) ile karşılaştırdık. Biyo-informatik analizler yaparak, farklı anlatımı olan genleri belirledik. Seçilen aday genlerin RNA-dizileme sonuçlarının doğrulamasını gerçek zamanlı yarı kantitatif polimeraz zincir reaksiyonu yöntemi ile gerçekleştirdik. Daha sonra, gen ontolojisi analizi yaparak farklı anlatımı olan genlerin, zenginleştirilmiş fonksiyonel sınıflarının karakterizasyonunu gerçekleştirdik. Analizlerimiz, IRF4'ün özellikle hücre bölünmesi ile ilişkili genleri ağırlıklı olarak aktifleştirdiğini, lipit metabolizmasını ile ilişkili genleri baskıladığını göstermiştir. Ek olarak, RNA-dizileme sonucu elde ettiğimiz veriler ışığında, IRF4'ün, öne çıkan bir melanosit transkripsiyon faktörü üzerinde etkisini ve belirli melanoma hücre hatlarındaki yaşamsal yolaktaki rolünü belirlemiş olduk.

TABLE OF CONTENTS

ACKNOWLEDGEMENTS iii
ABSTRACT iv
ÖZET v
LIST OF FIGURES xi
LIST OF TABLES xv
LIST OF SYMBOLS xvii
LIST OF ACRONYMS / ABBREVIATIONS xviii
1. INTRODUCTION 1
1.1. Cancer: Overview 1
1.2. Melanoma 3
1.2.1. Melanoma: Overview 3
1.2.2. Melanoma: Deregulated Pathways 5
1.3. Interferon Regulatory Factor 4 (IRF4) 9
1.3.1. IRF4: Overview 9
1.3.2. Role of IRF4 in Immune Cells and Related Cancers 9
1.3.3. IRF4 in Non-immune Cells, Including Melanocytes 12
1.3.4. IRF4 in Melanoma 15
1.4. Next-Generation Sequencing 17
1.4.1. Overview 17
1.4.2. RNA-seq 19
2. PURPOSE 23
3. MATERIALS 24
3.1. General Kits, Enyzmes and Reagents 24
3.2. Biological Materials 25
3.2.1. Bacterial Strains 25
3.2.2. Cell Lines 25
3.2.3. Plasmids 25
3.2.4. Primers 26
3.3. Chemicals 27

3.4. Buffers and Solutions 28
3.5. Antibodies 30
3.6. Disposable Labware 31
3.7. Equipments 32
4. METHODS 35
4.1. Cell Culture 35
4.1.1. Cell Line Maintenance 35
4.1.2. Transfection of Lentiviral Vectors for Virus Production by Calcium Phosphate Method 36
4.1.3. Harvesting Virus Containing Medium 36
4.1.4. Lentiviral Transduction 36
4.1.5. Transient Transfection of Episomal Vectors with K2 Transfection System 37
4.2. GFP Competition 37
4.3. Molecular Biological Techniques 38
4.3.1. Plasmid Isolation 38
4.3.2. Isolation of Total RNA 38
4.3.3. Preservation of Total RNA by RNAstable 39
4.3.4. cDNA Synthesis 39
4.3.5. Real Time Quantitative PCR (RT-qPCR) 39
4.3.6. Agarose Gel Electrophoresis 40
4.4. Western Blotting 41
4.4.1. Cell Lysis and Protein Extraction 41
4.4.2. BCA Assay for Protein Concentration Determination 41
4.4.3. Preparation of Protein Samples and SDS Gel Electrophoresis 42
4.4.4. Blotting - Transfer from SDS Gel to PVDF Membrane 42
4.4.5. Staining - Antibody Incubations 43
4.4.6. Chemiluminescence Detection 43
4.5. Intracellular Flow Cytometry 43
4.6. RNA-seq 44
4.7. Bioinformatic Methods for RNA-seq Analysis 45
4.7.1. Data Quality Control by FastQC via Galaxy Web Server 45
4.7.2. Fetching Sequenced Total Read Number From a FastQ File 45

4.7.3. Splitting FastQ Files 45
4.7.4. Mapping Reads to the Human Genome by Tophat Software 46
4.7.5. Selection of Uniquely Mapped Reads 47
4.7.6. Mapping Statistics by SAMtools 48
4.7.7. Quantification of Mapped Reads and Determination of Differentially Expressed Genes by Cuffdiff Software 48
4.7.8. Visualization of Cuffdiff Output by CummeRbund Software 49
4.7.9. Quantification of Mapped Reads by HTSeq 50
4.7.10. Determination of Differentially Expressed Genes by DESeq Software 50
4.7.11. Venn Diagrams 52
4.7.12. Correlation Graphs 52
4.7.13. Kaplan-Meier Plots 52
5. RESULTS 53
5.1. Detection of Basal IRF4 Expression in Melanoma Cell Lines 53
5.2. Optimizations for RNA-seq Experiments 55
5.2.1. Transduction Efficiency Optimization 55
5.2.2. Optimal Time-point Selection 57
5.3. Validation of IRF4 Knock-down in Samples Prepared for RNA-seq 60
5.3.1. SKMEL-28 60
5.3.2. SKMEL-5 60
5.4. Integrity Control of Total RNA Samples for RNA-seq 62
5.5. Bioinformatic Analysis of RNA-seq Results 63
5.5.1. Quality Check for Sequenced Reads 63
5.5.2. Mapping to Reference Human Transcriptome and Its Visualization 64
5.5.3. Identification of Significantly Differentially Expressed Genes via Cuffdiff 65
5.5.4. Correlation Between Biological Replicates 69
5.5.5. Assesment of RNA-seq Data with Global Statistics 70
5.6. Verification of RNA-seq Results with RT-qPCR 72
5.7. Gene Ontology Enrichment Analysis via GOrilla 75
5.7.1. Common IRF4-Activated Genes 77
5.7.2. Common IRF4-Repressed Genes 78
5.8. Alternative Pipeline to Find Significantly Differentially Expressed Genes 79

5.9. Regulation of MITF upon IRF4 Knock-down and Over-expression 81
5.10. Regulation of RAS Targets upon IRF4 Knock-down and Over-expression 83
6. DISCUSSION 88
APPENDIX A: KAPLAN MEIER PLOTS OF PATIENTS WITH LOW AND HIGH IRF4 EXPRESSION PROFILES 99
APPENDIX B: REPLICATION OF ENDOGENOUS IRF4 LEVEL DETERMINATION BY WESTERN BLOTTING AND RT-qPCR 100
APPENDIX C: REPLICATION OF GFP COMPETITIONS 101
APPENDIX D: INTRACELLULAR FLOW CYTOMETRY RESULTS FOR GOAT SERUM TREATED SKMEL-28 CELLS 103
APPENDIX E: INTRACELLULAR FLOW CYTOMETRY RESULTS OF shIRF4 AND shLUC TRANSDUCED SKMEL-28 CELL LINE 104
APPENDIX F: AGILENT BIOANALYZER ANALYSES 105
APPENDIX G: QUALITY CHECK FOR RNA-STABLE TREATED SAMPLES 107
APPENDIX H: PER BASE QUALITY GRAPHS 108
APPENDIX I: INTEGRATIVE GENOME VIEWER VISUALIZATION FOR IRF4 LOCUS IN SKMEL-28 110
APPENDIX J: COMPARISON OF UNIQUELY MAPPED READ NUMBERS OF SKMEL-5 AND SKMEL-5-ADJUSTED SKMEL-28 111
APPENDIX K: GLOBAL STATISTICS FOR RNA-SEQ DATA 112
APPENDIX L: CORRELATION GRAPHS OF FPKM VALUES OF SAME CONDITION'S BIOLOGICAL REPLICATES 115
APPENDIX M: GENE ENRICHMENT ANALYSIS OF IRF4 ACTIVATED GENES FOR GO_BP TERMS BY GORILLA 117
APPENDIX N: GENE ENRICHMENT ANALYSIS OF IRF4 REPRESSED GENES FOR GO_BP TERMS BY GORILLA 132
APPENDIX O: ENRICHED GENE ONTOLOGY (BIOLOGICAL PROCESS) TERMS IN IRF4-ACTIVATED GENE LIST SHARED BETWEEN SKMEL-5 AND SKMEL-28 136
APPENDIX P: ENRICHED GENE ONTOLOGY (BIOLOGICAL PROCESS) TERMS IN IRF4-REPRESSED GENE LIST SHARED BETWEEN SKMEL-5 AND SKMEL-28 139

APPENDIX Q: MITF LEVELS UPON IRF4 KNOCK-DOWN IN SKMEL-5 AND SKMEL-28 CELL LINES 140
APPENDIX R: MITF AND P-AKT LEVELS UPON IRF4 KNOCK-DOWN IN A2058 AND G-361 CELL LINES 141
APPENDIX S: MITF PROTEIN LEVELS IN IRF4 OVER-EXPRESSED SKMEL-28 CELL LINE 142
APPENDIX T: p-ERK1/2 LEVELS UPON IRF4 KNOCK-DOWN IN SKMEL-5 AND SKMEL-28 CELL LINES 143
APPENDIX U: p-AKT LEVELS UPON IRF4 KNOCK-DOWN IN SKMEL-5 AND SKMEL-28 CELL LINES 144
APPENDIX V: p-AKT LEVELS IN IRF4 OVER-EXPRESSED SKMEL-28 AND MEL-ST CELL LINES 145
REFERENCES 146

LIST OF FIGURES

Figure 1.1. Progression of melanocyte transformation. 5

Figure 1.2. Major deregulated pathways in melanoma. 8

Figure 1.3. Late stage B-cell cancers and their origins. 12

Figure 1.4. IRF4 expression of fibroblast, keratinocyte and melanocyte cells. 13

Figure 1.5. GEO Dataset showing IRF4 expression both in melanocytes and melanoma. 14

Figure 1.6. Relationship between IRF4, MITF and AP2α and their effects on the expression of *TYR*. 15

Figure 5.1. Intracellular flow cytometry results showing IRF4 protein levels of indicated cell lines. 54

Figure 5.2. GFP competition assay with high transduction efficiencies on SKMEL-28 cell line. 56

Figure 5.3. GFP competition assays with high and medium transduction efficiencies on SKMEL-28 and G-361 cell lines. 57

Figure 5.4. Western blotting results with SKMEL-28 lysates for optimal time point selection. 58

Figure 5.5. Western blotting results with G-361 lysates for optimal time point selection. 59

Figure 5.6. Intracellular flow cytometry for optimal time point selection for IRF4 knock-down in SKMEL-28. 59

Figure 5.7. Intracellular flow cytometry results of SKMEL-28 samples used for RNA-seq. 61

Figure 5.8. Western blotting results of SKMEL-5 samples prepared for RNA-seq. 61

Figure 5.9. Schematics of the pipeline followed for bioinformatics analysis of RNA-seq experiment. 63

Figure 5.10. Per base sequence quality graph for one of the biological replicates of SKMEL-5. 64

Figure 5.11. The number of genes significantly up-regulated or down-regulated, defined by Cuffdiff, upon IRF4 depletion in SKMEL-28 and SKMEL-5 cell lines. 66

Figure 5.12. Number of significantly differentially expressed genes, defined by Cuffdiff, distinct or shared between two cell lines. 67

Figure 5.13. Difference between DEGs before and after, when SKMEL-28 mapped number decreased to the level of SKMEL-5 mapped number. 67

Figure 5.14. Dendrograms for A) SKMEL-5 B) SKMEL-28 showing relatedness between samples. 71

Figure 5.15. Expression distribution (density) graph of SKMEL-5. 72

Figure 5.16. RT-qPCR results of 8 genes compared with RNA-seq results. 73

Figure 5.17. RT-qPCR results of selected 8 genes for shIRF4 and shLuc transduced A2058 and G-361 cell lines. 75

Figure 5.18. Highest ranked Gene Ontology (Biological Process) terms for common IRF4-activated gene list ($p < 10^{-9}$). 78

Figure 5.19. Gene Ontology (Biological Process) terms enriched in IRF4-repressed gene set ($p < 10^{-9}$). 79

Figure 5.20. The number of genes significantly up-regulated or down-regulated upon IRF4 depletion, defined by DESeq, in SKMEL-28 and SKMEL-5 cell lines. 80

Figure 5.21. Comparison of Cuffdiff and DESeq for the number of differentially expressed genes in each case. 80

Figure 5.22. MITF protein levels upon IRF4 knock-down in A) SKMEL-5 and B) SKMEL-28 cell lines, as detected by immunoblotting. 81

Figure 5.23. MITF protein levels upon IRF4 over-expression in A) SKMEL-5 and B) SKMEL-28 cell lines. 83

Figure 5.24. Phospho-ERK (p-ERK) protein levels upon IRF4 knock-down in A) SKMEL-5 and B) SKMEL-28 cell lines. 84

Figure 5.25. Phospho-AKT protein levels upon IRF4 knock-down in A) SKMEL-5 and B) SKMEL-28 cell lines. 86

Figure 5.26. Phospho-AKT protein levels upon IRF4 over-expression in A) SKMEL-5 and B) SKMEL-28 cell lines. 87

Figure 6.1. A model for IRF4 and MITF cross regulation. 96

LIST OF TABLES

Table 1.1. Estimations of the American Cancer Society for new melanoma cases and related deaths, in the United States, 2014. 4

Table 1.2. IRF4 expression levels when compared between melanoma patients grouped according to their overall survival (OS). 16

Table 1.3. Phred quality scores and corresponding probability of incorrect base call. 21

Table 3.1. List of kits, enzymes and reagents. 24

Table 3.2. Primers used in this study. 26

Table 3.3. Chemicals used in this study. 27

Table 3.4. Buffers and solutions used in this study. 28

Table 3.5. Antibodies used in this study. 30

Table 3.6. List of disposable labwares used in this study. 31

Table 3.7. List of equipment used in this study. 32

Table 5.1. RINs for isolated total RNAs from SKMEL-28 and SKMEL-5 cell lines. 62

Table 5.2. Tophat mapping statistics showing number of sequenced (Total) and uniquely mapped reads for each replicate and condition. 65

Table 5.3. Significant IRF4-activated genes having highest fold change in both cell lines. 68

Table 5.4. Significant IRF4-repressed genes having highest fold change in both cell lines. 68

Table 5.5. Spearman's correlation coefficients between each biological replicate. 69

Table 5.6. Comparison of fold changes determined in RT-qPCR and RNA-seq. 74

LIST OF SYMBOLS

bp	Base Pairs
g	Gravity
gr	Gram
kb	Kilobase
kDa	Kilodalton
L	Liter
M	Molar
mA	Milliamper
mg	Milligram
min	Minute
ml	Milliliter
mm	Millimeter
mM	Millimolar
ng	Nanogram
s	Second
V	Volt
α	Alpha
β	Beta
^{o}C	Centigrade degree
µg	Microgram
µl	Microliter

LIST OF ACRONYMS / ABBREVIATIONS

ABC-DLBCL	Activated B-cell like diffuse large B-cell lymphoma
AKT	V-Akt Murine Thymoma Viral Oncogene / Protein Kinase B
APS	Ammonium persulfate
BCL	B-cell lymphoma
BRAF	V-raf murine sarcoma viral oncogene homolog B
BRCA2	Breast cancer 2
BSA	Bovine serum albumin
$CaCl_2$	Calcium chloride
CDK4	Cyclin dependent kinase 4
CDKN2A	Cyclin dependent kinase inhibitor 2A
cDNA	Complementary DNA
c-KIT	V-kit Hardy Zuckerman 4 feline sarcoma viral oncogene homolog
CO_2	Carbon dioxide
DCT	Dopachrome tautomerase
DIAPH1	Diaphanous-related formin 1
ddH_2O	Double-distilled water
DMEM	Dubecco's modified eagle medium
DMSO	Dimethyl sulfoxide
DNA	Deoxyribonucleic acid
DTIC	Dacarbazine
E2F1	E2F transcription factor 1
ECL	Enhanced chemiluminescent solution
EDTA	Ethylenediaminetetraacetate
ERK1/2	Mitogen-activated protein kinase 3/1
EST	Expressed sequence tag
EtOH	Ethanol
FBS	Fetal bovine serum
FC	Fold change

FPKM	Fragments per kilobase of transcript per million mapped reads
gDNA	Genomic DNA
GFP	Green fluorescent protein
GDP	Guanosine 5’ -diphosphate
GO	Gene ontology
GO_BP	Gene ontology biological process domain
GTP	Guanosine 5’ –triphosphate
GWAS	Genome-wide association studies
HEK	Human embryonic kidney
HEPES	4-(2-hydroxyethyl)-1-piperazineethanesulfonic acid
HRP	Horseradish peroxidase
IRF4	Interferon regulatory factor 4
ISRE	Interferon-stimulated response element
LB	Luria-Bertani broth
MAPK	Mitogen activated protein kinase
MDM2	Mouse double minute 2 homologue
MEK1/2	Dual specificity mitogen-activated protein kinase kinase 1/2
$MgCl_2$	Magnesium chloride
MITF	Microthalmia-associated transcription factor
MM	Multiple myeloma
mRNA	Messenger RNA
mTOR	Mammalian target of rapamycin
MYC	V-Myc Avian Myelocytomatosis Viral Oncogene Homolog
N-terminal	Amino terminal
NF-κB	Nuclear factor kappa B
NGS	Next-generation sequencing
NRAS	Neuroblastoma v-ras oncogene homolog
PAGE	Polyacrylamide gel electrophoresis
PBS	Phosphate buffered saline
PCR	Polymerase chain reaction
PDK1	3-phosphoinositide dependent protein kinase-1
PE	Phycoerythrin
PFA	Paraformaldehyde

PH	Pleckstrin homology
PI3K	Phosphoinositide-3-OH kinase
PIP_2	Phosphatidylinositol (4,5)-bisphosphate
PIP_3	Phosphatidylinositol (3,4,5)-triphosphate
POU3F2	POU Class 3 Homeobox 2
PS	Polystrol
PTEN	Phosphate and tensin homologue
PVDF	Polyvinylidene fluoride
Q61R	Glutamine to arginine substitituon
Q61K	Glutamine to lysine substitituon
PerCP	Peridinin chlorophyll protein complex
RB	Retinoblastoma
RGP	Radial growth phase
RNA	Ribonucleic acid
RNA-seq	RNA sequencing
ROCK	Rho-associated protein kinase
rpm	Revolution per minute
rRNA	Ribosomal RNA
RT	Room temperature
RT-qPCR	Reverse transcriptase - quantitative PCR
SDS	Sodium dodecyl sulfate
shRNA	Short hairpin RNA
shLuc	Short hairpin RNA against Luciferase
SNP	Single nucleotide polymorphism
SQ	Subcutaneous
SQLE	Squalene Monooxygenase
TBS	Tris-buffered saline
TBS-T	Tris buffered saline with tween
TEMED	Tetramethylethylenediamine
TFAP2A	Activating enhancer binding protein 2 alpha
Th	T helper cell
TLR	Toll-like receptor
TP53	Tumor protein p53

Tris	Tris (hydroxylmethyl) aminomethane
Tween	Polysorbate
TRYP1	Tyrosinase-related protein 1
TYR	Tyrosinase
Unt	Untransduced
UV	Ultraviolet
UVR	UV radiation
VEGF	Vascular endothelial growth factor
VGP	Vertical growth phase
V600E	Valine to glutamic acid substitituon

1. INTRODUCTION

1.1. Cancer: Overview

Cancer is a disease resulting from abnormal cell growth and proliferation in an uncontrolled fashion due to genetic or epigenetic alterations in the genome. Abnormalities in the genomes of cancer cells let them to gain ability to skip cellular mechanisms that limit proliferation, such as cell death or senescence. If proliferation continues and those cells also gain the ability to migrate and invade into other tissues, the phenomenon called metastasis arises and the spread of tumor to other organs cause the disease to become fatal due to loss of functions in related organs. Hanahan and Weinberg sum up the hallmarks of cancer under six concepts as shown below (Hanahan and Weinberg, 2011):

(i) Self-sufficiency in growth signals
(ii) Insensitivity to anti-growth signals
(iii) Evading apoptosis
(iv) Limitless replicative potential
(v) Tissue invasion & metastasis
(vi) Sustained angiogenesis

Cancer cells sustain proliferative state either by constantly producing growth factors or stimulating normal cells in their stroma to do so. However, receptors of those growth factors or downstream elements of related pathway could also be mutated. In this case, the proliferative signaling pathway works in a ligand-free fashion and becomes constitutively active. For example, BRAF (v-raf murine sarcoma viral oncogene homolog B) and NRAS (neuroblastoma v-ras oncogene homolog) are the key elements for the mitogen activated MAPK (mitogen-activated protein kinase) pathway. Mutations affecting the structure of those proteins may lead to a constant proliferative state. Such genes are named as proto-oncogenes, where their high activity is sustained by, for example, gain-of-function mutations or increased expression (Hanahan and Weinberg, 2011).

Disruptions of the mechanisms for attenuating the proliferative signaling also help cancer cells evade senescence, and sustain the proliferative characteristic. Loss-of-function of PTEN (phosphatase and tensin homolog) protein is a prominent example for such a case. When PTEN loses its function by mutation, PI3K/AKT pathway (phosphatidylinositol-4,5-biphosphate 3-kinase / protein kinase B) becomes over-activated, as PTEN is the negative regulator of this growth promoting pathway (Chalhoub and Baker, 2009). Genes such as PTEN whose loss of activity contribute to cancer progression are named tumor suppressors. Other important tumor suppressors include RB (retinoblastoma) and TP53 (tumor protein p53) proteins. During cancer progression, cells encounter physiological stress due to elevated oncogene levels and DNA damage (Adams and Cory, 2007). In normal cells, RB and TP53 play roles in such stress situations by inducing cells to go into either senescence, or programmed cell death. Abnormalities in the functions of these gatekeeper proteins of proliferation are critical steps in most of the cancer cases (Ghebranious and Donehower, 1998).

Because tumor volume increases during tumor growth, cancer cells require more oxygen and nutrients, and more efficient removal of metabolic waste as well. For that reason tumor mass reaching 1- to 2-mm diameter necessitates the vascularization process (Talmadge and Fidler, 2010). This is accomplished by the secretion of angiogenic factors. The well known angiogenesis inducer up-regulated in tumor cells is VEGF (Vascular Endothelial Growth Factor) (Carmeliet, 2005). VEGF interacts with its tyrosine kinase receptor on the cell surface of endothelial cells and transmits signal to downstream proteins. As a result, endothelial cell proliferation and migration into the tumor is stimulated (Byrne *et al.*, 2005).

Metastasis, or the ability of cancer cells to colonize new tissues, occurs at the later stages after cancer cells gain the ability to invade. This relies on cancer cells' ability to activate or repress the transcription of certain genes. The best characterized gene deregulated in this process found in epithelial tumors is *CDH1* which encodes E-cadherin protein. E-cadherin is a key molecule playing a role in cell-to-cell adhesion. Reduction in E-cadherin expression therefore helps cancer cells to migrate to and invade the other tissues (Berx and van Roy, 2009).

Cancer progression is a multi-step process starting from transformation of normal cells into cancer cells. In each step of cancer progression, cells acquire new abilities by de-regulation of certain proto-oncogenes and tumor suppressor genes. For a proper prognosis and an accurate treatment, these genes and their mechanisms of activation (for oncogenes) and deactivation (for tumor suppressors) should be clearly defined.

1.2. Melanoma

1.2.1. Melanoma: Overview

Melanoma is the most aggressive type of skin cancer which originates from melanocytes (pigment producing cells). Other types of skin cancer, basal cell carcinoma and squamous cell carcinoma, are more frequent but less dangerous. The reason for melanoma to be more fatal relative to other skin cancers is its high metastatic potential. When diagnosed in early stage (Stage I), five year survival rate is around 90% and it could be treated with surgical excision. However, survival rate drops down to 15% in the late stages (Stage IV) where metastasis has already occurred (Balch *et al.*, 2009). The American Cancer Society estimates that 76,100 people in the United States will be diagnosed with melanoma and 9,710 deaths will occur related with this disease in 2014 (Table 1.1) (Siegel *et al.*, 2014).

Skin is the primary site where melanoma rises but rarely, it can also originate from the other parts of the body that contain melanocytes, such as eye (uveal melanoma), vulva (vulval melanoma) or vagina (vaginal melanoma). If originated from the skin, it is also called cutaneous malignant melanoma. Melanocytes are located at the basal layer of epidermis in skin where their homeostasis is regulated by keratinocytes. In response to UVR (UV radiation), keratinocytes secrete factors to stimulate melanocytes for the production of melanin pigments. These pigments protect the skin from the harmful effects of UVR by absorbing the light energy, so that they protect the cells from DNA damage. Being a barrier to UV rays, melanocytes, as well as keratinocytes, are affected from its damaging effects (Costin and Hearing, 2007). This causes UVR to be considered as the major risk factor for

melanoma and other skin cancers. Additional risk factors are genetic background and pigmentation status of the individual (Vultur and Herlyn, 2013).

Table 1.1. Estimations of the American Cancer Society for new melanoma cases and related deaths, in the United States, 2014 (Siegel *et al.*, 2014).

	ESTIMATED NEW CASES			ESTIMATED DEATHS		
	BOTH SEXES	MALE	FEMALE	BOTH SEXES	MALE	FEMALE
All sites	**1,665,540**	**855,220**	**810,320**	**585,720**	**310,010**	**275,710**
Skin (excluding basal & squamous)	**81,220**	**46,630**	**34,590**	**12,980**	**8,840**	**4,410**
Melanoma - skin	76,100	43,890	32,210	9,710	6,470	3,240

Malignant transformation of melanocytes to melanoma begins with deregulation of melanocyte homeostasis. This results in the proliferation and spread of the melanocytes, leading to the formation of benign neoplasms called nevi. When these cells acquire the ability to grow horizontally, the state is named as radial growth phase melanoma (RGP melanoma). This state is considered to be the primary malignant phase. Next stage is the growth in vertical manner (VGP melanoma - vertical growth phase melanoma) where cells acquire the metastatic capacity to invade dermis (Gray-Schopfer *et al.*, 2007). Figure 1.1 shows the transformation of melanocytes to malignant melanoma cells.

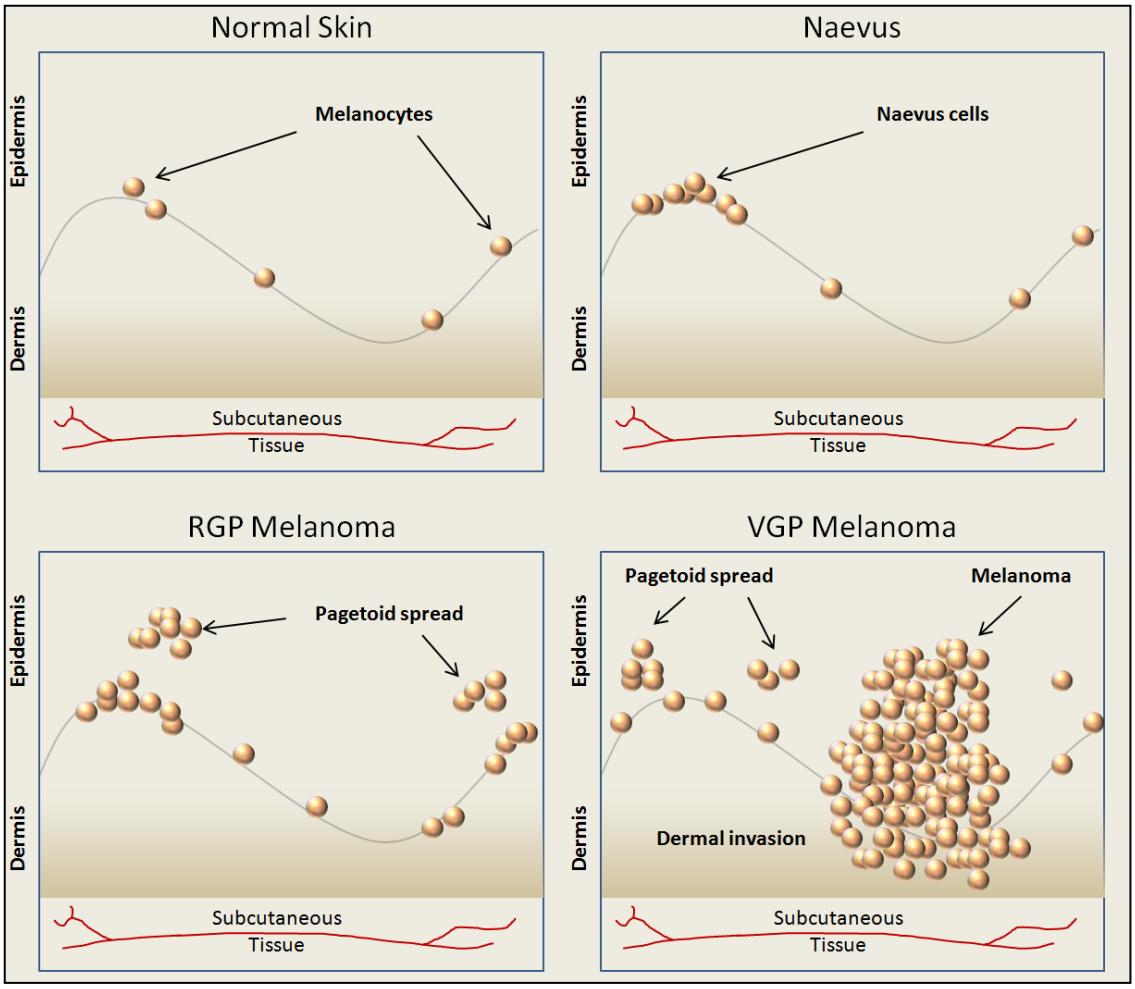

Figure 1.1. Progression of melanocyte transformation. Naevus cells firstly transforms into RGP, followed by VGP transformation. Pagetoid spread refers to an upward migration and vertical stacking of malignant cells (Adapted from Gray-Schopfer *et al.*, 2007).

1.2.2. Melanoma: Deregulated Pathways

Carcinogenesis involves genetic aberrations both in proto-oncogenes, resulting in gain-of function, and in tumor suppressor genes which lead to loss-of-function (Hanahan and Weinberg, 2011). Such genetic aberrations are also responsible for the transformation of melanocytes to melanoma cells.

One of the key pathways deregulated in melanoma, due to gain-of-function mutations, is the MAPK (Mitogen-activated protein kinase) pathway which regulates cell proliferation, invasion, migration and survival (Calipel *et al.*, 2003, Panka *et al.*, 2006, Sharma *et al.*, 2005). Certain members of this pathway, BRAF and NRAS, are the classical oncogenes of melanoma. Approximately 60% of melanomas harbor a point mutation at BRAF which leads to V600E (valine to glutamic acid) substitution, and around 20% of melanomas harbor a point mutation at NRAS which leads to Q61R (glutamine to arginine) or Q61K (glutamine to lysine) substitutions (Davies *et al.*, 2002, Ekedahl *et al.*, 2013). These mutations on BRAF and NRAS are mutually exclusive. Being a small G protein, NRAS is active when it is bound to GTP and inactive when GTP molecule is hydrolyzed to GDP. Indicated mutations on NRAS impairs the GTP hydrolysis so, NRAS becomes constitutively active. V600E substitution on BRAF makes it hyperactive and increases its kinase activity. This results in constitutively active downstream protein kinases, MEK1/2 (Dual specificity mitogen-activated protein kinase kinase 1/2) and ERK1/2 (Dahl and Guldberg, 2007). ERKs are known to activate transcription factors related with proliferation, survival and tumor growth (Gray-Schopfer *et al.*, 2005).

Although oncogenic NRAS and BRAF are very common in melanomas, they are not sufficient for a complete transformation unless combined with other genetic alterations. Most of the melanocytic nevi, benign precursors of melanoma, harbor either $BRAF^{V600E}$ or $NRAS^{Q61K/R}$ suggesting that activation of RAS/RAF/MAPK pathway is an important step in the initiation of melanocytic neoplasia but insufficient for a malignant transformation (Pollock *et al.*, 2003).

Distinct from BRAF, NRAS also regulates PI3K (Phosphoinositide 3-kinase) pathway which is another important signaling cascade in melanomagenesis (Tsao *et al.*, 2004). Upon activation by RAS, PI3K phosphorylates PIP_2 (Phosphatidylinositol 4,5-bisphosphate), generating a new product, PIP_3 (Phosphatidylinositol (3,4,5)-triphosphate). PIP_3 binds to the proteins with pleckstrin homology (PH) domain, such as PDK1 (3-phosphoinositide dependent protein kinase-1) and AKT (V-Akt Murine Thymoma Viral Oncogene). Later on, PDK1 phosphorylates threonine 308 residue of AKT. mTORC2 contributes to the full activation of AKT by phosphorylating it from serine 473 (Castellano

and Downward, 2011). AKT is a serine/threonine-specific protein kinase and has roles in cell proliferation and survival. Activity of AKT is kept under control by a tumor suppressor protein, PTEN which dephosphorylates PIP_3. Loss of PTEN function is reported between 5% to 20% in melanomas either by mutation, deletion or promoter methylation (Wu *et al.*, 2003). Overall, deregulation of PI3K pathway results in AKT hyper-activation in 60% of melanoma cases. Over activation of AKT targets, such as mTOR and NF-kB promote cell growth and survival (Nikolaou *et al.*, 2012, Stahl *et al.*, 2004, Xie *et al.*, 2013).

Upstream of NRAS, there is a receptor tyrosine kinase protein named c-KIT. Activation of c-KIT by growth factors leads to the stimulation of both MAPK and PI3K pathways. However, mutations on c-KIT, which makes it constitutively active, are rare (3%) (Willmore-Payne *et al.*, 2005).

One of the other key molecules in melanoma is CDKN2A gene. 30% to 70% of melanoma cells overcome the senescence barrier with the inactivation of CDKN2A. This gene encodes two tumor suppressor proteins, $p16^{INK4a}$ and $p14^{ARF}$ (Gray-Schopfer *et al.*, 2007). In the case of a mutation, $p16^{INK4a}$ can't inhibit certain cyclin dependent kinases (CDK4 and CDK6) and in turn, E2F1 transcription factor's activity increases. This increase is due to hyper phosphorylation of Retinoblastoma protein (Rb) by CDK4/6 (Bertolotto, 2013). Activity of E2F1 regulates the transcription of genes promoting S-phase of cell cycle and induces proliferation in $p16^{INK4a}$ mutated profiles. Alternatively, mutations on CDK4 inhibiting $p16^{INK4a}$ interaction result in a same phenotypic effect. Previous studies showed that $NRAS^{Q61K}$ and loss of $p16^{INK4a}$ expression are sufficient to promote melanoma formation in mice (Ackermann *et al.*, 2005). On the other hand, $p14^{ARF}$ binds to MDM2 and prevent its inhibitory and degredatory effect on p53. As a key tumor suppressor protein, p53 has multifunctional roles in cancer cells. It is involved in the regulation of cell cycle, DNA integrity, and cell survival (van Oijen and Slootweg, 2000). Hence, loss of activity in $p14^{ARF}$ gene causes p53 protein level reduction in the cell and consequently, leads to cell survival (Kamijo *et al.*, 1998).

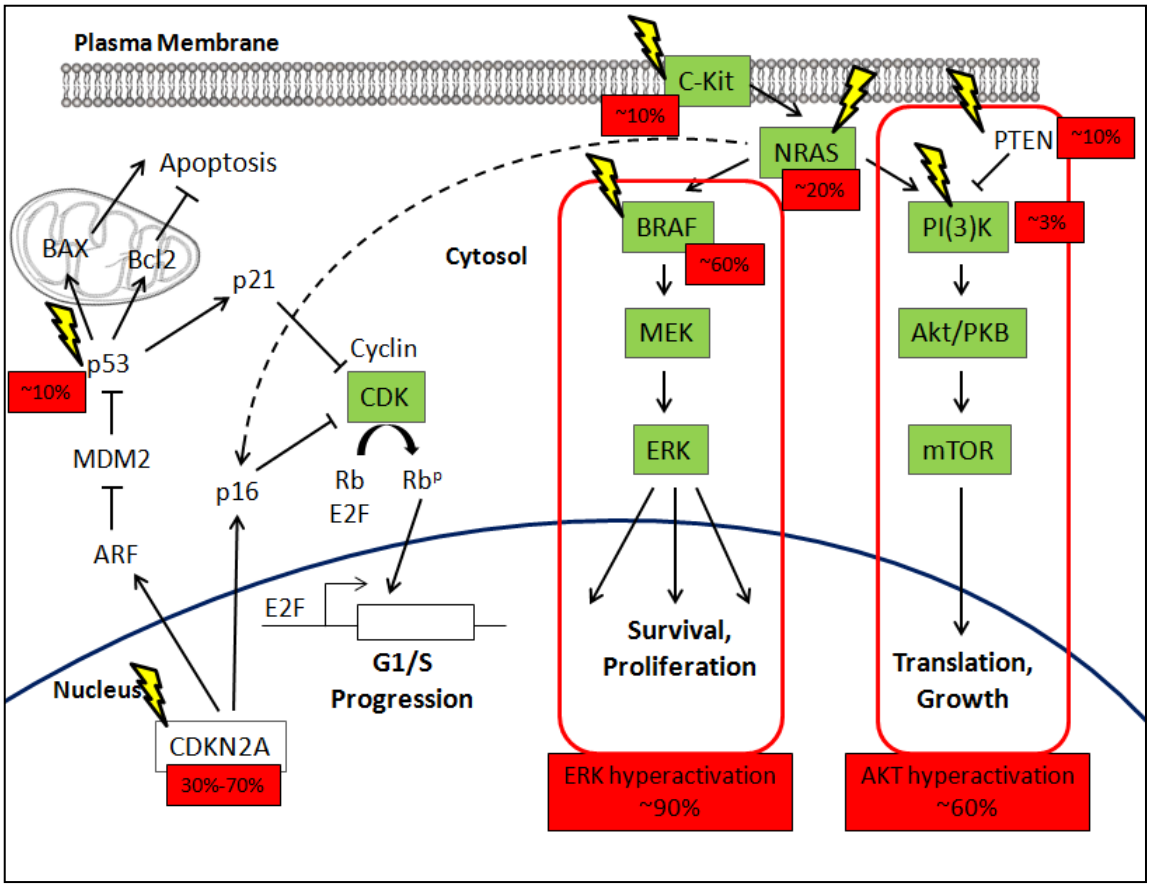

Figure 1.2. Major deregulated pathways in melanoma. Percentages show the frequency of genetic alteration in the related gene (Adapted from Gray-Schopfer *et al.*, 2007).

Microphthalmia-associated transcription factor (MITF) is the master regulator of melanocyte development. Genes involved in melanogenesis and melanin synthesis, such as *TYR*, *TRYP1* and *DCT*, are direct downstream targets of MITF (Cheli *et al.*, 2010). Apart from its role in normal cells, MITF contributes to melanomagenesis and is responsible for the survival and proliferation of melanoma cells (Levy *et al.*, 2006) Its amplification was shown in 10-20% of melanomas (Garraway *et al.*, 2005). However, it was observed that variable MITF levels in a melanoma cell contribute to different phenotypes (Hoek *et al.*, 2008a). High MITF levels induce cell proliferation through the activation of *DIAPH1* gene (Carreira *et al.*, 2006). High expression of MITF was also shown to induce the transcription of *miR-211* which suppresses the expression of *POU3F2 (BRN2)* gene. BRN2 is a transcription factor, capable of increasing invasive potential of melanoma cells *in vitro* (Boyle *et al.*, 2011). In contrast, low levels of MITF increases the activity of ROCK (Rho-

associated protein kinase) contributing to invasive and anti-proliferative characteristics (Carreira *et al.*, 2006).

1.3. Interferon Regulatory Factor 4 (IRF4)

1.3.1. IRF4: Overview

IRF4 is a member of Interferon Regulatory Factor family of transcription factors which has 9 members. Other designations of IRF4 are MUM1 (Multiple Myeloma Oncogene 1), LSIRF (Lymphocyte specific interferon regulatory factor), PIP (PU.1 interaction partner) or ICSAT (Interferon consensus sequence binding protein for activated T-cells). IRF family of proteins were initially identified due to their roles in the regulation of interferon-inducible genes (Yamagata *et al.*, 1996).

Various functions of IRF4 depend on the tissue in which it is expressed. With the ability to bind certain cofactors, it can function as activator or repressor. Its regulatory effect on transcription depends on the availability of these partners in the cell and the binding potential of IRF4 to target regions on the DNA. Expression of IRF4 was thought to be restricted to certain hematologic cells, like lymphocytes, macrophages and dendritic cells (Eisenbeis *et al.*, 1995, Politis *et al.*, 1992) but recently, its expression and functional roles in non-immune cells was also revealed.

1.3.2. Role of IRF4 in Immune Cells and Related Cancers

In immune cells, distinct from most other members of the IRF family, IRF4 is not induced by interferons but rather by mitogenic stimuli like antigen-receptor engagement, lipopolysaccharide binding or CD40 signaling, all of which have the NF-kB pathway in their downstream. Despite this unique characteristic, IRF4 binds to interferon-stimulated response element (ISRE), similarly to other IRF members, because IRFs share a conserved N-terminal containing the DNA-binding domain (Escalante *et al.*, 1998). IRF4 without its binding partners has a weak DNA-binding affinity because of its auto-inhibition capacity

(Brass *et al.*, 1996). However, upon interaction with its binding partners, such as PU.1, SPIB, E47, NFATC2, Foxp3, STAT6 or other certain IRF members, IRF4 can function as a potent transcriptional activator or repressor (De Silva *et al.*, 2012).

IRF4 is especially important in the activation and maturation of B and T lymphocytes. In B cell development, cellular IRF4 concentration plays an important role in differentiation from germinal center B cell to antigen secreting plasma cell where gradual increase is observed from former to latter (Figure 1.3) (Rui *et al.*, 2011). Regarding that, it was shown that IRF4 knockout mice lack plasma cells and germinal centers which are sites for B lymphocyte proliferation and differentiation. Together with its role in differentiation, IRF4 deficiency results in reduced immunoglobulin levels and poor B and T cell proliferative responses due to mitogenic stimulation (Mittrucker *et al.*, 1997). Moreover, IRF4 is required for immunoglobulin class switching at B cells (Sciammas *et al.*, 2006).

Differentiation of a subset of $CD4^+$ T cells also depends on IRF4. These include type 2 and type 17 T helper cells (Th2 and Th17). T helper cells are involved in the activation of other immune cells by producing cytokines. Cytokine production, as well as apoptosis, is regulated by IRF4 in these specific subtypes of T helper cells (Brustle *et al.*, 2007, Honma *et al.*, 2008).

In addition to critical roles in B and T cells, IRF4 also plays a part in myeloid lineage, precisely within dendritic cells and macrophages. Increase in the levels of IRF4 mRNA during the differentiation of monocytes into macrophages or dendritic cells has been shown (Lehtonen *et al.*, 2005). Studies on a subset of dendritic cells ($CD4^+$) showed the role of IRF4 on the expression of major histocompability complex class II and antigen presentation to T cells (Suzuki *et al.*, 2004). Whereas, in macrophages, IRF4 functions in TLR (Toll-like receptor) signaling, where it negatively regulates the cascade by competing with another member of the IRF family, IRF5 (Negishi *et al.*, 2005).

Having an important role on the activation (which involves increased survival and proliferation) and differentiation of immune cells, it is not surprising that deregulation on

IRF4 levels leads to a variety of hematological malignancies. Among those, it was firstly discovered in a malignancy of plasma cells, Multiple Myeloma (MM) where t(6;14)(p25;q32) translocation results in juxtaposition of immunoglobulin heavy chain locus to IRF4 gene. However, genetic aberrations of IRF4 are rare for MM (Iida *et al.*, 1997). IRF4 levels in MM patients is related with the outcome of the disease and it has been found that high IRF4 expression is associated with poor survival (Heintel *et al.*, 2008). Also, other study in the same year showed that IRF4 is required for multiple myeloma cell survival and even ~50% knock-down is sufficient to kill MM cell lines. Revealed targets of IRF4 in those cell lines showed its association with metabolic control, membrane biogenesis, cell cycle progression, cell death, and transcriptional regulation (Shaffer *et al.*, 2008). Such a dependency of MM cells on IRF4 expression without any genetic alteration on the gene is explained as "non-oncogenic addiction" by the authors of the paper (Shaffer *et al.*, 2009). On the other hand, over expression of such a critical factor, is not sufficient to cause the disease in the lymphocytes of transgenic mice (Saito *et al.*, 1999).

Activated B cell like diffuse large B cell lymphoma (ABC-DLBCL), which originates from late germinal center B cells, is an aggressive type of DLBCL (Figure 1.3). Over-expression of IRF4 on that type of cancer is a hallmark due to constitutively active NF-kB pathway (Saito *et al.*, 2007). Similar to MM, ABC-DLBCL cell lines were also dependent on IRF4 expression (Yang *et al.*, 2012). Germinal center B cell like diffuse large B cell lymphoma (GCB-DLBCL) has low levels of IRF4, due to absence of NF-kB signal and is not affected from IRF4 depletion (Figure 1.3).

Opposite to its role in MM and ABC-DLBCL, IRF4 in B cell acute lymphoblastic leukemia (B-ALL, originated from lymphoblasts), chronic myeloid leukemia (CML, originated from granulocytes), acute myeloid leukemia (AML, originated from myeloblasts) and chronic myelomonocytic leukemia (CMML, originated from hematopoietic stem cells) works as a tumor suppressor (Acquaviva *et al.*, 2008, Pathak *et al.*, 2011, Teng *et al.*, 2007). It is not surprising to observe tumor suppressor effect of IRF4 at these cancers which all are originated from immature immune cells. Roles of IRF4 in immature immune cells are distinct from its roles in mature immune cells. It was demonstrated that IRF4 ex-

pression in early B-cell development results in growth inhibition and cell-cycle arrest (Ma *et al.*, 2008).

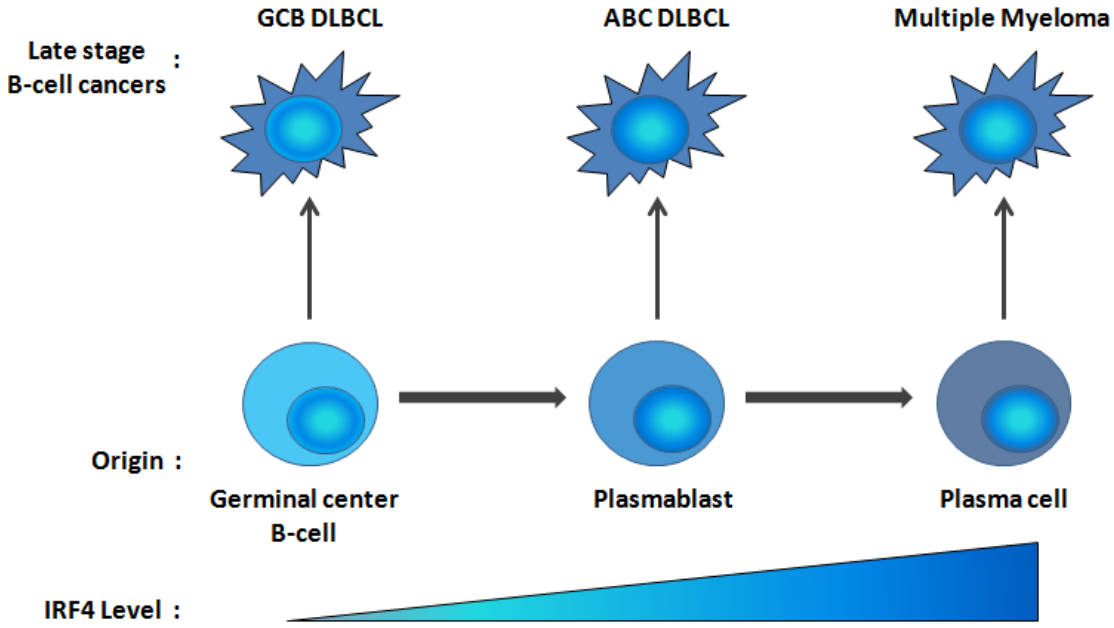

Figure 1.3. Late stage B-cell cancers and their origins. GCB DLBCL cells have low IRF4 levels and MM originated from mature B-cells (plasma cell) have the highest level of IRF4 (Adapted from Rui *et al.*, 2011).

1.3.3. IRF4 in Non-immune Cells, Including Melanocytes

Until recently, IRF4 expression was thought to be restricted to immune cells, however, recent studies show that various type of cells express IRF4. One of the IRF4 expressing non-immune cell type is the adipocytes. These are fat cells where excess energy is stored in the form of triglycerides. During fasting, triglycerides are broken down into free fatty acids and glycerol by a process named lipolysis. Eguchi *et al.* showed that IRF4 promotes lipolysis by inducing the expression of lipases (Eguchi *et al.*, 2008).

Recently, expression of IRF4 was shown in cardiac tissue and CNS (central nervous system) neurons. They concluded that IRF4 promotes cardiac hypertrophy, where heart

muscle is thickened due to an adaptive response to pressure (Jiang *et al.*, 2013). In neurons, IRF4 has a protective role where its expression rescues neurons from death and apoptosis. During ischemia and reperfusion, IRF4 is induced by an unknown mechanism, and its expression is correlated with milder outcomes of stroke damage (Guo *et al.*, 2014).

The first clues about IRF4 expression in melanocytes arose from a normal foreskin melanocyte expressed sequence tag library (EST library) (Grossman *et al.*, 1996). Additionally, online databases such as Oncomine (Rhodes *et al.*, 2004) or Cancer Cell Line Encyclopedia (Barretina *et al.*, 2012), sharing mRNA expression data are well-known sources to examine IRF4 mRNA levels in various cell types. In Figure 1.4, comparison of IRF4 mRNA expression between melanocytes and other types of skin cells is shown by using the data from a previous study (Bernstein *et al.*, 2010).

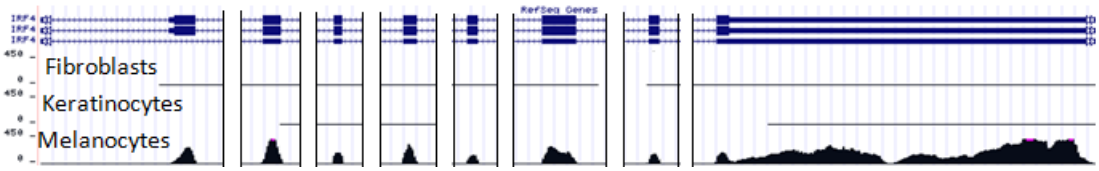

Figure 1.4. IRF4 expression of fibroblast, keratinocyte and melanocyte cells. Data was derived from NIH Roadmap Epigenomics Project. Intronic regions were shortened for a better view. At the top, three IRF4 transcripts from RefSeq were shown. Thick bars represent exonic regions. Visualization was performed by using UCSC Genome Browser.

Another database, Gene Expression Omnibus (GEO), also provides expression data from various studies (Edgar *et al.*, 2002). IRF4 expression in melanocytes, as well as in melanoma cells, can be observed from an expression study of Hoek *et al.* Expression graph showing IRF4 mRNA levels can be seen in Figure 1.5. Blue square in the graph represents the percentile rank of IRF4 expression in the whole expression profile of the corresponding sample. Red bars show the expression measurements from microarray experiments. Expression of IRF4 is high both in melanocyte and melanoma samples when compared to whole gene expression profiles (blue squares) except the second sample, GSM0206. (Hoek *et al.*, 2004).

In melanocyte biology, a SNP on IRF4 (rs12203592) has been linked to hair color and skin pigmentation by a number of genome-wide association studies (GWAS) (Han *et al.*, 2008, Sulem *et al.*, 2007). These were the first observations of possible role of IRF4 in pigmentation. A recent study showed it clearly that MITF, together with IRF4, activates the expression of one of the important pigmentation genes, TYR (tyrosinase) in melanocytes. Moreover, importance of the rs12203592 was shown by comparing the IRF4 expression in cells homozygous for CC allele and homozygous for TT polymorphism. Cells from T/T individuals has significantly ($p<10^{-3}$) lower level of IRF4 compared to C/C individuals both in mRNA and protein levels because, this SNP corresponds to the binding site of TFAP2A. If the binding site contains rs12203592-C variant, TFAP2A can bind to this region and induce the expression of IRF4, together with MITF as shown in Figure 1.6 (Praetorius *et al.*, 2013).

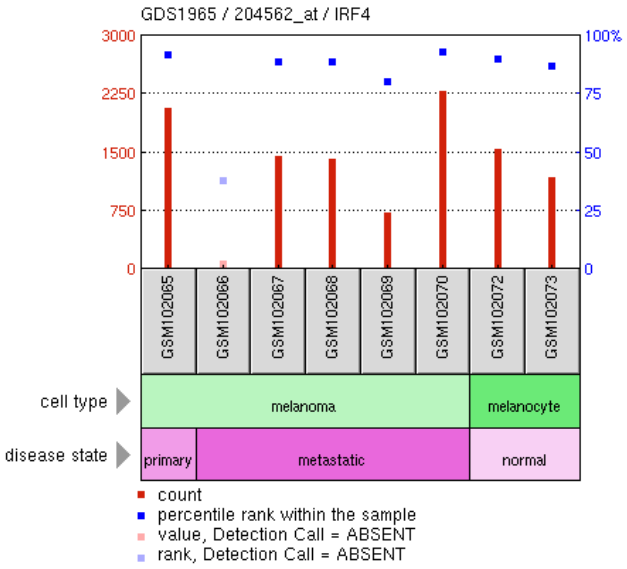

Figure 1.5. GEO Dataset showing IRF4 expression both in melanocytes and melanoma (Hoek *et al.*, 2004).

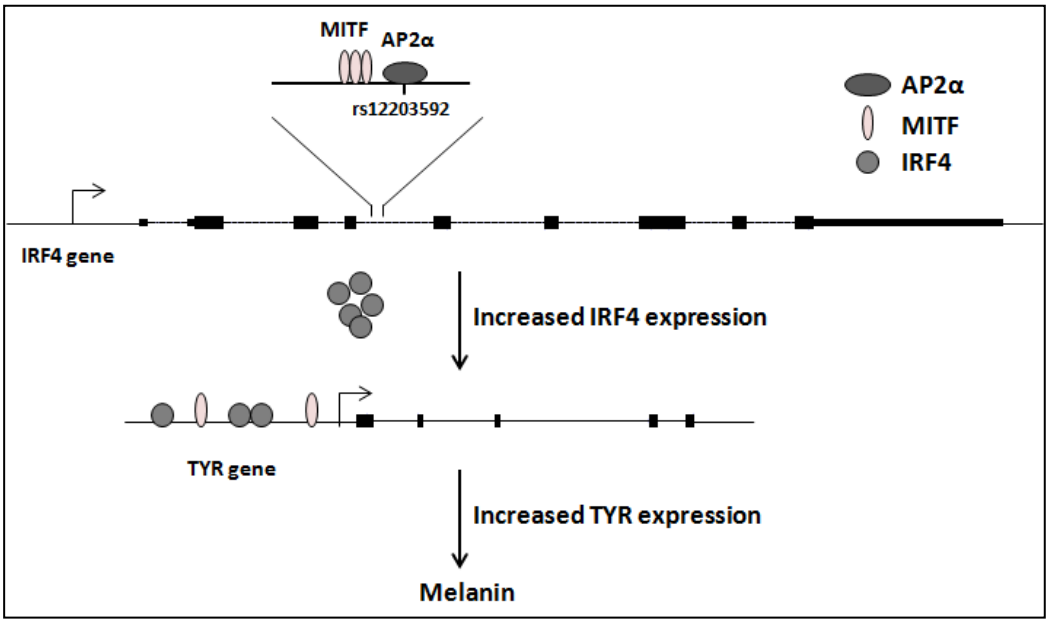

Figure 1.6. Relationship between IRF4, MITF and AP2α and their effects on the expression of *TYR* (Adapted from Praetorius *et al.*, 2013).

1.3.4. IRF4 in Melanoma

IRF4 expression in melanoma was initially detected in G-361 cell line (Grossman *et al.*, 1996). Another study showed its expression in protein level by immunohistochemistry in patient samples (Natkunam *et al.*, 2001). In a further study, they found that 92% of conventional primary and metastatic melanomas give positive staining for IRF4 and suggested its use in the diagnosis of melanoma (Sundram *et al.*, 2003). Other than expression studies, it has been found that the germline SNP rs12203592 (described above) in *IRF4* predisposes individuals to melanoma and other skin cancers (Duffy *et al.*, 2010, Han *et al.*, 2011, Pena-Chilet *et al.*, 2013)

Other than being a transcriptional target of MITF and its regulatory activity on *TYR* gene in melanoma (Figure 1.6), function of IRF4 in these cells are yet to be discovered (Hoek *et al.*, 2008b). However, when studies relating to melanoma patient survival and gene expression profiles were investigated, its potential critical role in melanomas can be seen. In one of these studies, Bogunovic *et al.* sub-grouped metastatic melanoma patients

according to their gene expression profiles and survival. When IRF4 expression and survival correlation is investigated on those patients without sub-grouping, we observed that melanoma patients expressing less IRF4 survive longer (Figure A.1) (Bogunovic *et al.*, 2009). Similar data come from the study of Journe *et al.* Although they are mostly concentrated on the effect of TYRP1 gene expression on clinical outcome, they show that IRF4 expression in melanoma metastases is significantly higher in the patients living relatively shorter (Journe *et al.*, 2011). Table 1.2 shows the IRF4 expression and overall survival association from this study. In contrast, another study shows an opposite effect of IRF4 on the clinical outcome of metastatic melanoma patients. However, as the authors also indicated, treatment of patients with dacarbazine (DTIC) in this study may have led to a high benefit rate in a group of patients characterized by high expression levels in the pigmentation genes (Jonsson *et al.*, 2010).

Table 1.2. IRF4 expression levels when compared between melanoma patients grouped according to their overall survival (OS) (Journe *et al.*, 2011) (Geom= geometric, FDR= false discovery rate, OS=overall survival).

Gene Symbol	p-value	FDR	Geom. Mean of intensities OS<30 monthes	Geom. Mean of intensities OS>30 monthes	Fold change	Probe set
IRF4	0.0161	0.3	150.04	56.2	2.67	204562_at

Researchers have been investigating the role of IRF4 mostly in immune cells (De Silva *et al.*, 2012). Mechanisms of certain drugs used to treat those cancers, like lenalidomide, have been linked to IRF4, suggesting more precise therapy options for certain cancer patients. For example, a study done by Lopez-Girona *et al.* showed that lenalidomide does not have an effect on low IRF4 expresser multiple myeloma patients but high IRF4 expressers treated with lenalidomide have significantly longer OS (overall survival) compared to those receiving other therapies (Lopez-Girona *et al.*, 2011). So far, except certain immune cancers, the only cancer type which IRF4 expression was observed is melanoma. Preliminary results showing its potential critical role *in vitro* and in patient survival studies in melanoma cases are encouraging for further investigations. For that purpose, it is important to study the biological processes and the signaling pathways in which IRF4 plays a role in melanoma.

1.4. Next-Generation Sequencing

1.4.1. Overview

Sanger sequencing has been the most commonly used method for DNA sequencing until recently. The method is based on chain termination by dideoxynucleotides (ddNTPs) during in vitro DNA replication (Sanger *et al.*, 1977). ddNTPs, lacking the 3'-OH group, terminate the elongation of DNA catalyzed by DNA polymerase. In the current protocol, fluorescently labeled ddNTPs provide the information about the corresponding base when the PCR products were run in capillaries (capillary electrophoresis) to sort the fragments according to size and order. At the end, depending on the fluorescent label, nucleotide is detected (Smith *et al.*, 1986). This method is considered as first generation sequencing.

Although Sanger method is still being used widely, sequencing of large genomes or transcriptomes requires a faster and cost effective technology. This demand prompted the creation of the next-generation sequencing methods (NGS). In this technique, millions of DNA fragments are sequenced at the same time, which is the reason why it is also called as massive parallel sequencing. Unlike Sanger method, nucleotides are detected along with their addition to the complementary strand rather than chain-termination, so separation step is not necessary as in Sanger technology. Nowadays, NGS is widely used for whole genome sequencing, *de-novo* sequencing, targeted resequencing, exome sequencing and mRNA sequencing which is actually reverse synthesized to cDNA before sequencing (Morozova and Marra, 2008).

Exome sequencing is generally used in identification of disease-causing mutations. Because researchers are generally interested in protein coding parts of the genome, they choose to sequence the whole "exome" rather than whole "genome", especially when pursuing Mendelian diseases. In the case of a suspected disease, targeted sequencing, where a specific region in the genome is sequenced, is preferable to whole exome sequencing. Thus, the technique brings advantage on cost and time (Grada and Weinbrecht, 2013). Whole genome sequencing is used for the characterization of an organism's complete DNA

sequence. If the method is used for an unknown genome where a reference genome for mapping the reads are not available, sequenced reads are assembled in an overlapping fashion forming contigs and it is named as *de-novo* sequencing (Ng and Kirkness, 2010).

Commonly used commercially available next-generation technologies belong to Roche/454, Illumina/Solexa and Life Tech/SOLiD. These platforms use different strategies for library preparation, sequencing and imaging steps. In the amplification step, just before sequencing, 454 and SOLiD use emulsion-PCR, and Illumina uses bridge amplification method to amplify DNA templates. In the sequencing step, 454 uses pyro-sequencing, Illumina uses fluorescently labeled reversible terminators and SOLID uses cleavable probes which are sequenced by ligation. Each platform has cons and pros due to using those different methodologies at each step. Roche/454 can generate relatively longer reads, which improve the mapping of repetitive regions. SOLiD produces relatively error-free, more accurate results. On the other hand, Illumina platform produces highest throughput per run (Loman *et al.*, 2012, Metzker, 2010).

Other commercial DNA sequencing platforms are Ion Torrent of Life Technologies and PacBio RS II of Pacific Biosciences. Ion torrent semiconductor sequencing is based on the detection of hydrogen ions released during DNA polymerization. Precisely, micro-wells in a chip contain the clonally amplified DNA fragments (by emulsion PCR), and these wells are flooded with a single type of nucleotide in each cycle. If nucleotide incorporates into template strand, hydrogen ions are released which causes pH alteration of the solution in the well. If there are two identical bases next to each other in the template strand, two nucleotides incorporate into the strand and this leads to a higher pH alteration which is detected by the machine (Rothberg *et al.*, 2011). PacBio machine uses single molecule real time sequencing technology. In this technology, a single DNA and a single DNA polymerase are immobilized to the bottom of a chamber, formed in a zero-mode waveguide (ZMW) structure. The chamber volume is extremely low, such that the detector can monitor any disturbance in wavelength throughout its detection area where DNA polymerase and the template stand. When a fluorescently labeled nucleotide is incorporated into the template, its dye is detected. The nucleotide releases its dye (since the dye is linked to phosphate chain of nucleotide) which diffuses out the detection area upon incorporation,

which allows the second cycle of nucleotide detection during polymerization (Eid *et al.*, 2009).

There is a new technology which has not been commercialized yet: nanopore sequencing, developed by Oxford Nanopore Technologies. In this method of sequencing, nanopores formed from pore-forming proteins or synthetic materials are the biosensors used to detect the nucleotides in a DNA strand as it passes through the pore. These nanopores are formed in an insulating membrane separating the two chambers. An ionic current is measured due to ion passage between chambers through the nanopores. When a DNA molecule passes through the pore, it causes disturbance in the current. Because each nucleotide causes a characteristic change in the magnitude of current, each nucleotide in a DNA strand can be detected while passing through the nanopore. Although the method is not commercialized yet, it is expected that it will fairly reduce the cost and time (Clarke *et al.*, 2009, Pennisi, 2012).

1.4.2. RNA-seq

In RNA-seq (shorthand for RNA-sequencing, which is actually cDNA sequencing) method, a snapshot of transcript levels at a given time and condition are determined. With this method, novel transcript discovery or transcript quantification can be accomplished (Wang *et al.*, 2009). When compared to microarray technology, which has been the traditional method for transcriptome profiling until recently, RNA-seq enables to get digital sequencing read counts rather than fluorescence intensity values. This creates a larger dynamic range in the expression quantification in RNA-seq. The method is not restricted to pre-designed probes as in microarrays, so there is no need for prior knowledge about the transcriptome of interest. By this way, novel isoforms or transcripts can be detected. Moreover, background noise is low when compared to microarrays, because there are no cross-hybridization issues (Zhao *et al.*, 2014).

As in all next-generation methods, RNA-seq protocol starts with library preparation. Unlike DNA sequencing, cDNAs are generated either from the total RNA or purified

RNA. Purification of total RNA is optional but, because rRNAs constitutes up 85% of total RNA, removal of rRNA is vital for an accurate mRNA sequencing (Morlan *et al.*, 2012). For this purpose, there are 2 common methods: rRNA removal and poly-A tail purification. In the first approach, a set of oligos targeting the rRNAs are used to capture and remove rRNAs, and in the latter approach, poly(T) oligos are used to target specifically poly(A)-tailed mRNAs (Tariq *et al.*, 2011). As expected, the second method is not convenient to be used for the quantification or detection of non-polyadenylated RNAs such as rRNAs and tRNAs.

Further steps in library preparation include mRNA fragmentation and first strand cDNA synthesis of fragmented RNAs by using random primers. Followed by second strand cDNA synthesis, those fragments are end-repaired and a single deoxyadenine nucleotide is added to form DNA having 3' dA-tails. At the next step, adapters are ligated. In order to multiplex different samples in a single lane of sequencing machine, adapters are indexed with specific barcodes which allows user to identify *in silico* the source of the read at the analysis step. At the end of library preparation, products are purified and enriched with a PCR step (Nagalakshmi *et al.*, 2010).

In the Illumina sequencing platform, adapter ligated fragments are attached to the flow cell with the help of single stranded oligonucleotides bound to the surface. Those oligos are complementary to adapter sequences. Just before sequencing, attached DNA fragments are "bridged amplified" where firstly, priming occurs at the free end of the fragment to the complementary sequence on the surface. This results in a shape like a bridge. Then, polymerase-based amplification with unlabeled dNTPs produce millions of clusters. Because imaging systems can't detect single fluorescent events yet, cluster generation is a necessity. Those clusters are sequenced along with synthesis after the addition of all four labeled and reversible terminators, primers, and DNA polymerase. At each cycle, a single fluorescent nucleotide incorporates to the newly synthesized complementary fragment. After each single base extension, emitted light is detected by high resolution imaging system and corresponding nucleotide is determined (Morozova and Marra, 2008).

Following sequencing, raw data is formed in "fastq" format. In the raw data, each read is grouped depending on their barcodes, so reads originated from different samples are bioinformatically separated (de-multiplexing). After grouping the reads, adaptor/index sequences should be removed. In the fastq format, each read has its 4 informatory lines which contain a record identifier, the sequence, and also quality scores corresponding to each base. Those scores are phred quality values assigned depending on base-calling accuracy (Ewing *et al.*, 1998). According to quality scores, manipulations could be applied on sequences and low scored bases can be trimmed for a better mapping. Table 1.3 shows phred quality scores and related error probabilities which were calculated according to the formula: "$Q = -10.\log_{10}P$" where Q is the phred quality score and P is base-calling error probability.

Table 1.3. Phred quality scores and corresponding probability of incorrect base call.

Phred Quality	**Probability of incorrect base call**	**Base call accuracy**
10	1 in 10	90%
20	1 in 100	99%
30	1 in 1,000	99.9%
40	1 in 10,000	99.99%

In a standard RNA-seq bioinformatic analysis, mapping is the next step after quality check. At this step, mapping to reference genome could be restricted to user defined regions on genome. If novel gene or transcript discovery is not an interest, the common way is to map on a known transcriptome. Other parameters, like mismatch number or mapping uniqueness, can also be adjusted. Bowtie and Tophat are two commonly used mapping software (Langmead *et al.*, 2009, Trapnell *et al.*, 2009). The latter actually uses the former's algorithmic core. Different than Bowtie, Tophat can align reads that span introns.

Following to mapping, if determination of differentially expressed genes between two or more conditions is an interest, Cuffdiff and DESeq are the commonly used software (Anders and Huber, 2010, Robinson *et al.*, 2010, Trapnell *et al.*, 2010). The output of those

programs is a list of differentially expressed genes with statistical significance levels. Researchers then typically use "gene ontology enrichment analysis" to get an insight into the biological meaning or pathways related with those differentially expressed genes.

Gene Ontology (GO) project is a collaborative initiative to unite genes under biologically meaningful representations (Gene Ontology, 2008). GO terms have a systematic representation as each term has defined relationships to other certain GO terms which can be a synonym or a parent term (relatively more general) or a child term (relatively more specific). GO terms are distributed under three major domains: Biological Process, Cellular Compartment and Molecular Function. GO database is generally used for comparison with a list of genes, generated by high-throughput experiments, to see if any GO term is enriched for input genes (Gene Ontology Enrichment Analysis). Software (some of which are web-based programs) for gene ontology enrichment analyses includes GOrilla (Gene ontology enrichment analysis and visualization tool), DAVID (Database for Annotation, Visualization and Integrated Discovery) and GSEA (Gene Set Enrichment Analysis) (Eden *et al.*, 2009, Huang da *et al.*, 2009, Subramanian *et al.*, 2005).

2. PURPOSE

Studies on IRF4 protein have established a solid background about its role in certain hematopoietic cells and hematological cancers. Recently, its role in pigmentation in melanocytes has also been identified. Our group also recognized high IRF4 expression in melanoma cell lines, besides lymphoid and myeloid malignancies, in publicly available expression databases. Preliminary results showed that melanoma cells have non-oncogenic addiction to IRF4, as in the case of B-cell origin cancers such as multiple myeloma and activated B-cell like diffuse large B-cell lymphoma.

The purpose of this thesis is to identify the IRF4 transcriptional targets and to understand which pathways and biological processes it modulates in human melanoma cell lines. For this purpose, we decided to knock-down IRF4 expression in two melanoma cell lines, via RNA interference against IRF4, for expression profiling. We chose RNA-seq method for expression profiling analysis and a bioinformatic pipeline to identify differentially expressed genes after IRF4 knock-down. These genes are expected to be transcriptionally regulated by IRF4. Given our group's recent studies suggesting a critical role in the viability of IRF4 positive melanoma cells, identification of IRF4 target genes in such an aggressive cancer type can help us to understand IRF4's role in melanoma biology and to provide a basis for generating more accurate and effective treatment options.

3. MATERIALS

3.1. General Kits, Enyzmes and Reagents

Table 3.1. List of kits, enzymes and reagents.

BCA Protein Assay Kit	Thermo Scientific, USA
DMEM	Gibco, LifeTechnologies, USA
FBS	Gibco, LifeTechnologies, USA
Plasmid Midiprep Kit	Roche, Switzerland Qiagen, Germany
EndoFree Plasmid Maxi Kit	Qiagen, Germany Macherey Nagel, Germany
First Strand cDNA Synthesis Kit	New England Biolabs (AMV), USA Thermo Scientific (RevertAid), USA
RNAstable Kit	Biomatrica, USA
Non Essential Amino Acids	Gibco, LifeTechnologies, USA
Penicillin / Streptomycin	Gibco, LifeTechnologies, USA
RNA Isolation Kits	Roche (High Pure), Switzerland Macherey Nagel, Germany
Protein Molecular Weight Marker	New England Biolabs (P7709 V), USA
Protease Inhibitor Coctail Tablets	Roche, Switzerland
Taqman Mastermix	Roche, Switzerland Life Technologies, USA
Trypsin	Gibco, LifeTechnologies, USA
Chemiluminescent HRP Substrate	Thermo Scientific, USA
Western Developer Solution, 500 ml	Ilford PQ Universal, Switzerland
Western Fixer Solution, 500 ml	Ilford Rapid Fixer, Switzerland
Phosphatase Inhibitor	Roche (PhosStop), Switzerland
K2 Transfection Reagent	Biontex Labaroteries, Germany

3.2. Biological Materials

3.2.1. Bacterial Strains

Escherichia coli STBL3 strain was used for the transformations as competent cells. It shows recombinational stability for the transformations of lentiviral vectors. The genotype of *Escherichia Coli* STBL3 strain is F– mcrB mrr hsdS20 (rB–, mB–) recA13 supE44 ara-14 galK2 lacY1 proA2 rpsL20 (StrR) xyl-5 λ– leu mtl-1.

3.2.2. Cell Lines

SKMEL-28, G-361 (human melanoma cell lines; kindly provided by Dr. Marisol Soengas), MALME-3M (human melanoma cell line; kindly provided by Dr. Ali Osmay Güre), A2058, SKMEL-5 (human melanoma cell lines; kindly provided by Yetiş Gültekin and Dr. David M. Sabatini), MEL-ST (human immortalized melanocyte cell line; kindly provided by Yetiş Gültekin and by Dr. David M. Sabatini), MCF-7 (human breast cancer cell line; kindly provided by Dr. Nesrin Özören), HEK-293FT (human embryonic kidney cell line; kindly provided by Dr. Nesrin Özören), cell lines were used in the experiments.

3.2.3. Plasmids

KH1 (lentiviral RNAi vector), and helper constructs pRSV-rev, pHCMV-G, pMDLg-pRRE (kindly provided by Dr. Nesrin Özören) were used. Small hairpin RNA triggers (shLuc and shIRF4) were sub-cloned into KH1 plasmid as double-stranded oligonucleotides by Mustafacan Ayhan (Ayhan, 2014).

For IRF4 up-regulation, pIRES2-eGFP (kindly provided by Dr. Necla Birgül-İyison) plasmid was used. GFP and IRF4 coding sequences were sub-cloned into that plasmid by Ekin Ece Erkan.

3.2.4. Primers

Table 3.2. Primers used in this study.

Primer ID	Sequence	Application
IRF4 – FAM	Probe: 5'-/56-FAM/AGCCCAGCA/ZEN/ GGTTCACAACTACAT/3IABkFQ/-3' Primer1: 5'-GGGACATTGGTACGGGATT-3' Primer2: 5'-CTACACCATGACAACGCCTTA-3'	qRT-PCR
IRF4 - HEX	Probe: 5'-/5HEX/AAGCAGGAC/ZEN/ TACAACCGCGAGG/3IABkFQ/-3' Primer1: 5'-GAGAACGAGGAGAAGAGCATC-3' Primer2: 5'-CTTTCCTTTAAACAGTGCCCAAG-3'	qRT-PCR
IRF4-FAM	Probe: 5'-/56-FAM/AAGCAGGAC/ZEN/ TACAACCGCGAGG/3IABkFQ/-3' Primer1: 5'-GAGAACGAGGAGAAGAGCATC-3' Primer2: 5'- CTTTCCTTTAAACAGTGCCCAAG-3'	qRT-PCR
GAPDH - FAM	Probe: 5'-/56-FAM/AAGGTCGGA/ZEN/ GTCAACGGATTTGGTC/3IABkFQ/-3' Primer1: 5'-TGTAGTTGAGGTCAATGAAGGG-3' Primer2: 5'-ACATCGCTCAGACACCATG-3'	qRT-PCR
GAPDH - FAM	Probe: 5'-/56-FAM/CCATCACCA/ZEN/ TCTTCCAGGAGCGAG/3IABkFQ/-3' Primer1: 5'-TACTCAGCGCCAGCATC-3' Primer2: 5'-TGTTCCAATATGATTCCACCCA-3'	qRT-PCR
MITF - FAM	Probe: 5'-/56-FAM/CCAGTGCTC/ZEN/ TTGCTTCAGACTCTGT/3IABkFQ/-3' Primer1: 5'-GATTGTCCTTTTTCTGCCTCTC-3' Primer2: 5'-CTCACCATCAGCAACTCCTG-3'	qRT-PCR
MITF - FAM	Probe: 5'-/56-FAM/AGGAGTTGC/ZEN/ TGATGGTGAGGCC/3IABkFQ/-3' Primer1: 5'-CTTGATGGATCCTGCTTTGC-3' Primer2: 5'-TTATGTTGGGAAGGTTGGCT-3'	qRT-PCR
PGK1 - HEX	Probe: 5'-/5HEX/TCATCAAAA/ZEN/ ACCCACCAGCCTTCTGT/3IABkFQ/-3' Primer1: 5'-TTTGGCACTGCTCACAGAG-3' Primer2: 5'-TTGCAAAGTAGTTCAGCTCCT-3'	qRT-PCR
TYR - FAM	Probe: 5'-/56-FAM/CCCTTTTAA/ZEN/ CATTTTCCCCTAAGCCAA/3IABkFQ/-3' Primer1: 5'-GTGTAGCCTTCTTCCAACTCA-3' Primer2: 5'-GTTCCTCATTACCAAATAGCATCC-3'	qRT-PCR

Table 3.2. Primers used in this study (cont.).

Primer ID	Sequence	Application
SQLE - FAM	Probe: 5'-/56-FAM/ /ZEN/ CATTTTCCCCTAAGCCAA/3IABkFQ/-3' Primer1: 5'-GTACAAGGATAAAGAGACTGGAGA-3' Primer2: 5'-GCCAACAAAATGAGATGATACAGA-3'	qRT-PCR
MYC - FAM	Probe: 5'-/56-FAM/TGGGCGGTG /ZEN/TCTCCTCATGG/3IABkFQ/-3' Primer1: 5'-TCCTCGGATTCTCTGCTCTC-3' Primer2: 5'-TCTTCCTCATCTTCTTGTTCCTC-3'	qRT-PCR
CDKN2A - FAM	Probe: 5'-/56-FAM/TAGCAGTGT/ZEN/ GACTCAAGAGAAGCCAGT/3IABkFQ/-3' Primer1: 5'-AGCTGTCGACTTCATGACAAG-3' Primer2: 5'-TGAGCTTTGGTTCTGCCATT-3'	qRT-PCR
BRCA2 - FAM	Probe: 5'-/56-FAM/CCACCGCCG /ZEN/CAAAAGACACC/3IABkFQ/-3' Primer1: 5'-GCGAGCTTCTGAAACTAGGC-3' Primer2: 5'-GTCACAAATCTGTCCCCTCAC-3'	qRT-PCR
NRAS - FAM	Probe: 5'-/56-FAM/TGAAACCTC/ZEN/ AGCCAAGACCAGACAG/3IABkFQ/-3' Primer1: 5'-GATACAAAACAAGCCCACGAAC-3' Primer2: 5'-GCGTATTTCTCTTACCAGTGTG-3'	qRT-PCR

3.3. Chemicals

Table 3.3. Chemicals used in this study.

Ethidium Bromide	Merck, USA
EDTA	Merck, USA
Hydrochloric Acid	Merck, USA
Sodium Chloride	Merck, USA
Bromophenol Blue Indicator	Merck, USA
Tween 20	Merck, USA
Methanol	Merck, USA
Acetic Acid	Merck, USA
LB Broth	Merck, USA
Glycine	Merck, USA
DMSO	Merck, USA

Table 3.3. Chemicals used in this study (cont.).

Ethanol	Merck, USA
Nonidet P40	Fluka, USA
Hexadimethrine bromide	Sigma Aldrich, USA
Chloroquine diphosphate	Applichem, Germany
Ammonium persulfate	Applichem, Germany
SDS	Applichem, Germany Sigma Aldrich, USA
Ampicilllin	Applichem, Germany
Acrylamide	Sigma Aldrich, USA
Sodium Deoxycholate	Sigma Aldrich, USA
N,N'-Methylenbisacrylamide	Sigma Aldrich, USA
DEPC-treated water	Fisher Scientific, USA
Agarose	Sigma Aldrich, USA
Kanamycin	Applichem, Germany
Glycerol	Merck, USA
2-Mercaptoethanol	Merck, USA
TEMED	Merck, USA
Tris-Cl	Merck, USA
Calcium Chloride	Merck, USA
BSA	Applichem, Germany
Saponin	Sigma Aldrich, USA
Tris-Base	Sigma Aldrich, USA
Ponceau S powder	Applichem, Germany
Paraformaldehyde	Sigma-Aldrich, USA (P6148)
Isopropanol	Merck, USA
Milk Powder	Pinar, Turkey
HEPES	Gibco Invitrogen, USA

3.4. Buffers and Solutions

Table 3.4. Buffers and solutions used in this study.

10X SDS Running Buffer	1% SDS 1.92M Glycine 250 mM Tris-Base

Table 3.4. Buffers and solutions used in this study (cont.).

10X SDS Running Buffer	1% SDS 1.92M Glycine 250 mM Tris-Base
10X Transfer Buffer	1.92M Glycine 250 mM Tris-Base
1X Transfer Buffer	10% 10X Transfer Buffer 20% Methanol
4X Protein Loading Dye	200 mM Tris-Cl (pH: 6.8) 8% SDS 40% Glycerol 4% β-mercaptoethanol 50 mM EDTA 0.8% Bromophenol Blue
Cell Lysis Buffer	150 mM NaCl 50 mM Tris (pH: 8.0) 0.1% SDS 0.5% Sodium deoxycholate 1.0% NP-40
10% SDS-PAGE Gel, Resolving Part (20ml)	8 ml ddH2O 6.66 ml 30% Acrylamide/Bisacrylamide mix 5ml 1.5M Tris, pH: 8.8 200 µl 10% SDS 120 µl 10% APS 20 µl TEMED
4% SDS-PAGE Gel, Stacking Part (8ml)	7788 µl ddH2O 1072 µl 30% Acrylamide/Bisacrylamide mix 1ml 1 M Tris, pH: 6.8 200 µl 10% SDS 50 µl 10% APS 10 µl TEMED
10X TBS	200 mM Tris-Cl (pH: 7.6) 1.5 M NaCl
1X TBS-T	50 mM Tris-Base (pH: 7.4) 150 mM NaCl 0.1% Tween 20
Paraformaldehyde (4%)	1 g Paraformaldehyde 25 ml distilled water
5% Blocking Solution	5% BSA (w/v) in 1X TBS-T 5% Milk Powder (w/v) in 1X TBS-T

Table 3.4. Buffers and solutions used in this study (cont.).

5% Blocking Solution	5% BSA (w/v) in 1X TBS-T 5% Milk Powder (w/v) in 1X TBS-T
10X PBS	1,37 M NaCl 270 mM KCl 80 mM NaH2PO4 20 mM KH2PO4
1X PBS+	1X PBS 0.5% BSA
1X PBS+S	1X PBS 0.5% BSA 0.3% Saponin
Freezing Medium	1X DMEM 20% FBS 1X Pen/Strep 100 μM MEM-NEAA 10% DMSO
400X Choloroquin	10 mM Choloroquin
1000X Polybrene	4 mg/ml Polybrene
2X HBS	50 mM HEPES (pH: 7.0) 280 mM NaCl 1.5 mM NaH2PO4
LB Medium	10 g/L Tryptone 5 g/L NaCl 5 g/L Yeast Extract
1000X Ampicillin	100 mg/ml in ddH2O
1000X Kanamycin	50 mg/ml in ddH2O

3.5. Antibodies

Table 3.5. Antibodies used in this study.

Name	**Species**	**Dilution**	**Source**
Anti-Actin	Rabbit	1:2500	4967S, Cell Signaling
Anti-IRF4 X (M-17)	Goat	1:5000	Sc-6059, Santa Cruz
Anti-MITF	Mouse	1:3000	Ab12039, Abcam
Anti-total-Erk	Rabbit	1:2500	4695S, Cell Signaling
Anti-p-Erk	Rabbit	1:1000	4270S, Cell Signaling

Table 3.5. Antibodies used in this study (cont.).

Anti-total-Akt	Rabbit	1:2500	9272S, Cell Signaling
Anti-p-Akt (Thr308)	Rabbit	1:1000	2965S, Cell Signaling
Anti-p-Akt (Ser473)	Rabbit	1:1000	9271S, Cell Signaling
Anti-Rabbit-HRP	Mouse	1:2500	7074S, Cell Signaling
Anti-Goat-HRP	Rabbit	1:2500	Sc-2768, Santa Cruz
Anti-Mouse-HRP	Horse	1:2500	7076S, Cell Signaling
Normal Goat IgG	Goat	-	Sc-2028, Santa Cruz
Anti-Goat-IgG-PerCP	Goat	-	Sc-45091, Santa Cruz
Anti-Goat-IgG-PE	Goat	-	Sc-3743,Santa Cruz

3.6. Disposable Labware

Table 3.6. List of disposable labwares used in this study.

Western Blotting Paper	Whatman, UK
Parafilm	Brand, Germany
Scalpel	Swann-Morton, UK
Centrifuge Tubes, 15 ml	Vwr, USA
Centrifuge Tubes, 15 ml	Vwr, USA
Serological pipette, 5ml	Tpp, Switzerland
Serological pipette, 10ml	Tpp, Switzerland
Serological pipette, 25ml	Tpp, Switzerland
Pipette Tips, filtered	Biopointe, USA
Pipette Tips, bulk	Biopointe, USA
Microcentrifuge tubes	Axygen, USA
PCR Tubes, 0.2 ml	Axygen, USA
Medical Gloves	Vwr, USA Broche Medikal, Turkey
Syringe Filters	Sartorius, Germany
Cryovial	Tpp, Switzerland
Cell Culture Plates, 10 cm	Tpp, Switzerland
Cell Culture Plates, 6-well	Tpp, Switzerland
Cell Culture Plates, 96-well	Tpp, Switzerland
Cell Culture Flasks, $75cm^2$	Tpp, Switzerland
Insulin Syringes, 1 ml	Vwr, USA
Syringe, 10ml	Becton Dickinson, USA

Table 3.6. List of disposable labwares used in this study (cont.).

PS Test Tubes, 5 ml	Becton Dickinson, USA Isolab, Germany
Glass Pasteur Pipette, 230 mm	Witeg, Germany
Chemiluminescent Detection Film	Roche, Switzerland
96 well plates for qRT-PCR	Thermo Scientific, USA

3.7. Equipments

Table 3.7. List of equipment used in this study.

Beaker, 100 ml	Duran, Germany
Beaker, 600 ml	Duran, Germany
Erlenmeyer, 250 ml	Duran, Germany
Erlenmeyer, 500 ml	Duran, Germany
Bottle, 1000 ml	Vwr, USA
Bottle, 500 ml	Vwr, USA
Bottle, 100 ml	Vwr, USA
Forceps	RSG Solingen, Germany
Magnetic Stirring Bar	Vwr, USA
Cryobox	Tenak, Denmark
Autoclave Indicator Tape	Llg, Germany
Measuring Cylinder 100 ml	Kartell, Italy
Measuring Cylinder 250 ml	Kartell, Italy
Measuring Cylinder 1000 ml	Kartell, Italy
pH Meter	Hanna, USA
Microtube Racks	Vwr, USA
Electronic Balance	Sartorius AY123, Germany
Microcentrifuge	Vwr Galaxy Ministar, USA
Horizontal Electrophoresis	Cleaver Scientific Multi Sub Mini, UK
Micropipettes	Cleaver Scientific, UK Gilson Pipetman Neo PCR Kit, USA Axygen, USA

Table 3.7. List of equipment used in this study (cont.).

Heat Block	Cleaver Scientific EL-01, UK
Pipettor	Greiner Labopet 240, Germany
Vortex	Vwr, USA
Vertical Electrophoresis	Cleaver Scientific Omni-page Mini, UK
Centrifuges	J2-21, Beckman Coulter, USA Allegra X-22, Beckman Coulter, USA 5415R, Eppendorf, USA
Rotor	Beckman Coulter JA-14, USA
Cell Culture Incubator	Binder C-150, Germany
Documentation System	GelDoc XR System, Bio-Doc, Italy
Flow Cytometer	FACSCalibur , Becton Dickinson, USA
Freezers	-20°C, Ugur UFR 370 SD, Turkey -80°C, Thermo Scientific TS368, USA -150°C, Sanyo MDF1156, Japan
Microplate Reader	680, Biorad, USA
Microscopes	Inverted Microscope, Nikon Eclipse TS100, Japan Fluoroscence Microscope, Observer Z1, Zeiss, Germany
Thermal Cycler	Antarus MyCube ANT101, USA
Power Supply	Vwr, USA
Real Time PCR Machine	Thermo Scientific Piko Real 96, USA
Shaker	VIB Orbital Shaker, InterMed, Denmark Vwr Mini Orbital Shaker, USA
Spectrophotometer	NanoDrop 1000, USA
Stirrer - Heater	Dragonlab MS-H-S, China
Rotator	Grant Bio Multifunctional Rotator PTR-35, UK
Safe Light	Kodak Model B, USA
Safe Light Filter	Kodak GBX-2, USA
Hybridization Oven	Thermo Scientific Hybaid Shake'n'Stack, USA
Refrigerator	4°C, Ugur USS 374 DTKY, Turkey
Refrigerated Vapor Trap	Thermo Scientific SPD111V, USA
Oil-free Gel Pump	Thermo Scientific Savant VLP110, USA
Vacuum Pump Oil Filter	Thermo Scientific VPOF110, USA
SpeedVac	Thermo Scientific SPD111V, USA
Carbon dioxide Tank	Genc Karbon, Turkey
Ice Maker	Brema, Italy Scotsman Inc. AF20, Italy
Autoclave	Model ASB260T, Astell, UK

Table 3.7. List of equipment used in this study (cont.).

Dishwasher	Miele Mielabor G7783, Germany
Cold Room	Birikim Elektrik Soğutma, Turkey
Stella	Raytest, Germany
Freezing Container	Nalgene, USA
Oven	Nüve KD200, Turkey
Local Server with 5 x Quad-Core Intel Xeon Processor	HP, USA

4. METHODS

4.1. Cell Culture

4.1.1. Cell Line Maintenance

Cell lines used in this study were grown in DMEM - high glucose which contains the additives of 10% FBS, 1% penicillin/streptomycin and 1% non-essential amino acids. They were incubated in an incubator with the following conditions, 5% CO_2 and 37°C. To passage cells, old medium was aspirated and cells were washed with 1X PBS. Trypsin (0.05%) was used to detach the cells in 37°C with a 5 minute incubation. After detachment was complete, equal amount of DMEM was added on the trypsinized cells to deactivate the trypsin activity, and they were transferred into a 15ml falcon for the centrifugation at 500g for 5 min. Medium-trypsin mix aspirated and cells were resuspended in a proper volume of fresh DMEM by pipetting. Proper ratio of cells were seeded back into new flasks or plates.

In order to stock the cells for long periods; after cells were trypsinized and centrifuged, old medium was aspirated and cell pellet was resuspended in freezing medium (Table 3.4). If 10-cm cell culture plate was fully confluent, it was divided into 5 cryovials which contains 1ml of cell and freezing medium mix. Cryovials were placed into Nalgene Freezing Container filled with isopropanol. Container was kept at -80°C for a day and then cryovials were transferred into cryoboxes at -150°C.

In order to thaw the cells from cell line stocks which are kept at -150°C freezers; one vial for one 10-cm cell culture plate was thawed quickly in water bath. Immediately, after thawing was complete, they were transferred into 15ml falcon tubes previously filled with 5 ml of fresh and warm DMEM. Cells were centrifuged at 500g for 5 min. After aspirating the medium to remove DMSO, cells were resuspended and seeded into proper plates.

4.1.2. Transfection of Lentiviral Vectors for Virus Production by Calcium Phosphate Method

Transfection of lentiviral vector and helper plasmids (pRSV-rev, pHCMV-G and pMDLg-pRRE) to HEK293FT cells were performed by calcium phosphate method for virus production. The method is based on combination of positively charged calcium and DNA mix with phosphate solution (Graham and van der Eb, 1973). When added onto cells, the precipitate is taken up by the cells.

The day before transfection, HEK cells were passaged into 10 cm plates with a 70% confluency. At the day of transfection, chloroquine was added into fresh medium with a 25μM final concentration. 6μg of lentiviral plasmid and 6μg of each helper plasmids were mixed with 62.5μl of 2M $CaCl_2$ (125 mM), and then dH_2O was added to a final volume of 500μl. 500μl of 2X HBS was added onto DNA - $CaCl_2$ mix in a dropwise manner and the solution was aerated by pipetting. Mix was incubated for 5 minutes at room temperature and later on, it was added drop by drop onto HEK293FT cells. Medium of each plate was changed after 6 hours.

4.1.3. Harvesting Virus Containing Medium

Efficiency of transfection was determined after 2 days under the fluorescent microscope with the help of GFP marker in the lentiviral vector. If transfection was successful, medium of each HEK cell plates were passed through a 0.45μm filter. Collected medium was aliqouted into 2 ml tubes in 1 ml volumes and stored in -80°C.

4.1.4. Lentiviral Transduction

A day before transduction, cells to be transduced were passaged to a confluency of 60%. At the day of transduction virus containing medium was thawed and mixed with polybrene with a final concentration of 4μg/ml. Mix was combined half and half with fresh medium and added to the cells.

4.1.5. Transient Transfection of Episomal Vectors with K2 Transfection System

Transfection by K2 system is a lipofection method which uses cationic lipids to form liposomes around DNA by "K2 Transfection Reagent". Another solution, K2 Multiplier, decreases the detectability of DNA by transfected cell to avoid immune reactions by the transfected cells.

Two hours before transfection, 10µl K2 Multiplier was mixed with 500µl of fresh medium (serum containing DMEM) and added onto cells in a 24-well plate. If there were multiple wells, mastermix was prepared for K2 Multiplier - fresh medium mix. 30 minutes before transfection, plasmids should be diluted in a proper concentration, preferentially as 500ng/µl to avoid any pipetting mistakes in further steps. In a 96-well plate; solution A, containing 30µl of serum-free medium and 0.5µg plasmid, and solution B, containing 30µl of serum-free medium and 3µl of K2 Transfection Reagent were prepared in separate wells. At this step, they should not be kept in separate solutions for longer than 5 minutes. In the following step, solution A, containing the plasmid was added onto solution B, containing the K2 Transfection Reagent and mixed by pipetting. Mixed solution was incubated for 15 to 20 minutes and then, it was added onto cells in a drop-wise manner. 6 hours later, medium of the wells were refreshed with serum containing fresh DMEM. Transfection efficiency was determined by flow cytometry analysis, 2 days after transfection.

4.2. GFP Competition

GFP competition procedure was started by transducing cells with shIRF4 or shLuc (negative control) expressing lentiviruses. After 2 days, trypsinized and detached cells were transferred into separate 5 ml polystyrene tubes. One fourth of the cells were taken back into wells to perform next round of GFP competition experiment and fresh medium was added to deactivate trypsin effect. At this step, untransduced cells were also taken into a tube to determine the GFP threshold during flow cytometry analysis. All tubes were firstly centrifuged at 500g for 5 minutes and then medium was poured into viral waste carefully. Cell pellet at the bottom of the tube was resuspended in 1ml 1X PBS and vortexed vig-

orously as the solution should be cell aggregate-free for a proper flow cytometry analysis. At the step of flow cytometry analysis (done by BD FACScalibur machine and CellQuestPro Software), firstly, untransduced cells were analyzed to determine the signal of self-fluorescence at FL-1 detector of FACScalibur which is for GFP signal. When analyzing the cells transduced with shIRF4 or shLuc, percentage of GFP-containing cells were determined based on the threshold, which were defined by self-fluorescence GFP intensity value of untransduced cells. Same procedure was repeated in 3-4 day intervals depending on the confluency of the cells.

4.3. Molecular Biological Techniques

4.3.1. Plasmid Isolation

Plasmids isolated were always used either for calcium phosphate transfection to HEK293FT cells to produce virus, or used for K2 Transfection System to transfect desired cells transiently. Since such experiments require a pure plasmid batch, isolations were performed with endotoxin-free maxi plasmid isolation kits. For the plasmid isolation purposes either QIAGEN EndoFree Plasmid Maxi Kit or Macharey-Nagel NucleoBond Xtra MaxiPlus EF was used according to the manufacturer's instructions.

4.3.2. Isolation of Total RNA

Cells were detached by trypsinization after washing with PBS. Detached cells were transferred into a 15ml falcon tube along with the same volume of fresh medium to deactivate the effect of trypsin. Falcon tube was centrifuged at 500g for 5 minutes and medium was aspirated. Afterwards, cells were resuspended in 2 ml of 1X PBS for washing. Centrifugation was repeated and cell pellet was lysed by lysis buffer, supplied with the kit. Roche High Pure RNA Isolation kit or Macherey-Nagel NucleoSpin RNA Isolation kit was used according to the manufacturer's instructions. Total RNA was stored at -20°C for short periods (1-2 weeks), and for longer periods, samples were kept at -80°C.

4.3.3. Preservation of Total RNA by RNAstable

Total RNA samples extracted for library preparation of RNA-seq step were processed with RNAstable Kit (Biomatrica) to preserve the integrity during shipping in room temperature. The procedure was performed according to manufacturer's instructions. Briefly, 1.1 mg total RNA in 11ul volume was added into RNAstable tubes which contain RNAstable as a coating at the bottom. Following mixing with RNAstable, solutions for each sample were transferred into 0.2 ml PCR strips. Samples were dried by SpeedVac (Thermo Scientific SPD111V) in 30 minutes. Tubes were kept at room temperature in sealed moisture barrier foil bags till shipping.

4.3.4. cDNA Synthesis

Reverse transcription and cDNA synthesis were performed with RevertAid First Strand cDNA Synthesis Kit (Thermo Scientific) according to the manufacturer's instructions. During first strand synthesis, oligo-dt and random hexamer primers were used separately, or at certain experiments they were mixed in half to half volumes. Final volume of 20µl was completed to 200µl by adding 180µl of nuclease free distilled water. cDNA products were kept at -20°C for further use.

4.3.5. Real Time Quantitative PCR (RT-qPCR)

Master-mix, which includes 5µl TaqMan Gene Expression Master Mix, 0.5µl primer/probe mix and 2.5µl of nuclease free distilled water for 1 well of 96-well qPCR plate, was prepared. Primer-probe mix and TaqMan® Gene Expression Master Mix were kept in dark during the experiment as they contain fluorescent dyes. After master-mix was distributed into each well in 8µl volumes, 2µl of corresponding cDNA templates were added where each cDNA batch was diluted in 1:50 from cDNA stocks. Adhesive sealing films were attached onto the 96-well qPCR plate surface. Plate was vortexed carefully and centrifuged at 500g for 2 minutes. This step ensures that all the solution is at the bottom of the wells after vortexing. Plate was placed into PikoReal 96 real time PCR machine and proto-

col was set up as starting with initial denaturation at 50°C for 2 minutes then at 95°C for 10 minutes. AmpliTaq Gold DNA Polymerase in the master mix is designed for hot start PCR so it is also activated during the initial denaturation step. As next steps, protocol includes 40 cycles of 95°C for 15 seconds incubation and annealing-elongation incubation at 60°C for 1 minute. At the end of qPCR, automatic threshold determined by the software for the fluorescent signal was used. Depending on the threshold, Ct (threshold cycle) values were determined by the program, so Ct values are inversely proportional to the amount of target cDNA in the sample. At the step of analysis, Ct values are subtracted from 40 (total cycle number) and the result is used as the exponent of 2 by assuming that at each cycle nucleic acid amount of target cDNA is doubled. For several primer/probe pairs, selected randomly, we showed the high amplification efficiency (90%-105%) (data not shown). Because more than 3 technical replicates are used in the design of experiment, median value of "Ct over 2" was taken as the representative. Median value of target gene's expression data was normalized to the median value of normalization gene's expression data. Standard errors were calculated with the formula of (Standard Deviation of Expression Values from "n" Sample) / ("n"^0.5).

4.3.6. Agarose Gel Electrophoresis

Agarose gel was prepared as 1% of weight to volume ratio in 1X TAE buffer in a beaker. Solution was boiled at a microwave until agarose was completely dissolved. 3µl of ethidium bromide was added for a volume of 40ml. Samples, mixed with loading dye to a final concentration of 1x, were loaded into wells and gel was run at 100V for half an hour. Detection was done by Bio-Rad GelDoc XR System under UV.

4.4. Western Blotting

4.4.1. Cell Lysis and Protein Extraction

Medium of the cells to be lysed were aspirated and cells were washed with PBS once. Adherent cells were trypsinized and transferred to a 15ml falcon tube with the same amount of fresh DMEM. After centrifugation at 500g for 5 minutes, medium was aspirated carefully, and cells were washed with PBS twice to completely remove trypsin. RIPA buffer was mixed with 50X protease inhibitor just before addition on to the cells. 500µl of protease inhibitor containing RIPA buffer was used to lyse cells from an almost confluent 6-well plate. Following the addition of the lysis buffer, the solution should be mixed harshly by pipetting to lyse the cell pellet efficiently. Protein lysate was transferred into a 1.5ml tube, then, was kept in ice for 30 minutes and syringed with a 22-gauge needle afterwards. Lysate was centrifuged at 14,000g for 15 minutes at 4°C. By leaving precipitates in the tube, total protein lysate was transferred into a new 1.5ml micro centrifuge tube.

4.4.2. BCA Assay for Protein Concentration Determination

Pierce BCA Protein Assay Kit was used for the determination of protein concentrations. BSA standards in the concentrations of 125, 250, 500, 750, 1000, 1500 and 2000 µg/ml were prepared from the stock given in the kit by serial dilution in 1X PBS. If the cell lysates were taken from a confluent 6-well plate, they were diluted as 1:5 to get an OD in the range of standards. All the samples were prepared in at least 3-replicates. BCA solution was prepared by mixing 150µl of Reagent A and 3µl of Reagent B for each sample. After BCA solution was prepared as a mastermix, 150µl per well was distributed into a 96-well plate. 5µl of standards and diluted lysates were added into corresponding wells. Plate was kept on ice while adding the protein lysates. Plate was incubated at 37°C for 30 minutes and absorbance values were determined at 562 nm on the plate reader. Blanks were subtracted from median OD values of samples and standards. Standard blank is the PBS and sample blank is the RIPA buffer. To calculate concentration of samples, firstly, a standard curve was prepared in Microsoft Excel for standards by pushing the line to cross from (x,y) = 0,0 where x is the concentration and y is the absorbance value. Formula of the standard

curve was used to calculate the samples' concentrations. Results were multiplied by 5 as they were in a 1:5 dilution.

4.4.3. Preparation of Protein Samples and SDS Gel Electrophoresis

Protein lysates were prepared by adding 4X laemni loading dye and boiling the mix at 95°C for 5 minutes. Those lysates were loaded into the wells of SDS-gel prepared at Cleaver Omni-Page Gel Casting System where resolving gel (10%) polymerized at the bottom and stacking gel (4%) at the upper part (Table 3.4). The amount of lysates loaded were calculated according to the BCA assay results and the lowest concentrated protein lysate was the limiting factor for how much protein would be loaded into each well. Lysates were loaded into the wells in the vertical gel electrophoresis chamber, filled with 1X running buffer and the system was run at 100V until the loading dye gets into resolving gel, and then at 120V until the loading dye reached to the end of the gel.

4.4.4. Blotting - Transfer from SDS Gel to PVDF Membrane

Blotting papers and PVDF membrane, cut in the size of the blotting pad, were prepared. PVDF membrane was activated in methanol for 10 seconds, then washed in dH_2O for 1 minute and kept in 1X transfer buffer until it was placed in the blotting system. Meanwhile, glasses of running apparatus were separated from each other, by leaving the SDS gel on one of the glasses. Under distilled water the stacking part was removed and the gel was placed on the blotting paper. Under the blotting paper, there was one of the blotting cassettes and one blotting pad. Membrane was placed on the gel by paying attention not to leave any bubbles between blotting paper and gel, and between gel and membrane for an efficient transfer. For that purpose, those steps were performed in a container partially filled with transfer buffer, so bubbles could be removed easily. Another blotting paper and blotting pad was placed onto the membrane. After other part of the cassette was placed on the pad, clips were closed to compress the system. Transfer cassette was placed into the transfer chamber in the right orientation. Membrane should be at positive, and gel should be at the side of negative pole because proteins are negatively charged due to SDS. Transfer was performed at 250 mAh for 1hour and 45min. After transfer was complete,

membranes were cut to a smaller size depending on the size of the protein of interest. Membranes were washed with 1X TBS-T (0.1% Tween 20) for several times to remove methanol.

4.4.5. Staining - Antibody Incubations

Prior to staining with antibodies, the membrane was blocked for 1 hour at room temperature with 5% BSA (w/v) prepared in TBS-T. Membrane was incubated overnight at 4°C, in certain dilution of the desired antibody, also prepared in 5% BSA solution. Membrane was washed 3 times with TBS-T with 5 minute intervals before incubation with HRP linked secondary antibody, diluted in TBS-T. Secondary antibody incubation was performed at room temperature for 2 hours. Membranes were washed 3 times with TBS-T in 5 minute intervals. Blocking, washing and antibody incubations were performed on a benchtop orbital shaker.

4.4.6. Chemiluminescence Detection

ECL (enhanced chemiluminescent solution) was prepared by mixing 1 volume of peroxide and 1 volume of substrate in a Falcon tube wrapped with aluminum foil to protect from light. Before placing the membrane on a glass plate for detection of luminescent signal at imaging system (Stella), membrane was incubated in the ECL solution in a small-size container for a minute, paying attention to keep it away from light. Then, membrane placed on a glass plate was put in Stella and exposure duration was determined by the help of Xstella software. Detection was done after focusing was adjusted.

4.5. Intracellular Flow Cytometry

Cells to be analyzed were transferred into 3 separate 5 ml polystyrene tubes after washing and trypsinization steps. One tube should include about 500,000 cells. Among 3 tubes; one of them was used to adjust the threshold (no staining), another for normal serum treatment as the negative control (control antibody treated), and one of the tubes was pre-

pared to get the actual signal from target protein (test tube). Cells in each tube were centrifuged at 500g for 5 minutes to remove trypsin solution. Cells were washed 3 times with cold PBS+, where they were centrifuge at each step and PBS+ were discarded. After the last wash, 500µl 2% PFA was added drop by drop while the tube was being vortexed in a slow mode. Tubes were incubated for 10 minutes at room temperature and then they were washed with PBS+ once and resuspended in PBS+S. At this step, the tube which would be used to determine the threshold for dye signal intensity was ready for the analysis and it was kept on ice till the end of the procedure. Other tubes were incubated for 10 minutes in PBS+S and the solution was removed after each centrifugation step. 500µl of primary antibody solution, diluted in PBS+S, was added on the cells. Dilutions were prepared according to manufacturer's instructions, by paying attention to add same amount of normal serum IgG and primary antibody. Tubes were incubated in primary antibody solution for 15 minutes and then washed with PBS+S twice. After the last wash, 500µl of secondary antibody diluted in PBS+S in 1 to 200, was added onto the cell pellet. Cells were incubated with secondary antibody solution for 15 minutes at room temperature. After secondary antibody solution additions, tubes were kept in dark. Cells were washed once with PBS+S and twice with PBS+ afterwards. At the last step, they were resuspended in PBS+ to be analyzed at flow cytometry.

4.6. RNA-seq

Following total RNA extraction and integrity control with an Agilent Bioanalyzer 2100 (performed at Department of Chemical Engineering, Bogazici University), RNA samples were sent to UCLA (University of California, Los Angeles) Genomics Core. TruSeq RNA Sample Preparation Kit was used for library preparation step. Briefly, library preparation starts with purification of mRNA by poly-A selection using oligo-dT attached magnetic beads. Following purification, mRNAs are fragmented and copied into first strand cDNA by using random hexamers. Then second strand cDNA synthesis is performed. End repair and addition of adenine base follows the procedure. At the end, adaptors with barcodes are ligated and products are enriched with PCR.

Samples from both cell lines were sequenced as single-end 50bp reads. HiSeq2000 (Illumina) was used for sequencing of SKMEL-28 samples and HiSeq2500 (Illumina) in Rapid Run Mode was used for sequencing of SKMEL-5 samples.

4.7. Bioinformatic Methods for RNA-seq Analysis

4.7.1. Data Quality Control by FastQC via Galaxy Web Server

Fastq files, containing all the sequencing reads, for each sample were uploaded into Galaxy Server (http://galaxyproject.org/). FastQC program (http://www.bioinformatics.babraham.ac.uk/projects/fastqc/) was selected from the "NGS: QC and manipulation" menu and run with default parameters.

4.7.2. Fetching Sequenced Total Read Number From a FastQ File

All of the reads sequenced for each sample are stored in separate fastq files. Command line to learn how many reads there are in a fastq file is shown below:

```
> cat <raw_data>.fastq | paste - - - - | wc -l
```

4.7.3. Splitting FastQ Files

Fastq files were splitted for SKMEL-28, to decrease the number of mapped reads to the level of SKMEL-5 mapped read number. In order to do that, each fastq file was split into parts by using number of lines in the file. Representation of a single read by 4 lines should be taken into consideration when determining the line number to be split. Command below shows how to split a fastq file with indicated number of lines:

```
> split -l <# of lines> <name>.fastq
```

Outputs of this command line are files named xaa, xab, xac etc. File named xaa can be used in further steps by renaming:

```
> mv xaa <name>.fastq
```

4.7.4. Mapping Reads to the Human Genome by Tophat Software

Tophat Software v2.0.8b (http://ccb.jhu.edu/software/tophat/index.shtml) was installed to the local server of the department, which runs with Ubuntu (12.04.1 LTS) operating system. It was run remotely via PuTTY software (http://www.chiark.greenend.org.uk/~sgtatham/putty/download.html). Command line to run the program with selected parameters (http://ccb.jhu.edu/software/tophat /manual.shtml) in linux, is given below:

```
> tophat -p 8 -o <output_file_name> -T -G <path_to_the_.gtf file> --no-novel-juncs <path_to_the_human_genome_file> <path_to_the_fastq_file>
```

"-p" designates the number of processors to be used for the run and it was determined as 8, which is the maximum capacity of the computer.

"-o" allows to define the name of the output file.

"-T" option restricts the mapping only to the defined transcriptome which is also defined by the user. This transcriptome file is in the .gtf format and was downloaded from "UCSC Table Browser". The file is under the "Mammal" clade, "Human" genome, "Feb. 2009 (GRCh37/hg19)" assembly, "Genes and Gene Prediction Tracks" group, "RefSeq Genes" track, and "refFlat" table. "GTF" was selected as the output file format. Additionally, this parameter can only be used when the transcriptome file path is defined with "-G" option.

"-G" allows user to define the path of transcriptome file.

"--no-novel-juncs" is an option which restricts junctional alignments to the defined transcriptome. The parameter is valid when only used with "-G" option.

All other options are used in default if not defined in the command line.

Human genome sequence index, which is the reference genome file, was downloaded from Illumina's iGenomes collection (http://support.illumina.com/sequencing/ sequencing_software/igenome.ilmn) with the UCSC source and hg19 build.

4.7.5. Selection of Uniquely Mapped Reads

Tophat does not have a parameter to discard sequencing reads with ambiguous mapping (i.e., hitting multiple locations in the genome/transcriptome). In default options, it allows a read to map up to 20 different locations (-g 20) in the genome (or in the transcriptome if defined). We used the command line below to select uniquely mapped reads after Tophat analysis from files in bam format:

```
> samtools view -bq 50 -o <file_name> accepted_hits.bam
```

"-b" is used to get the output in bam format.

"-q" is used to skip alignments with MAPQ smaller than defined.

MAPQ is mapping quality and it is defined in 4 different values with the formula of "$-10\log_{10}$ Probability(mapping position is wrong)". A value of 50 indicates that the mapping is unique.

4.7.6. Mapping Statistics by SAMtools

SAMtools is a program to acquire information from or perform manipulations on the files in bam or sam format (Li *et al.*, 2009). Software was installed to the local server. Input files were the "accepted_hits.bam" (filtered for uniquely mapped reads) files. Command line to learn the read number in a bam file is given below:

```
> samtools flagstat "<name>.bam"
```

4.7.7. Quantification of Mapped Reads and Determination of Differentially Expressed Genes by Cuffdiff Software

Cuffdiff software, as a part of Cufflinks v2.1.1 (http://cufflinks.cbcb.umd.edu/index.html), was installed to the local server. Command line to run the program in linux is below:

```
> cuffdiff -p 8 -o <output_file_name> -L KD,WT <path_to_the_.gtf file> <path_to_the_KD_first_replicate> <path_to_the_KD_second_replicate><path_to_the_KD_third_replicate> <path_to_the_WT_first_replicate> <path_to_the_WT_ second_replicate><path_to_the_WT_third_replicate>
```

"-p" designates the number of processors to be used for the run and it was determined as 8, which is the maximum capacity of the computer.

"-o" allows user to define the name of the output file.

"-L" allows user to label the samples. KD stands for the shIRF4 transduced samples and WT stands for the shLuc transduced samples.

GTF file is the same as used in Tophat run.

For the further processes, only "genes.*" output files were used.

4.7.8. Visualization of Cuffdiff Output by CummeRbund Software

The statistical software package R v3.0.1 (R Core Team, 2014) was downloaded and installed to run CummeRbund R package (Goff *et al.*, 2012). To set up the package, command lines below were used;

```
> source("http://bioconductor.org/biocLite.R)
```

```
> biocLite("cummeRbund")
```

The package was loaded with the following command;

```
> library (cummeRbund)
```

Then cuffdiff output was loaded with a database name of "cuff":

```
> cuff <- readCufflinks()
```

Plotting the density plot requires the command below:

```
> csDensity(genes(cuff), "KD", "WT"))
```

Plotting the scatterplot requires the command below:

```
> csScatter(genes(cuff), 'KD', 'WT')
```

Plotting a dendrogram requires the command below:

```
> dend <- csDendro(genes(cuff),replicates=T)
```

Plotting a MvsA plot requires the command below:

```
> m <- MAplot(genes(cuff),"KD","WT")
```

4.7.9. Quantification of Mapped Reads by HTSeq

DESeq is another tool to be used for the determination of differentially expressed genes. Unlike Cuffdiff which uses FPKM values, DESeq uses raw count numbers in differential analysis. After Tophat run, we used HTSeq (v0.6.1) to generate a table indicating which gene has how many counts for each biological replicate and condition.

Command line to run HTSeq in Windows PowerShell is given below:

```
> python -m HTSeq.scripts.count -s no -m intersection-strict <.bam file> <.gtf file> > <name of the output>
```

4.7.10. Determination of Differentially Expressed Genes by DESeq Software

DESeq (v2.14) is a bioconductor package, running in R platform. Installation is accomplished with the command line below, in R:

```
> source("http://bioconductor.org/bioclite.R")
```

```
> bioclite("DESeq2")
```

Following commands were used in the further steps:

```
> library('DESeq2')

> directory < "<path_to_the_working_directory_ containing_HTSeq_outputs>"

> sampleFiles < grep("sh",list.files(directory),value=TRUE)

> sampleCondition <- c("KD","KD","KD","WT","WT","WT")

> sampleTable <- data.frame(sampleName=sampleFiles, fileName=sampleFiles, condition=sampleCondition)

> ddsHTSeq <- DESeqDataSetFromHTSeqCount(sampleTable=sampleTable, directory=directory, design=~condition)

> colData(ddsHTSeq)$condition <- factor(colData(ddsHTSeq)$condition, levels=c("KD","WT"))

> dds<-DESeq(ddsHTSeq)

> res<-results(dds)

> res<-res[order(res$padj),]
```

```
> mcols(res,use.names=TRUE)
```

```
> write.csv(as.data.frame(res),file="name")
```

4.7.11. Venn Diagrams

Venn Diagrams were created by "Venn Diagram Plotter" (http://omics.pnl.gov/software/venn-diagram-plotter)

4.7.12. Correlation Graphs

Correlation graphs were plotted and corresponding Spearman correlation values were calculated by GraphPad Prism 6. Correlation was chosen under XY Table & Graphs menu.

4.7.13. Kaplan-Meier Plots

Kaplan Meier Plots were plotted by BRB-Arraytools (Zhao and Simon, 2008) in Microsoft Excel.

5. RESULTS

5.1. Detection of Basal IRF4 Expression in Melanoma Cell Lines

IRF4 expression in human melanoma cell lines was verified by RT-qPCR and western blotting after a comprehensive analysis of publicly available gene expression databases (Ayhan, 2014). Here, we replicated those results by intracellular flow cytometry, showing IRF4 protein levels in cell lines we have been using (Figure 5.1).

When fluorescent signals detected from IRF4 antibody and normal goat IgG treated counterparts (negative control) are compared; among the cell lines analyzed, 4 of 5 human melanoma cell lines (SKMEL-28, SKMEL-5, G-361 and A-2058) have high endogenous IRF4 protein levels (Figure 5.1). On the other hand, 1 immortalized human melanocyte line (MEL-ST), 1 melanoma cell line (MEWO) and 1 human embryonic kidney cell line (HEK-293) has no detectable IRF4 protein.

We also replicated RT-qPCR (Figure B.1) and western blotting (Figure B.2) experiments for the determination of IRF4 expressing cell lines independently (Ayhan, 2014). Taken together, the cell lines used in RNA-seq experiments, SKMEL-5 and SKMEL-28, are among IRF4 positive melanoma cell lines.

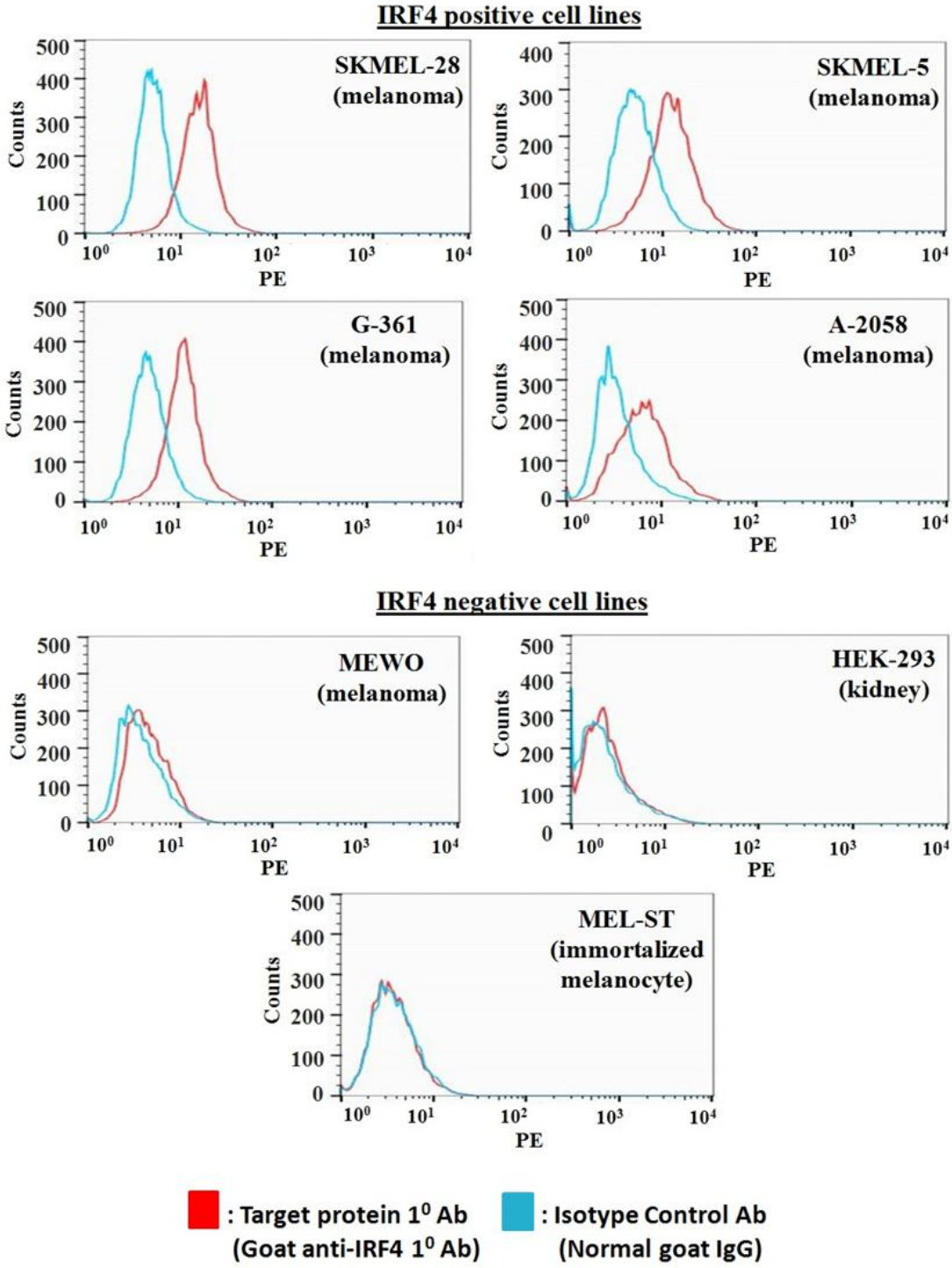

Figure 5.1. Intracellular flow cytometry results showing IRF4 protein levels of indicated cell lines. Intensities of fluorescence emitted from phycoerythrin (PE), which is conjugated to secondary antibodies are shown on the x-axis and cell counts are shown on the y-axis. Isotype control antibody was used as the negative control.

5.2. Optimizations for RNA-seq Experiments

As we have already detected IRF4 expressing melanoma cell lines, the next step was to adjust transduction efficiency and to determine the time point to collect total RNA samples from selected cell lines to be sent to UCLA (University of California, Los Angeles) Neuroscience Genomic Core Facility where library preparation and RNA-seq steps were performed (see Section 4.6).

5.2.1. Transduction Efficiency Optimization

We aimed a transduction efficiency which is high enough to down-regulate IRF4 efficiently (by shIRF4), but in the meantime, not causing a serious phenotypic effect, such as cell death. To monitor such phenotypic effects, we used GFP competition assay as a parameter. It was previously shown that shIRF4 transduced melanoma cells (marked with GFP expression) lost their competitive fitness, and viability of those cells decreased over time relative to shRNA-free cells, which does not express GFP and are grown in the same cell culture population (Ayhan, 2014). In the experimental procedure, shLuc transduced cells, which are also marked with GFP but grown in a separate cell culture plate, were used as negative control. It is expected that GFP percentage of shLuc transduced cells in the cell culture population should stay stable over time. At the end, alterations in the GFP levels of shIRF4 transduced cells were normalized to fluctuations in GFP levels of shLuc transduced counterparts.

We replicated these GFP competition assays for SKMEL-28 and G-361 cell lines (Figure C.1A, Figure C.1B and Figure C.1C). As expected and coherent with previous results (Ayhan, 2014), shIRF4 transduced cells lost their competitive fitness and shLuc transduced counterparts showed stable GFP percentage over time at indicated transduction efficiencies in melanoma cell lines. Additionally, IRF4 negative cell line (negative control), HEK293FT, didn't show any decrease in GFP percentage for shIRF4 introduced cells as expected (Figure C.1D).

In Figure 5.2, GFP competition assay was performed with high transduction efficiencies; 97% and 98% for shIRF4 and shLuc, respectively. We observed that shLuc transduced cells lost their viability along with shIRF4 over time. However, it should also be noted that the effect of transduction on the viability of shLuc transduced cells were observed after a longer period of time relative to shIRF4 transduced cells.

Viability loss observed in control cells transduced with shLuc, at high transduction efficiencies, was suspected to have the potential to cause experimental bias at the RNA-seq step, so we performed a more comprehensive experiment to see the effect of high transduction efficiency (over 98%), along with cell lines transduced in medium level efficiency (around 60%) counterparts (Figure 5.3). In this case, transductions were performed only with shLuc plasmid. We observed higher decrease in the viability of shLuc transductions in high efficiency.

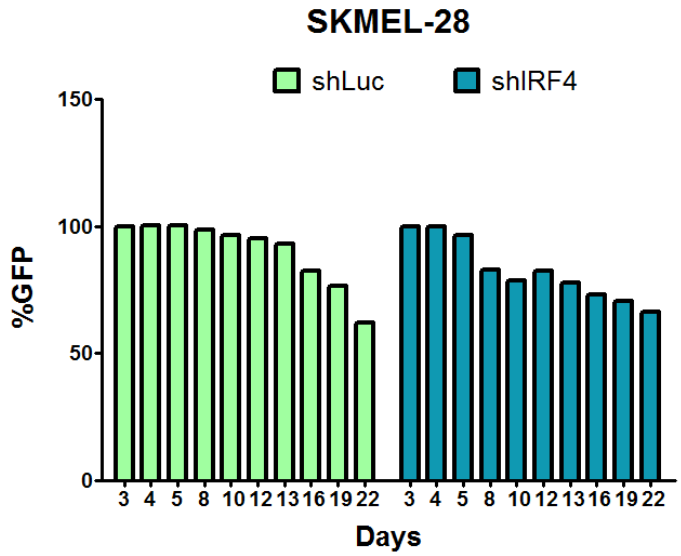

Figure 5.2. GFP competition assay with high transduction efficiencies on SKMEL-28 cell line. Transduction efficiencies are 97% and 98% for shIRF4 and shLuc, respectively.

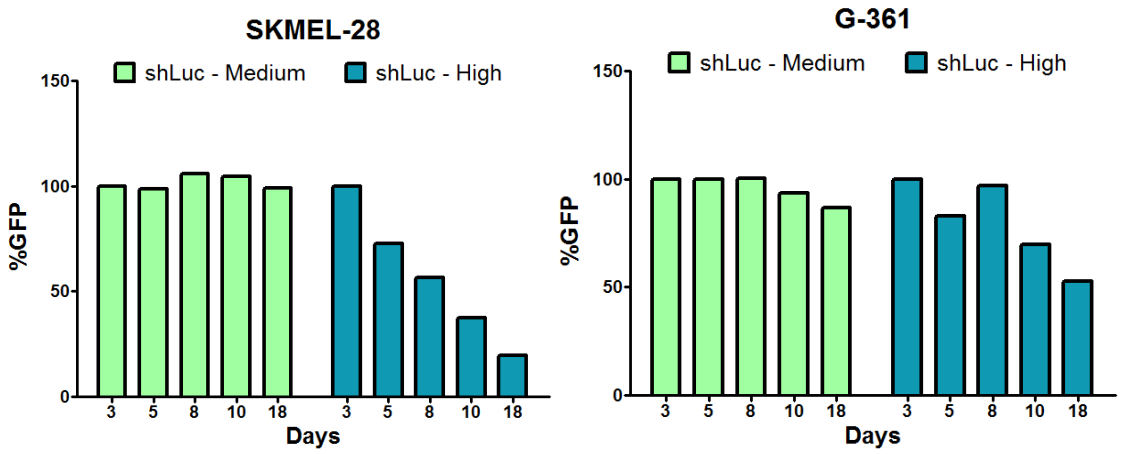

Figure 5.3. GFP competition assays with high and medium transduction efficiencies on SKMEL-28 and G-361 cell lines."High" represents a transduction efficiency over 98% and "Medium" represents a transduction efficiency around 60%, both for G-361 and SKMEL-28. High-efficiency-transduced cells were combined with untransduced cells in 1:1 proportion to balance the population and so to be able to see the effect more clearly.

We have observed that under 90% transduction efficiency, viability loss was not detected, either in short or long term, in control population (shLuc transduced) (Figure C.1). In order to keep the experiment away from the effects of high efficiency transduction but in the mean time to down-regulate IRF4 as efficiently as we can, we aimed a transduction efficiency around 90% in the following experiments.

5.2.2. Optimal Time-point Selection

For the determination of optimal time-point in which to collect total RNA to be analyzed via RNA-seq, we transduced SKMEL-28 and G-361 melanoma cell lines with shIRF4 and shLuc. At the first step, we started with a broader time-range to see the effect of knock down in SKMEL-28 cell line (Figure 5.4).

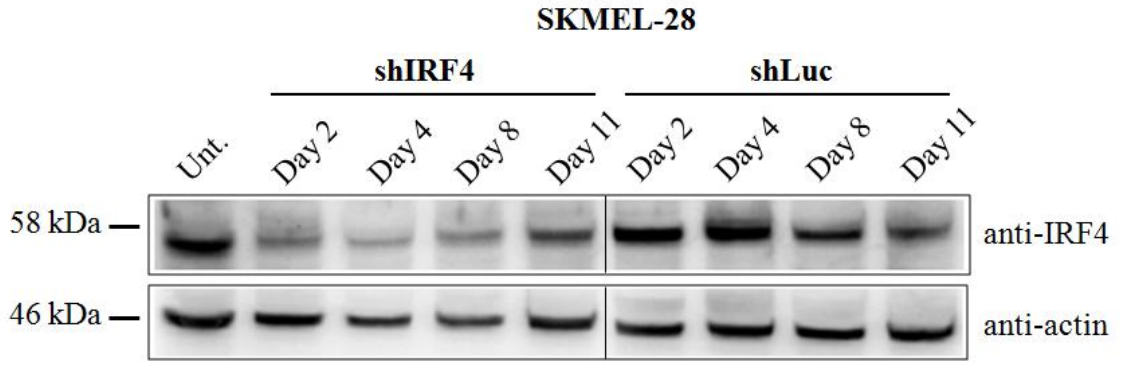

Figure 5.4. Western blotting results with SKMEL-28 lysates for optimal time point selection. Transduction efficiencies are 83% and 86% for shIRF4 and shLuc, respectively (Unt.: Untransduced cells, day 2).

After we decided that shIRF4 was able to reduce IRF4 protein levels in early timepoints, transductions were repeated for SKMEL-28 and G-361 cell lines, but this time to narrow down the time range, IRF4 protein levels were analyzed in the first 4 days after transduction by western blotting for G-361 (Figure 5.5) and by intracellular flow cytometry for SKMEL-28 cells (Figure 5.6). Goat serum controls for intracellular flow cytometry results of SKMEL-28 are shown in Figure D.1. Intracellular flow cytometry analysis with SKMEL-28 was also repeated with another dye, PerCP (Figure E.1)

Based on the experiments to find the optimal time point for total RNA collection, we observed that IRF4 protein level reduction could be detected after 48h. Due to relatively higher reduction in IRF4 levels compared to 48h time point, we selected 72h for subsequent RNA-seq analysis.

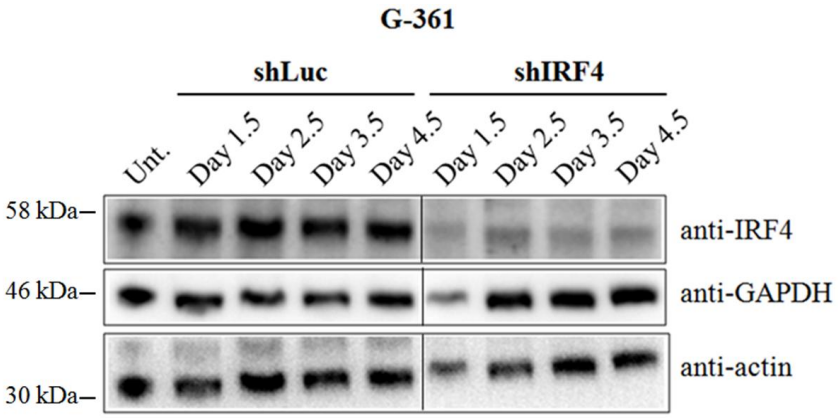

Figure 5.5. Western blotting results with G-361 lysates for optimal time point selection. Transduction efficiencies are 83% and 86% for shIRF4 and shLuc, respectively (Unt.: Untransduced cells, day 1.5).

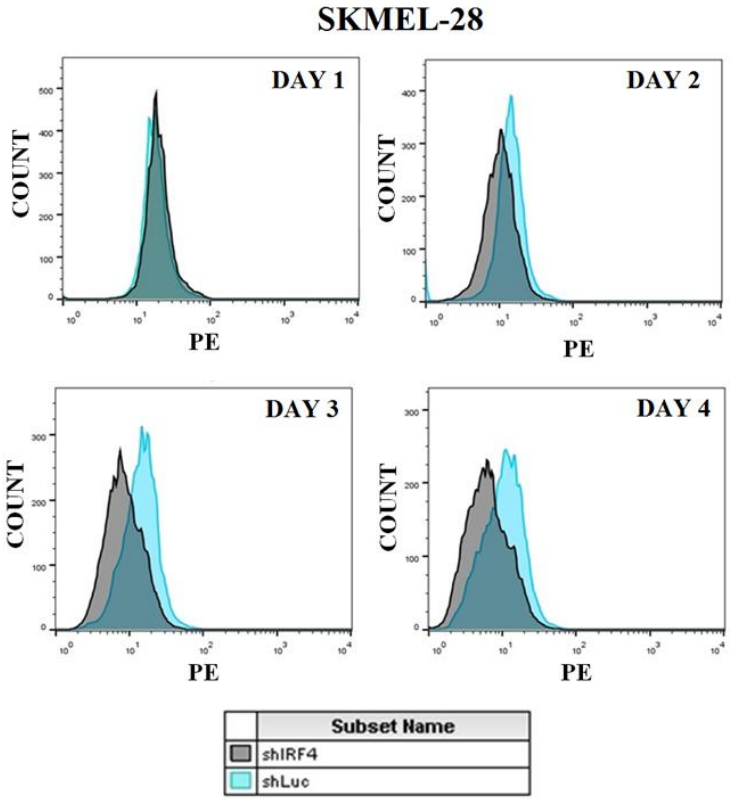

Figure 5.6. Intracellular flow cytometry for optimal time point selection for IRF4 knock-down in SKMEL-28.Transduction efficiencies were 83% and 86% for shIRF4 and shLuc, respectively.

5.3. Validation of IRF4 Knock-down in Samples Prepared for RNA-seq

Total RNA samples collected at 72h time-point were prepared from shIRF4- and shLuc-transduced SKMEL-28 and SKMEL-5 melanoma cell lines, as 3 biological replicates from each condition. These two cell lines differ in gender (SKMEL-28, male origin; SKMEL-5, female origin), in the tissue the cell line was isolated from (SKMEL-28, skin; SKMEL-5, axillary node metastasis), and in IRF4 protein levels (Figure B.2). This diversity among the characteristics of SKMEL-28 and SKMEL-5 was the reason of their selection among IRF4 expressing melanoma cell lines for RNA-seq analysis.

Before sending the samples for sequencing, we validated IRF4 knock-down in protein levels either by intracellular flow cytometry or western blotting.

5.3.1. SKMEL-28

Intracellular flow cytometry results for IRF4 levels in shIRF4 and shLuc transduced SKMEL-28 cells are shown in Figure 5.7. Although we ultimately used the 72h time point for RNA-seq, both 48h and 72h samples were analyzed. At both of the time points, IRF4 protein level reduction was detected.

5.3.2. SKMEL-5

Western blotting results for IRF4 levels in shIRF4 and shLuc transduced SKMEL-5 cells are shown in Figure 5.8. Although 72h time point was selected for RNA-seq analysis, both 48h and 72h collections were analyzed. IRF4 protein level reduction was observed at 72h time point.

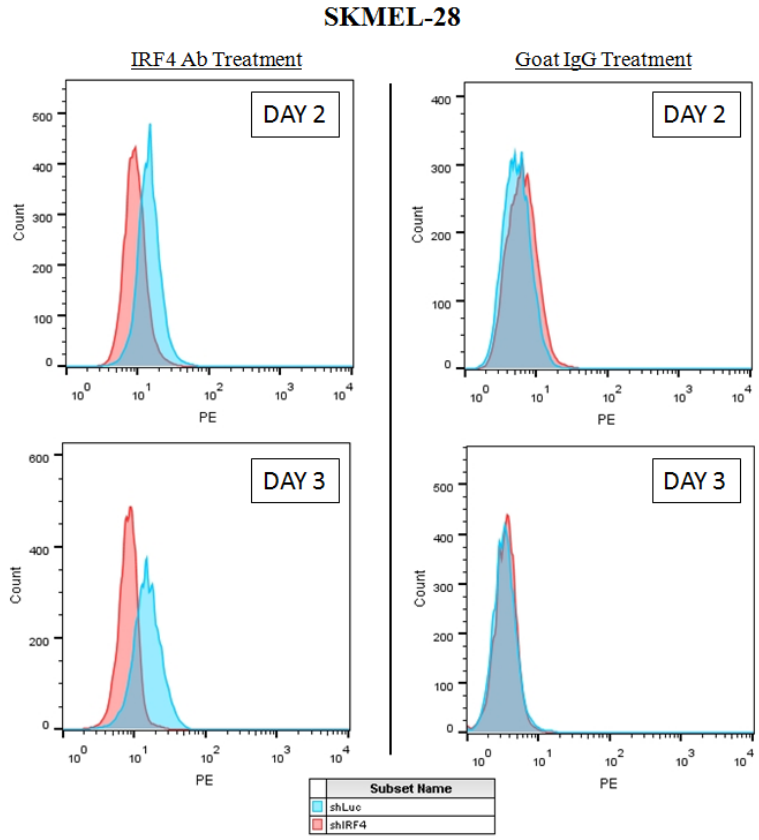

Figure 5.7. Intracellular flow cytometry results of SKMEL-28 samples used for RNA-seq. One of three replicates from each condition was analyzed as representative of whole. Transduction efficiencies for shIRF4 and shLuc are 90% and 80%, respectively.

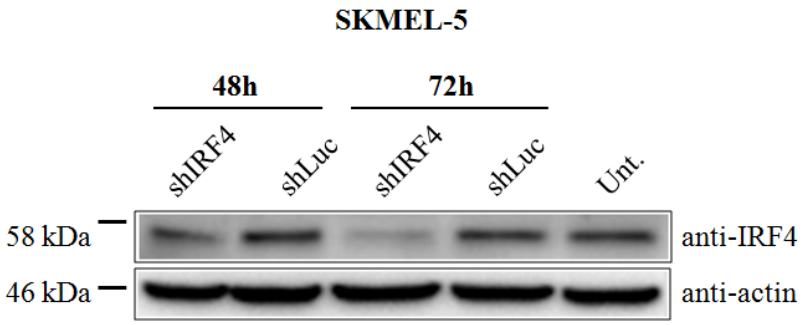

Figure 5.8. Western blotting results of SKMEL-5 samples prepared for RNA-seq. Biological replicates from each condition were pooled for each time point (Unt.: Untransduced, 48h). Transduction efficiencies for both conditions (shIRF4 and shLuc) are around 80%.

5.4. Integrity Control of Total RNA Samples for RNA-seq

Following extraction of total RNA, their integrity was checked by Agilent Bioanalyzer 2100. Output is RNA integrity number (RIN number) where 1 represents fully degraded RNA and 10 represents intact RNA. At the step of library preparation of RNA-seq experiment, values above 8 for RIN number are highly recommended (Sigurgeirsson *et al.*, 2014). In Table 5.1, RIN numbers for both SKMEL-5 and SKMEL-28 total RNA samples, prepared for library preparation step of RNA-seq experiment, are given. Detailed graphs showing the 18S and 28S rRNA peaks and representative simulated gel photos are depicted in Figure F.1 and Figure F.2. High RIN numbers confirm the intactness of total RNA samples used at RNA-seq experiment.

Table 5.1. RINs for isolated total RNAs from SKMEL-28 and SKMEL-5 cell lines.

Samples	**SKMEL-28**	**SKMEL-5**
shIRF4 Replicate-1	9.6	9.7
shIRF4 Replicate-2	10	9.7
shIRF4 Replicate-3	9.8	9.9
shLuc Replicate-1	9.9	9.6
shLuc Replicate-2	9.8	9.6
shLuc Replicate-3	10	9.9

Total RNA samples were treated with RNAstable (Biometrica) to inhibit degradation in room temperature during transportation to the sequencing facility. To ensure that the kit was working properly, we treated one of the samples with RNAstable kit and resuspended it in dH_2O after a week. Sample from same batch but stored in -80^oC for a week was thawed to be compared with RNAstable treated samples. We observed intact 18S and 28S rRNA bands in both of the conditions (Figure G.1).

5.5. Bioinformatic Analysis of RNA-seq Results

Sequenced reads were received from the sequencing facility in fastq file format. Raw data were already de-multiplexed and adaptor sequences were removed along with barcodes. We applied the bioinformatics pipeline summarized in Figure 5.9.

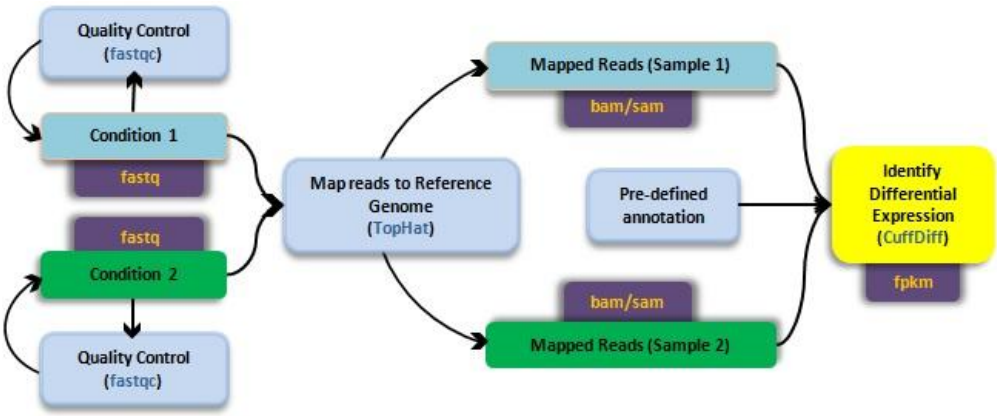

Figure 5.9. Schematics of the pipeline followed for bioinformatics analysis of RNA-seq experiment. After quality control of sequenced reads, they are mapped onto reference genome. Then, expression of each gene is quantified and differential expression analysis is applied between two conditions.

5.5.1. Quality Check for Sequenced Reads

Prior to mapping reads to the genome, we analyzed the quality of the reads by FASTQC software (http://www.bioinformatics.babraham.ac.uk/projects/fastqc/) through Galaxy Web Server to decide if any trimming or filtering was necessary. As a representative figure, quality score graph for one of the biological replicates of shIRF4 transduced SKMEL-5 is shown in Figure 5.10. All of the quality graphs corresponding to each biological replicate are shown in Figure H.1 and H.2.

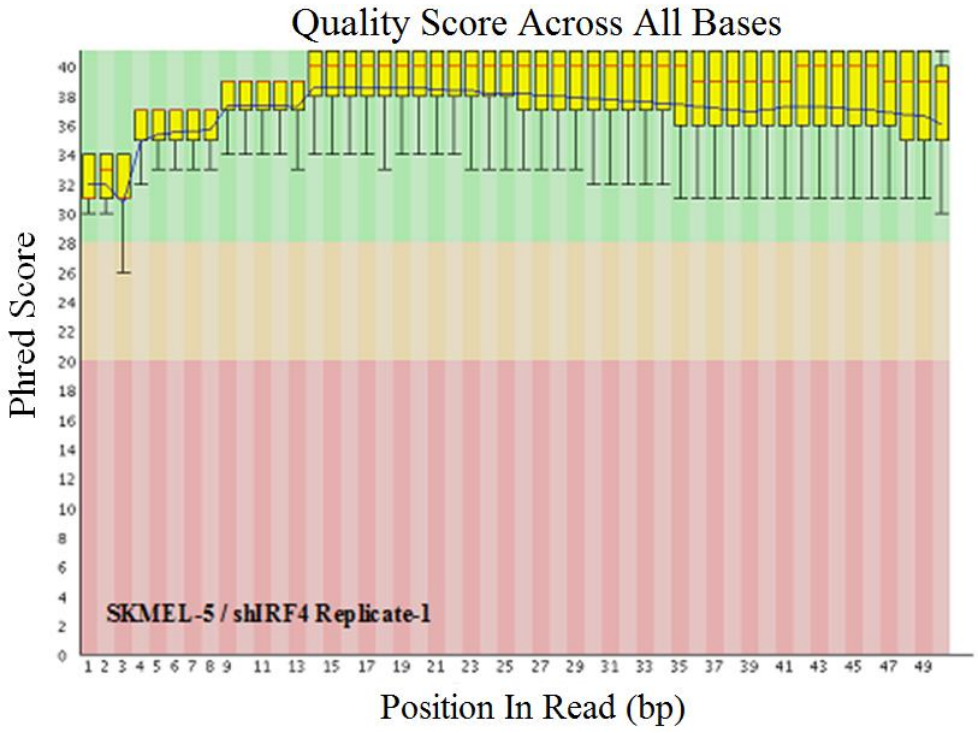

Figure 5.10. Per base sequence quality graph for one of the biological replicates of SKMEL-5. X-axis shows the overall quality of each base in each position in a read. Y-axis shows the Phred Scores which define the quality.

Based on the results shown in Figure H.1 and H.2, we didn't perform any trimming or filtering since qualities of bases in each position were satisfactory. Most of the bases have a Phred quality score more than 30 (base call accuracy > 99.9%). Therefore all the reads were used without any manipulation at the mapping step.

5.5.2. Mapping to Reference Human Transcriptome and Its Visualization

We used Tophat software (Kim *et al.*, 2013) to map sequenced reads to human genome (hg19). We restricted mapping only to known transcriptome, where also only known exon junctions were used. Then, we selected "unique hits", which are the reads mapping only once to the defined transcriptome, as explained in Materials and Methods. Mapping statistics is presented in Table 5.2.

Table 5.2. Tophat mapping statistics showing number of sequenced (Total) and uniquely mapped reads for each replicate and condition.

SKMEL-28	Uniquely Mapped	TOTAL	Mapped %
shIRF4 Replicate-1	19,170,015	30,878,570	62%
shIRF4 Replicate-2	19,256,767	29,769,865	64%
shIRF4 Replicate-3	22,233,254	35,252,637	63%
shLuc Replicate-1	18,382,566	31,079,022	59%
shLuc Replicate-2	15,662,788	26,505,662	59%
shLuc Replicate-3	18,568,155	32,303,067	57%
TOTAL	113,273,545	185,788,823	61%

SKMEL-5	Uniquely Mapped	TOTAL	Mapped %
shIRF4 Replicate-1	12,761,453	18,193,809	70%
shIRF4 Replicate-2	12,058,698	17,424,039	69%
shIRF4 Replicate-3	11,117,188	16,041,555	69%
shLuc Replicate-1	12,979,486	19,226,817	67%
shLuc Replicate-2	12,779,152	19,410,420	66%
shLuc Replicate-3	12,313,966	18,201,915	68%
TOTAL	74,009,943	108,498,555	68%

We visualized the reads mapped by Tophat using Integrated Genome Viewer (Thorvaldsdottir *et al.*, 2013). A representative figure, showing IRF4 locus for all shIRF4 and shLuc replicates of SKMEL-28, is shown in Figure I.1.

5.5.3. Identification of Significantly Differentially Expressed Genes via Cuffdiff

After reads were mapped by Tophat, we used Cuffdiff software (Trapnell *et al.*, 2012) to normalize and quantify expression levels which is calculated as FPKM (Fragments Per Kilobase of transcript per Million mapped reads), and to test them for significant differences in gene level between two conditions. Differential expression of genes was determined between two conditions with a significance test where false discovery rate (FDR) adjusted p-values (i.e., q-value) were used. We used 0.01 threshold for q-value, calculated

by Cuffdiff, to define significantly differentially expressed genes (DEGs) between shIRF4 and shLuc transduced replicates. Results are shown in Figure 5.11. We named genes down-regulated upon IRF4 depletion as "IRF4-activated" and genes up-regulated upon IRF4 depletion as "IRF4-repressed". Number of significantly differentially expressed genes ($q < 0.01$), shared or distinct for each cell line, are shown in Figure 5.12.

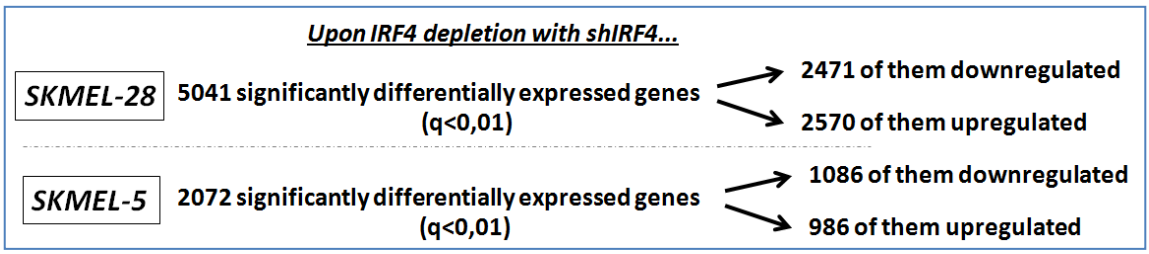

Figure 5.11. The number of genes significantly up-regulated or down-regulated, defined by Cuffdiff, upon IRF4 depletion in SKMEL-28 and SKMEL-5 cell lines.

As we have detected a high number of significantly DEGs unique to SKMEL-28, we asked if this is a result of relatively lower number of mapped reads of SKMEL-5 (Table 5.2). To investigate this, we decreased the number of mapped reads of SKMEL-28 by randomly omitting sequence reads (from fastq files) in order to adjust the number of mapped reads to a similar level for both cell lines (Table J.1). After using Cuffdiff to determine differentially expressed genes in this condition, we found that the change in the number of DEGs between SKMEL-28 and SKMEL-28-Adjusted is only modest (Figure 5.13). Therefore, we concluded that the source of difference is not the low read number produced in SKMEL-5 experiment.

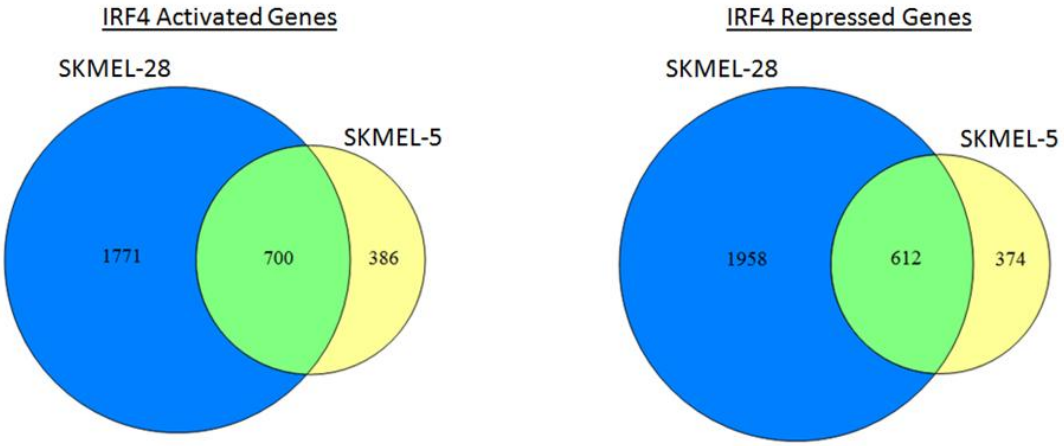

Figure 5.12. Number of significantly differentially expressed genes, defined by Cuffdiff, distinct or shared between two cell lines.

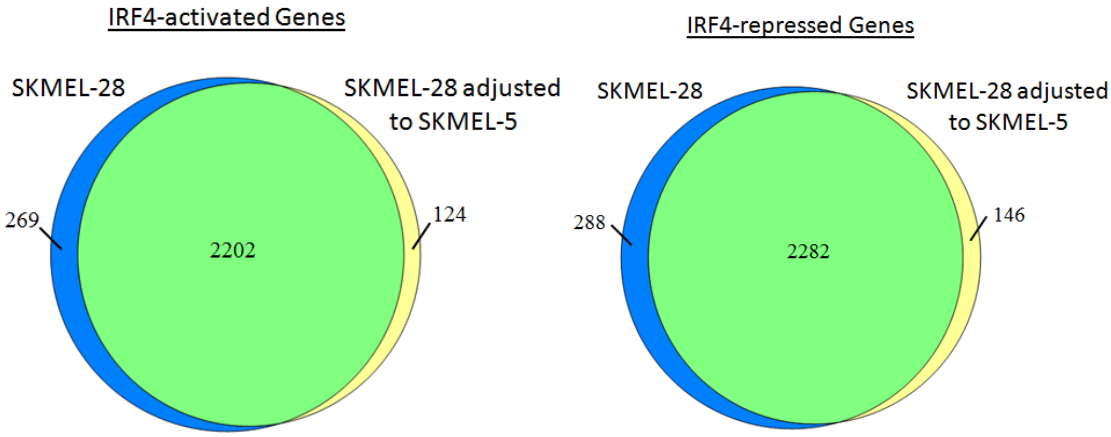

Figure 5.13. Difference between DEGs before and after, when SKMEL-28 mapped number decreased to the level of SKMEL-5 mapped number.

We ranked significantly differentially expressed genes depending on their fold changes between two conditions which were determined by CuffDiff. Common genes in the top ranked list of both cell lines (the first 100 genes) are shown separately for IRF4-activated (Table 5.3) and IRF4-repressed group (Table 5.4).

Table 5.3. Significant IRF4-activated genes having highest fold change in both cell lines ($q<10^{-3}$).

Common IRF4-activated Genes in Top 100		SKMEL-28	SKMEL-5
		Log_2 Fold Change	Log_2 Fold Change
EPHB3	Ephrin type-B receptor 3	3.65	1.12
H19	H19, Imprinted Maternally Expressed Transcript (Non-Protein Coding)	2.61	1.58
ECE1	Endothelin Converting Enzyme 1	2.42	1.36
MTFP1	Mitochondrial Fission Process 1	2.30	1.28
PON2	Paraoxonase 2	2.26	1.27
ADAM9	ADAM Metallopeptidase Domain 9	2.00	1.43
SLC2A3	Solute Carrier Family 2 (Facilitated Glucose Transporter), Member 3	1.95	1.41
PRKRA	Protein Kinase, Interferon-Inducible Double Stranded RNA Dependent Activator	1.93	1.06
VAMP8	Vesicle-Associated Membrane Protein 8	1.87	0.92
TPI1	Triosephosphate Isomerase 1	1.84	1.24
LAMP1	Lysosomal-Associated Membrane Protein 1	1.82	1.46
BAK1	BCL2-Antagonist/Killer 1	1.80	1.04
SLC44A1	Solute Carrier Family 44 (Choline Transporter), Member 1	1.63	1.30
SNRNP40	Small Nuclear Ribonucleoprotein 40kDa (U5)	1.58	0.93
M6PR	Mannose-6-Phosphate Receptor (Cation Dependent)	1.47	0.95

Table 5.4. Significant IRF4-repressed genes having highest fold change in both cell lines ($q<10^{-3}$).

Common IRF4-repressed Genes in Top 100		SKMEL-28	SKMEL-5
		Log_2 Fold Change	Log_2 Fold Change
CEND1	Cell cycle exit and neuronal differentiation 1	-3.67	-2.36
CCDC109B	Coiled-coil domain containing 109B	-2.22	-2.34
PDIA6	Protein disulfide isomerase family A, member 6	-1.71	-2.29
FKBP9	FK506 binding protein 9, 63 kDa	-2.16	-2.15
LEPREL1	Leprecan-like 1	-2.02	-1.56
TM7SF2	Transmembrane 7 superfamily member 2	-2.00	-1.50
STS	Steroid sulfatase (microsomal), isozyme S	-2.04	-1.40
TAPBP	TAP binding protein (tapasin)	-1.80	-1.37
SLC5A9	Solute carrier family 5 (sodium/sugar cotransporter), member 9	-1.83	-1.30
MXRA8	Matrix-remodelling associated 8	-1.71	-1.27
MARCKSL1	MARCKS-like 1	-1.70	-1.26

Table 5.4. Significant IRF4-repressed genes having highest fold change in both cell lines ($q<10^{-3}$) (cont.).

ST3GAL6	ST3 beta-galactoside alpha-2,3-sialyltransferase 6	-1.87	-1.23
CCM2	Cerebral cavernous malformation 2	-1.92	-1.16
MAP2	Microtubule-associated protein 2	-1.68	-1.08
PTCRA	Pre T-cell antigen receptor alpha	-2.77	-1.07
GYPC	Glycophorin C (Gerbich blood group)	-1.62	-0.95
ITFG3	Integrin alpha FG-GAP repeat containing 3	-1.65	-0.95
MYO1D	Myosin ID	-1.73	-0.93
DTNA	Dystrobrevin, alpha	-1.80	-0.93
NANOS1	Nanos homolog 1 (Drosophila)	-1.71	-0.86
EIF4EBP2	Eukaryotic translation initiation factor 4E binding protein 2	-1.96	-0.79
C1QC	Complement component 1, q subcomponent, C chain	-1.86	-0.77

5.5.4. Correlation Between Biological Replicates

When FPKM values were calculated for each gene in each biological replicate, a high overall correlation between the replicates of same condition in terms of FPKM values is expected. To check this, we plotted graphs comparing the FPKM values between each replicates using Graphpad Prism 6 (Figure L.1). Calculated Spearman's correlation coefficients are given in the Table 5.5.

Table 5.5. Spearman's correlation coefficients between each biological replicate.

	Spearman's Correlation Coefficients			
	SKMEL-28		**SKMEL-5**	
REPLICATES	**shIRF4**	**shLuc**	**shIRF4**	**shLuc**
Replicate- 1 vs. 2	0.9632	0.9578	0.9631	0.9650
Replicate- 1 vs. 3	0.9644	0.9611	0.9609	0.9586
Replicate- 2 vs. 3	0.9633	0.9598	0.9609	0.9611

All the pair-wise Spearman's correlation values were high (>0.95), indicating a good reproducibility between biological replicates. This suggests that the sample and library preparation steps were reproducible (Yamaguchi *et al.*, 2013).

5.5.5. Assesment of RNA-seq Data with Global Statistics

The output of differential gene expression analysis by Cuffdiff is a table of all the genes in the human transcriptome with FPKM values and fold changes between conditions, with associated significance test results. High amount of data make it difficult to visualize the whole output and to understand if anything is abnormal about the analysis. In order to gain an overall insight of the whole data, we used CummeRbund bioconductor package (Goff *et al.*, 2012) which provides graphical outputs of global data statistics. For example, dendrogram of the samples shows clustering among the biological replicates of the same condition, confirming the sample identities (Figure 5.14). In Figure 5.15, and Figure K.1, density graphs for SKMEL-5 and SKMEL-28 show the distribution of FPKM values for all genes across two conditions, providing visualization of expression distribution in the transcriptome. When quantified, the mean FPKM value of the genes are 25.13 (shIRF4 transduced samples) and 24.53 (shLuc transduced samples) for SKMEL-5; and 23.81 (shIRF4 transduced samples), 22.87 (shLuc transduced samples) for SKMEL-28. In both cell lines, global gene expression of the cells are higher in shIRF4 transduced condition.

The M vs. A plot shows the log fold change between test and control (M) against the log of FPKM values (A). Originally developed to detect dye biases in microarray experiments, these graphs helped us to observe high fold-change variance at low RPKM values, an expected phenomenon where signals close to background are measured with less precision (Figure K.2A and K.2B)

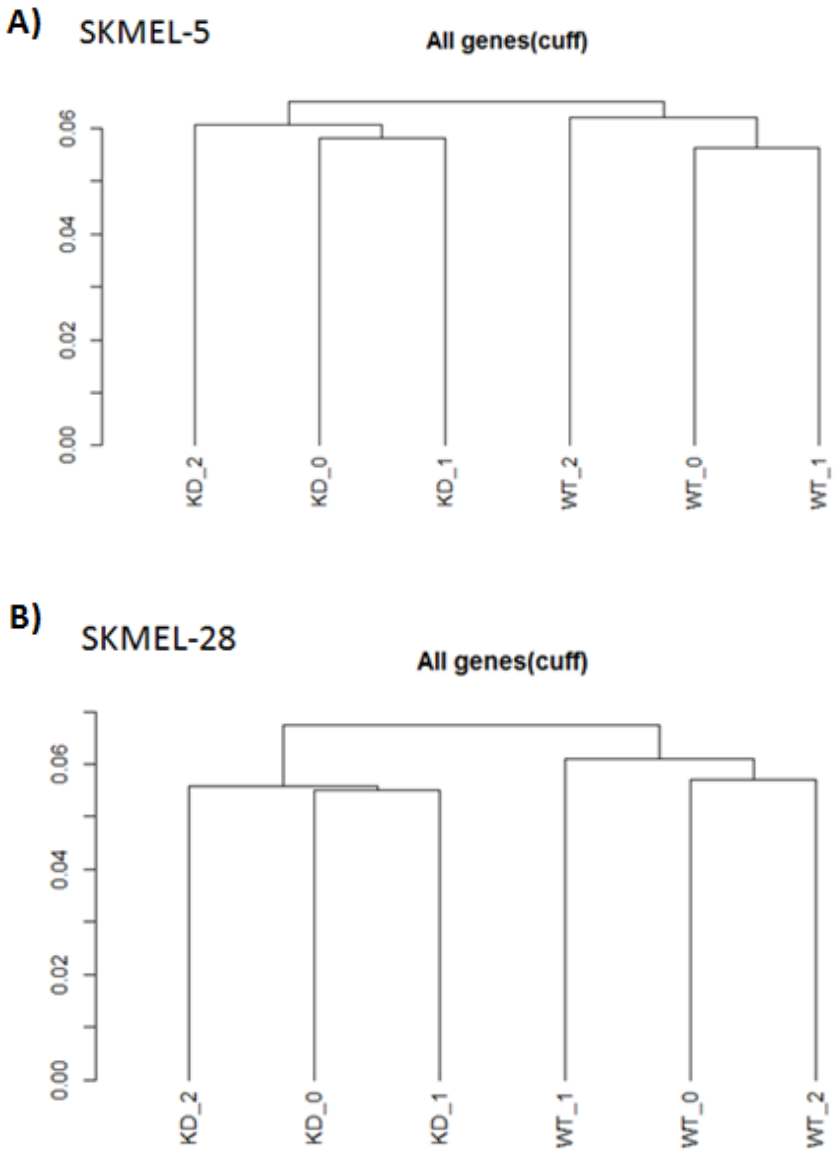

Figure 5.14. Dendrograms for A) SKMEL-5 B) SKMEL-28 showing relatedness between samples (KD: shIRF4 transduced samples, WT: shLuc transduced samples).

Scatterplots comparing the expression of each gene between two conditions are shown in Figure K.3. The scatterplots of significant DEGs appear uniform across expression levels (i.e., do not show a bias for low FPKM values), suggesting that the statistical test used by Cuffdiff was able to eliminate noisy data at low FPKM values. In M vs. A plot, it can also be observed that high FCs belong to low-expressed genes as a result of high variability between replicates.

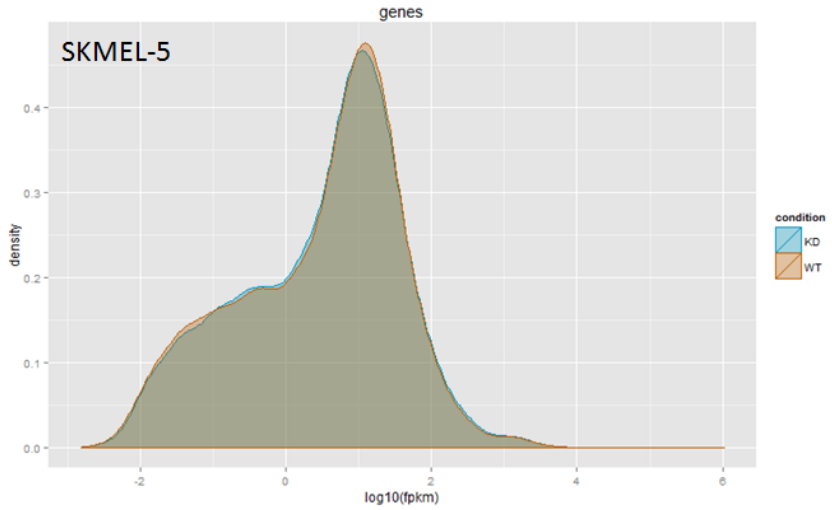

Figure 5.15. Expression distribution (density) graph of SKMEL-5 (KD: shIRF4 transduced samples, WT: shLuc transduced samples).

5.6. Verification of RNA-seq Results with RT-qPCR

In RNA-seq studies aiming to find the genes which are differentially expressed between 2 conditions, RT-qPCR is a common method used for validation (Fang and Cui, 2011). For that purpose, we chose certain genes based on their biological interest, FPKM values and fold change to control the sensitivity and reproducibility of RNA-seq results. Genes selected for RT-qPCR analysis are *MITF, BRCA2, NRAS, CDKN2A, MYC, SQLE* and *TYR*. In Table 5.6 and Figure 5.16, a comparison of RT-qPCR and RNA-seq results are shown for the cell lines we used in this study.

Depending on the comparison of RNA-seq and RT-qPCR, fold changes (FCs) were correlative in overall.

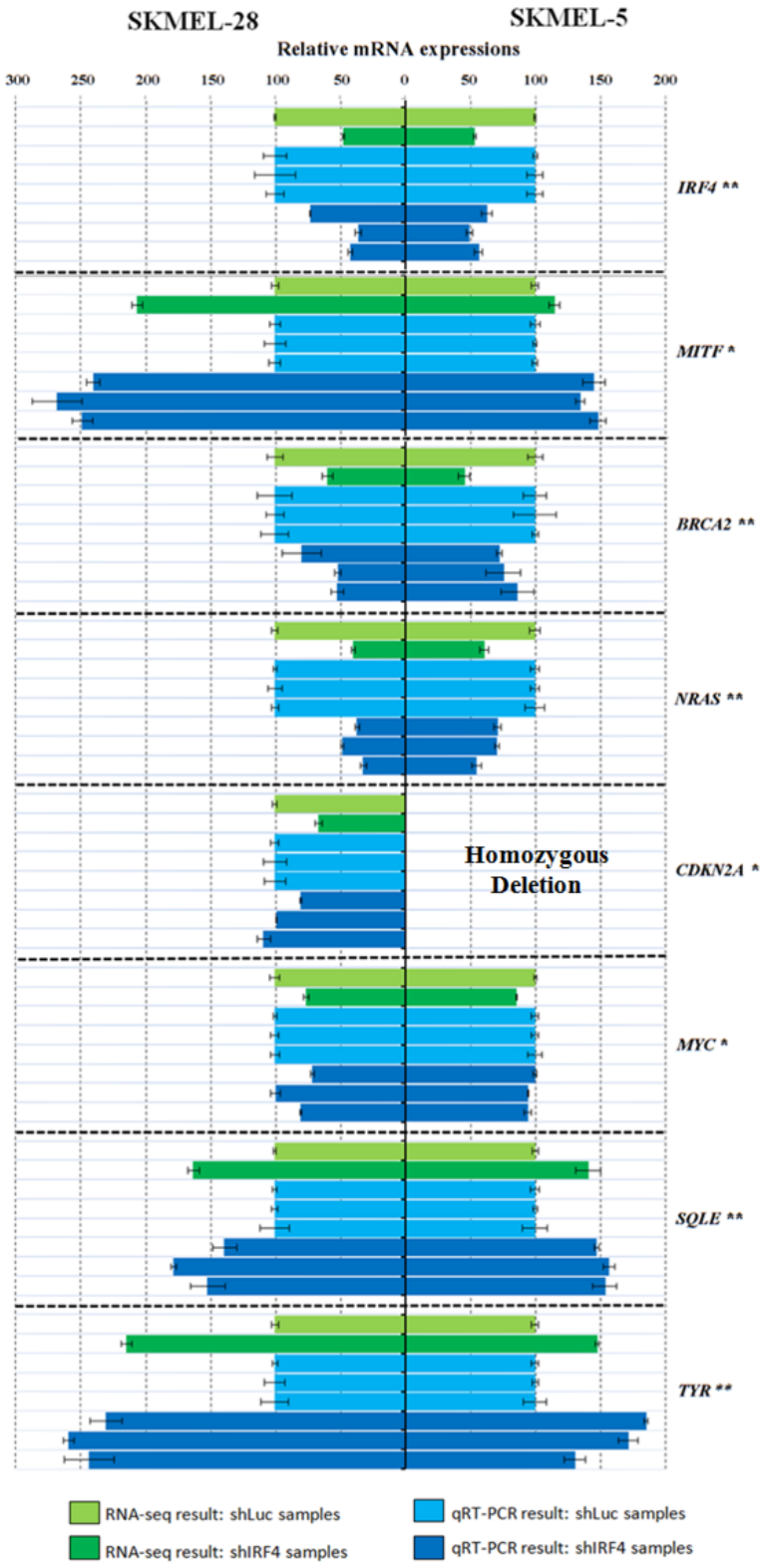

Figure 5.16. RT-qPCR results of 8 genes compared with RNA-seq results.shIRF4 data is normalized to corresponding shLuc data and error bars shows the standard error (*: significant DEG only in SKMEL-28; **: significant DEG in both cell lines).

Table 5.6. Comparison of fold changes determined in RT-qPCR and RNA-seq. RT-qPCR values are the means of 3 biological replicates.

		FOLD CHANGE (shLuc / shIRF4)							
		IRF4	*MITF*	*BRCA2*	*NRAS*	*CDKN2A*	*MYC*	*SQLE*	*TYR*
SKMEL -28	RNA-seq	-2.12	2.06	-1.68	-2.53	-1.50	-1.32	1.62	2.14
	RT-qPCR	-2.00	2.51	-1.64	-2.58	-1.05	-1.20	1.54	2.43
SKMEL -5	RNA-seq	-1.87	1.15	-2.19	-1.64	-	-1.17	1.41	1.48
	RT-qPCR	-1.77	1.40	-1.28	-1.52	-	-1.04	1.53	1.59

In order to see the effect of IRF4 down-regulation on the expression of selected genes (*MITF*, *BRCA2*, *NRAS*, *CDKN2A*, *MYC*, *SQLE* and *TYR*) in other IRF4 positive cell lines, A-2058 and G-361, we performed RT-qPCRs with primers used for the verification of RNA-seq results (Figure 5.17). Total RNA samples were collected in 72h time point as in RNA-seq experiment.

Results from Figure 5.17 indicate that compared to G-361, A2058 is more closely related to the IRF4-downregulated characteristics of SKMEL-5 and SKMEL-28, showing regulation on MITF, SQLE and TYR. On the other hand, except BRCA2 and NRAS, indicated genes in G-361 are unaffected from IRF4 down-regulation.

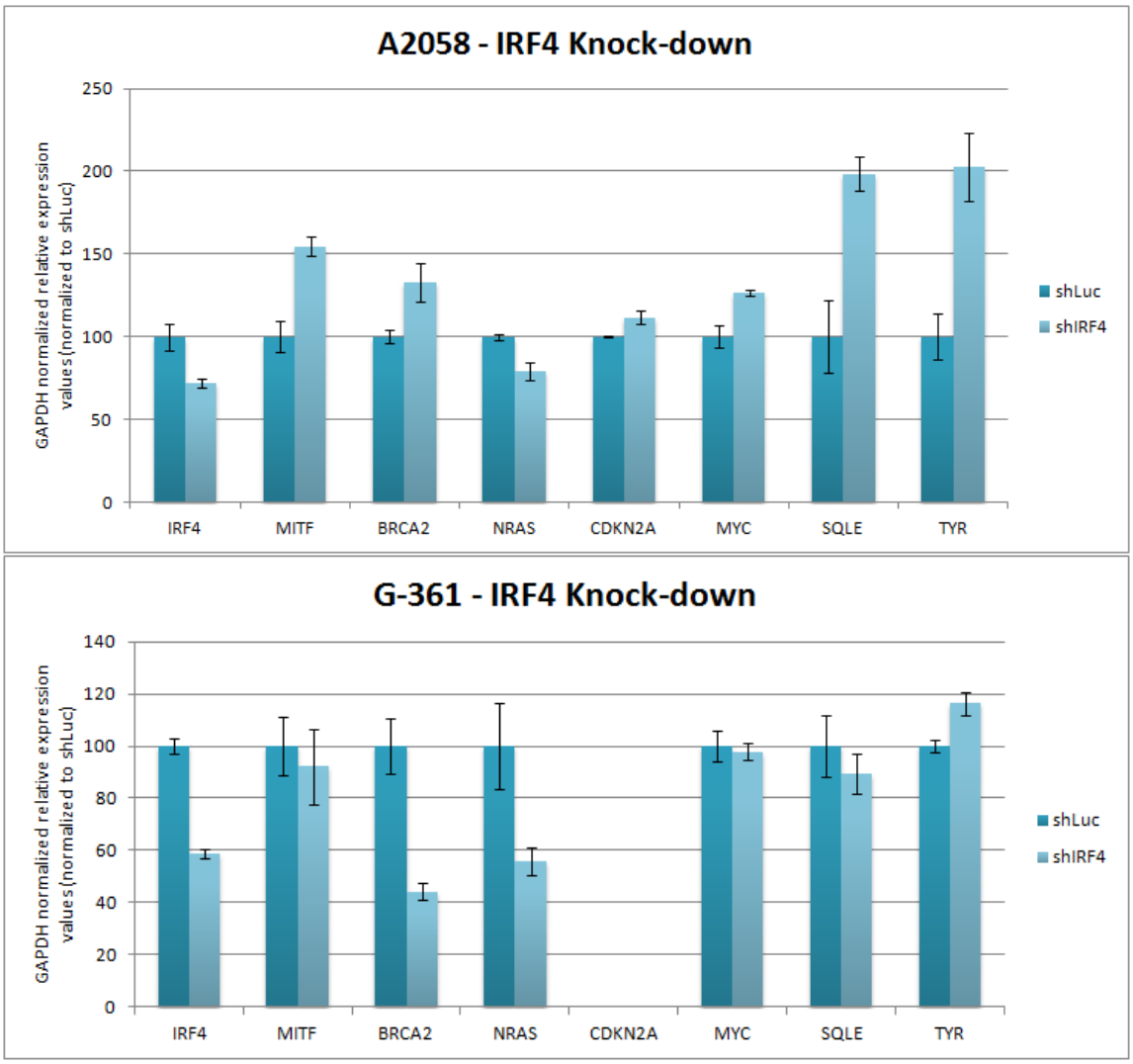

Figure 5.17. RT-qPCR results of selected 8 genes for shIRF4 and shLuc transduced A2058 and G-361 cell lines. Samples were collected at 72h time point. shIRF4 data is normalized to corresponding shLuc data and error bars shows the standard error.

5.7. Gene Ontology Enrichment Analysis via GOrilla

With the goal of revealing the enriched GO terms in Biological Process domain (GO_BP), significant DEGs defined by Cuffdiff were loaded into GOrilla (Gene ontology enrichment analysis and visualization tool) (Eden *et al.*, 2009).

GOrilla analysis generates a list with GO terms and corresponding p- and q- values with visualization in a hierarchical structure (parent-child term relations) called directed acyclic graph (DAG). At the first step, we applied GOrilla analysis separately to the IRF4-activated and IRF4-repressed lists of cell lines to find over-represented GO_BP terms. Whole list of significantly ($q < 10^{-3}$) over-represented GO_BP terms for IRF4-activated genes were shown in Table M.1 for SKMEL-5 and in Table M.2 for SKMEL-28.

In the DAG structure, end of branches (i.e., bottom of the graphs) tend to have more specific GO terms. In order to achieve an overall visualization with reduced redundancy, we mostly focused on bottom parts of the graph. In the bottom part of DAG of IRF4-activated GO term list of SKMEL-5, we observed the following GO terms at the bottom: "DNA replication", "DNA strand elongation", "DNA-repair", "mitotic cell cycle", "G1/S transition of mitotic cell cycle", "microtubule cytoskeleton organization", "chromatin modification", "mitotic nuclear division", "regulation of mitotic cell cycle phase transition" (Figure M.1 and M.2). IRF4-activated genes of SKMEL-28 were found to have enriched GO terms, very significantly, as followings: "regulation of transcription", "transcription", "positive regulation of RNA metabolic process", "regulation of protein modification process", "mitotic cell cycle process", and "chromatin modification" (Figure M.3 and M.4).

GO enrichment analysis with IRF4-repressed genes, for SKMEL-5, shows; "lipid", "sterol", "sphingolipid", "membrane lipid", "glycosaminoglycan" metabolic processes (Table N.1 and Figure N.1). Over-represented GO terms for IRF4-repressed genes in SKMEL-28 include "cholesterol biosynthetic process", "oxoacid metabolic process" and "intracellular protein transport" at the end of each main branch of DAG graph (Figure N.2). Moreover, not shown in DAG as it only includes highest ranked GO_BP terms ($q<10^{-11}$), "vesicle-mediated transport" and "melanin biosynthetic process" are present in the list of over-represented GO terms ($q<10^{-3}$) for IRF4 repressed genes (Table N.2).

Following analyses were performed with the intersection of IRF4-activated or IRF4-repressed genes between SKMEL-28 and SKMEL-5, in order to get insight into common IRF4 regulatory biological processes in both of the cell lines.

5.7.1. Common IRF4-Activated Genes

Gene Ontology - Biological Process (GO_BP) terms enriched with IRF4-activated genes, which are common in both cell lines (n=700) (Figure 5.12), were determined and visualized by GOrilla (Figure 5.18). To make visualization possible, this scheme is generated by GO terms with lowest p-values ($p < 10^{-9}$), showing highest ranked GO_BP terms, but parent terms with lower p-values are also placed into DAG by GOrilla to show the relation of "child" term to the “parent” term. Full list of GO_BP terms with less stringent p-value cutoff ($q < 10^{-3}$) for IRF4-activated gene list is shown in Table O.1.

Most significantly enriched GO terms are related to mitotic nuclear division and cell cycle. When SKMEL-28 and SKMEL-5 IRF4-activated genes were analyzed separately, related terms were also among the highest rankings (Figure M.1, M.2, M.3 and M.4).

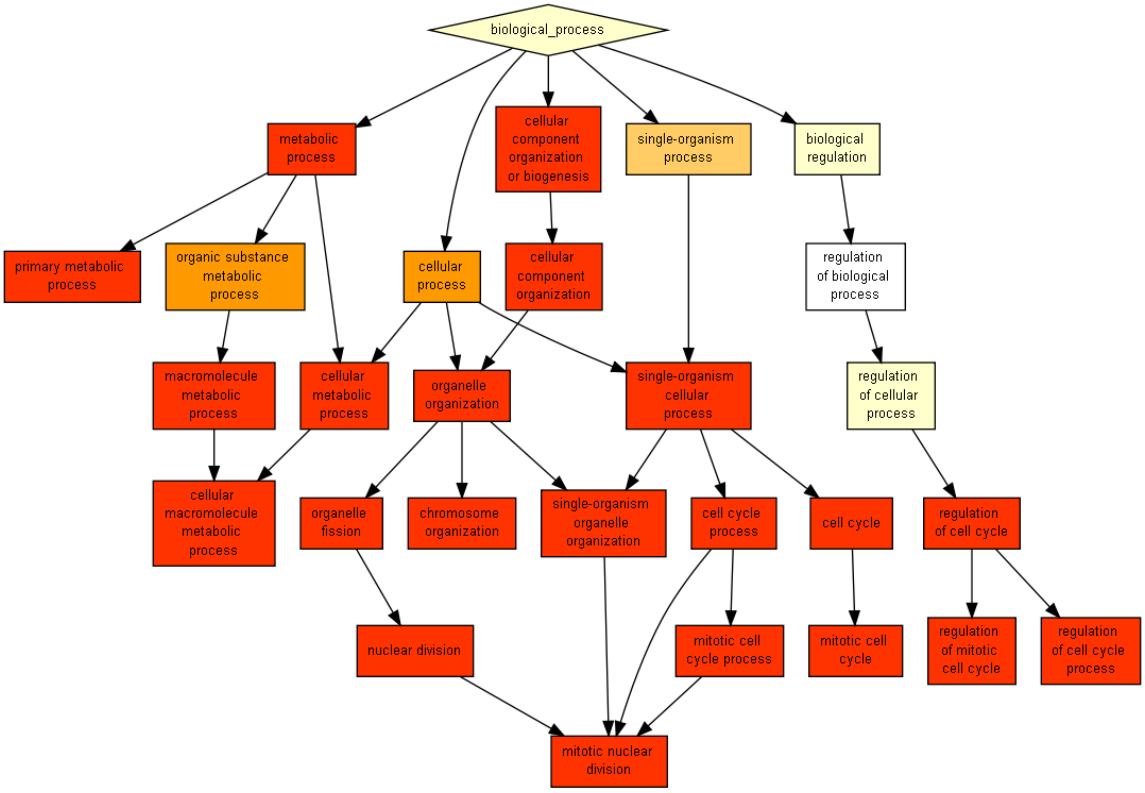

Figure 5.18. Highest ranked Gene Ontology (Biological Process) terms for common IRF4-activated gene list ($p < 10^{-9}$).

5.7.2. Common IRF4-Repressed Genes

Over-represented Gene Ontology - Biological Process (GO_BP) terms for IRF4-repressed genes in common (n=612) (Figure 5.12) were analyzed and visualized by GOrilla. DAG in Figure 5.19 shows GO terms with lowest p-values ($p < 10^{-9}$) but full list of GO_BP terms with less stringent p-value cutoff ($q < 10^{-3}$) is also shown in Table P.1.

Lipid biosynthetic process is the term with the lowest p-value. Many of the other terms in the list (Table P.1) are also related to lipid metabolism.

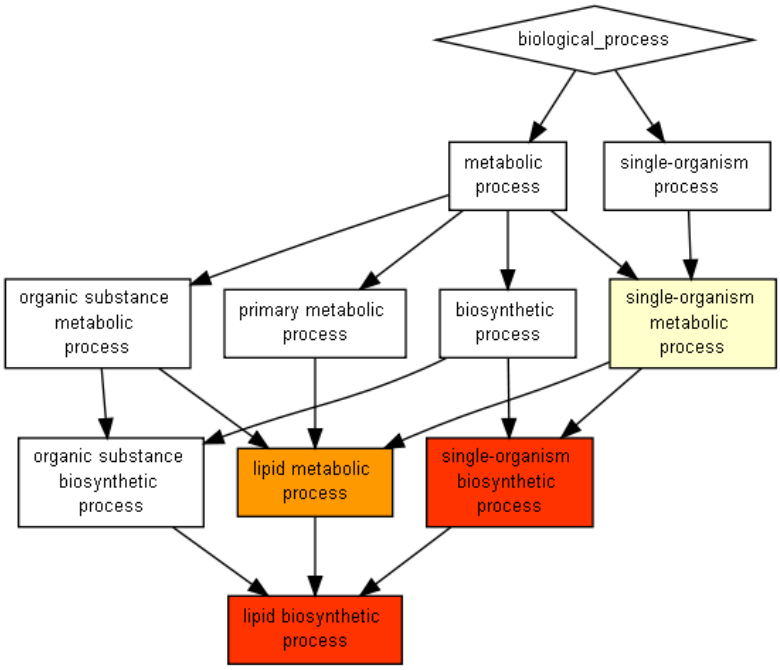

Figure 5.19. Gene Ontology (Biological Process) terms enriched in IRF4-repressed gene set ($p < 10^{-9}$).

5.8. Alternative Pipeline to Find Significantly Differentially Expressed Genes

A number of packages have been developed to find differentially expressed genes between different conditions. However, there is no clear consensus about which one is "better" relative to others (Seyednasrollah *et al.*, 2013). For this reason, we used another pipeline, DESeq which uses raw gene-level counts instead of FPKMs. In order to get raw counts for each gene, HTSeq was used (see Materials and Methods) (Anders *et al.*, 2014). Output of HTSeq is a table with mapped read counts for each gene. When DESeq was used for differential expression analysis, we got a number of genes differentially expressed as shown in Figure 5.20.

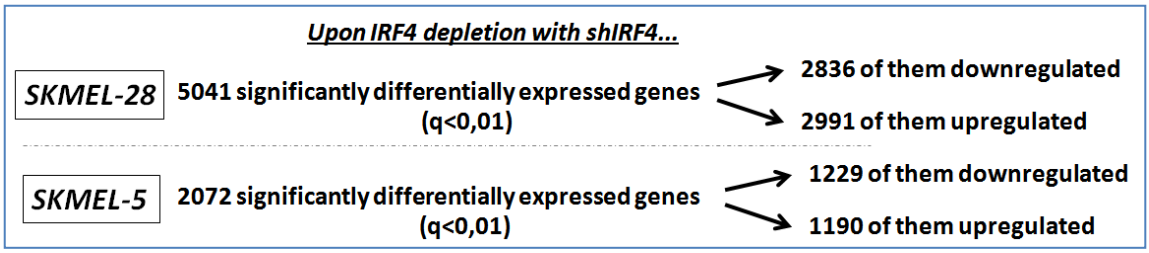

Figure 5.20. The number of genes significantly up-regulated or down-regulated upon IRF4 depletion, defined by DESeq, in SKMEL-28 and SKMEL-5 cell lines.

When compared to differentially expressed genes defined by Cuffdiff, we observed moderate to high levels of overlap (Figure 5.21).

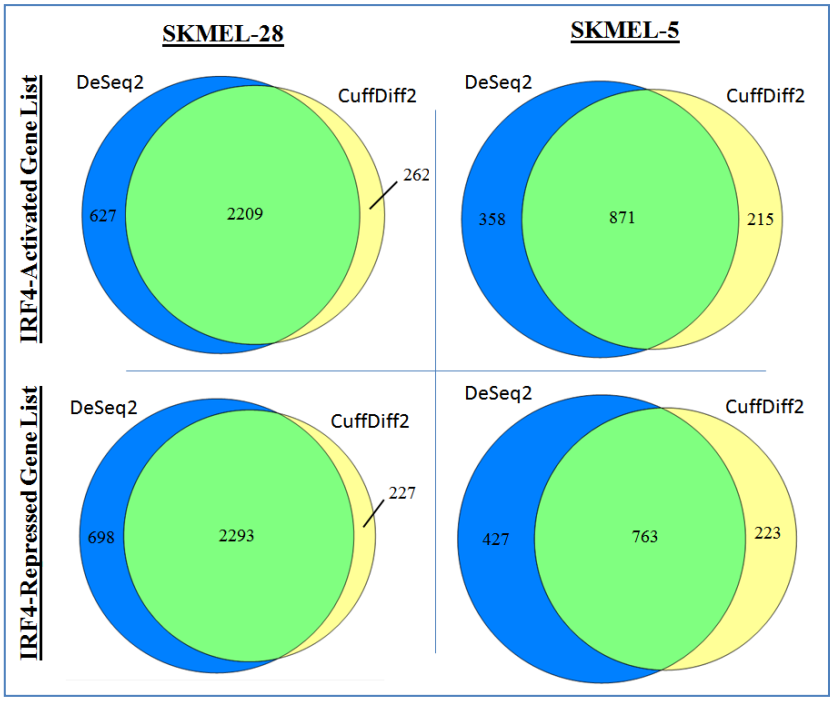

Figure 5.21. Comparison of Cuffdiff and DESeq for the number of differentially expressed genes in each case.

5.9. Regulation of MITF upon IRF4 Knock-down and Over-expression

Microphthalmia-associated transcription factor (MITF) is a master regulator of melanocyte development and pigment production (Cheli *et al.*,2010). In melanoma, MITF is considered as an oncogene and plays roles in cell cycle, proliferation, cell survival, metastasis and invasion (Levy *et al.*,2006). Due to its key role in melanoma, we focused on MITF after we observed that it is upregulated upon IRF4 knock-down. Although MITF is a significantly differentially expressed gene in RNA-seq upon IRF4 depletion in SKMEL-28, it is not significant in SKMEL-5. On the other hand, RT-qPCR results showed a modest alteration of MITF expression levels in SKMEL-5 cell line (Figure 5.16). As a further step to verify MITF increase due to IRF4 depletion in protein level, we performed western blotting analysis on the whole cell lysates of SKMEL-5 (Figure 5.22A and Figure Q.1A) and SKMEL-28 (Figure 5.22B and Figure Q.1B). In SKMEL-5, although undetectable in 48h, a slight increase for MITF was observed in shIRF4 transduced sample at 72h time point (Figure 5.22A). In SKMEL-28, MITF increase is detectable at both time points upon IRF4 knock-down (Figure 5.22B). In Figure Q.1A and Q.1B, alteration in MITF especially at 72h, 78h and 84h time points are very clear for SKMEL-5 and SKMEL-28.

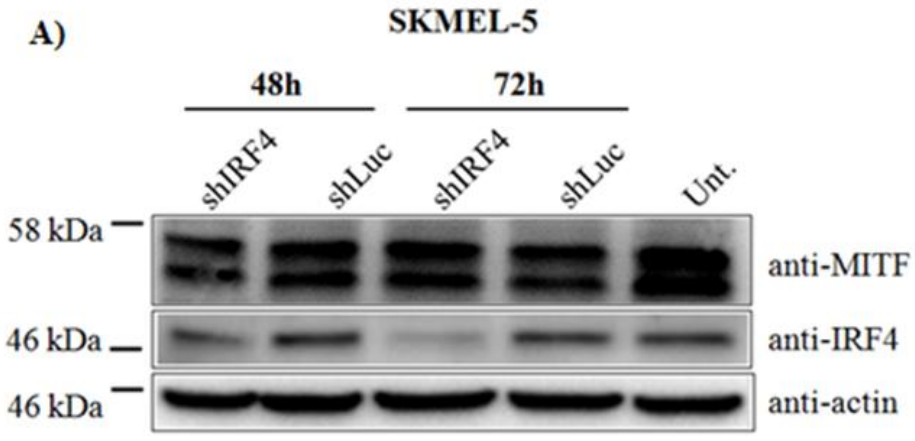

Figure 5.22. MITF protein levels upon IRF4 knock-down in A) SKMEL-5 and B) SKMEL-28 cell lines, as detected by immunoblotting. Total ERK is used as loading control.

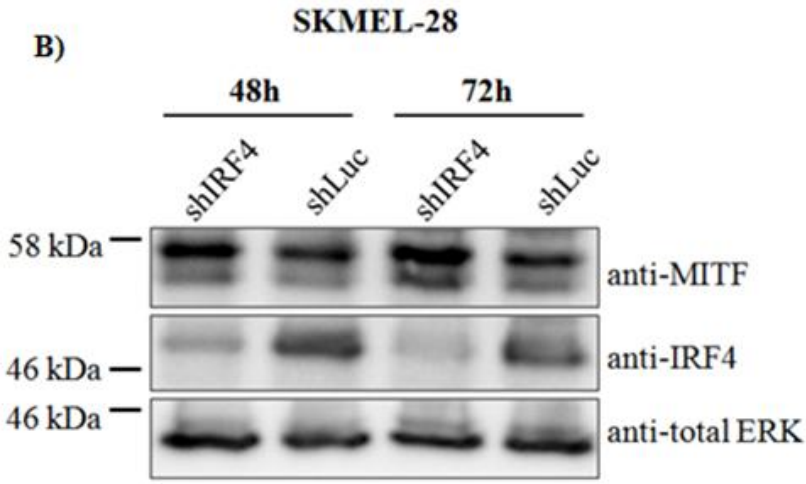

Figure 5.22. MITF protein levels upon IRF4 knock-down in A) SKMEL-5 and B) SKMEL-28 cell lines, as detected by immunoblotting (cont.). Total ERK is used as loading control.

We also performed IRF4 knock-down in A2058 and G-361 which are among IRF4-positive melanoma cell lines. We did not observe MITF protein level changes upon IRF4 knock-down in either of the cell lines (Figure R.1A and R.1B).

In order to verify the effect of IRF4 on MITF expression in a complementary assay, we over-expressed IRF4 ectopically. For this purpose we used mammalian pIRES2-eGFP-IRF4 and pIRES2-eGFP-GFP (control) episomal expression vectors (see Materials and Methods). We observed with western blotting MITF decrease when IRF4 is over-expressed in both cell lines, SKMEL-5 (Figure 5.23A) and SKMEL-28 (Figure 5.23B and S.1).

In conclusion, we showed the IRF4-repressed characteristic of MITF expression in SKMEL-5 and SKMEL-28 cell lines both by down-regulation and up-regulation of IRF4, but not in A2058 and G-361 cell lines.

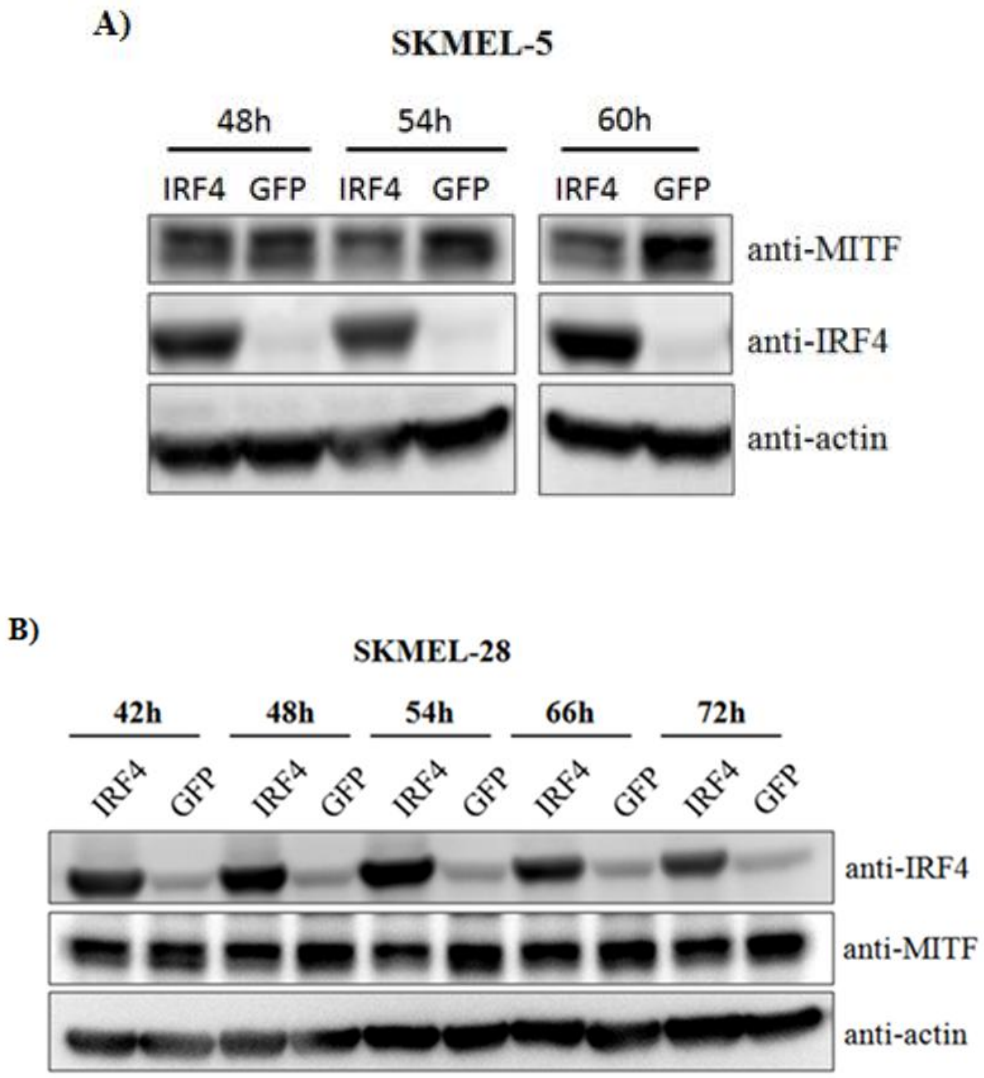

Figure 5.23. MITF protein levels upon IRF4 over-expression in A) SKMEL-5 and B) SKMEL-28 cell lines.

5.10. Regulation of RAS Targets upon IRF4 Knock-down and Over-expression

NRAS is a key player in melanoma: either NRAS or its downstream effector BRAF is mutated in most of the melanoma cases. Both of the cell lines, SKMEL-28 and SKMEL-5 have the BRAF V600E substitution and therefore they have an over-active MAPK/ERK pathway. ERK1/2 become activated upon phosphorylation which turns on their kinase activity. Activated ERKs can promote cell cycle entry and induce proliferation. NRAS, in

addition to being an upstream modulator of BRAF, is also at the upstream of PI3K/AKT pathway. PI3K signaling pathway is often activated alongside the ERK pathway by active NRAS. In this pathway, AKT becomes active by phosphorylation on Thr308 when pathway is triggered (Chambard *et al.*, 2007) (see Section 1.2.2). As we have detected NRAS mRNA levels decrease upon IRF4 down-regulation both by qRT-PCR and RNA-seq, we decided to investigate the effect of this modulation might have on the activity of these pathways by checking the phosphorylation status of two important downstream targets, ERK1/2 and AKT.

We first performed immunoblotting for phosphorylated ERK on IRF4 down-regulated SKMEL-5 (Figure 5.24A and T.1A) and SKMEL-28 cells (Figure 5.24B and T.1B). We have not observed an alteration in p-ERK levels upon IRF4 knock-down.

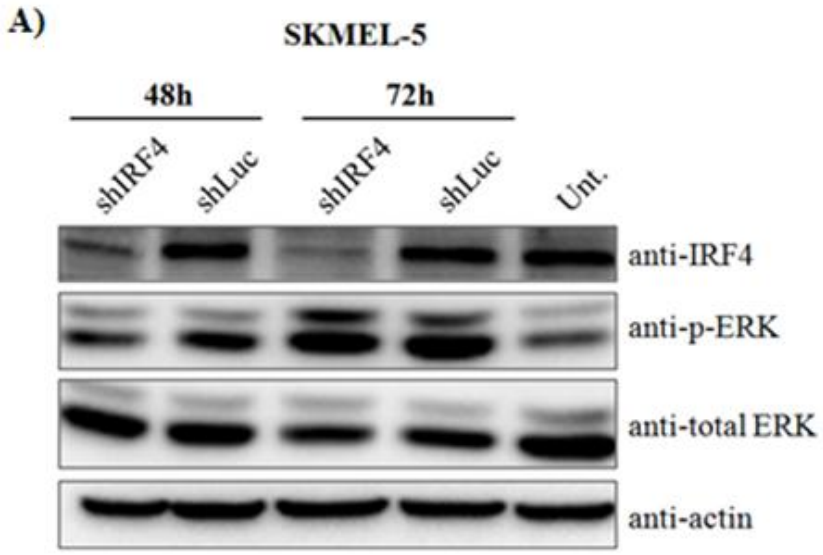

Figure 5.24. Phospho-ERK (p-ERK) protein levels upon IRF4 knock-down in A) SKMEL-5 and B) SKMEL-28 cell lines. Anti-total ERK is used as loading control in Figure B.

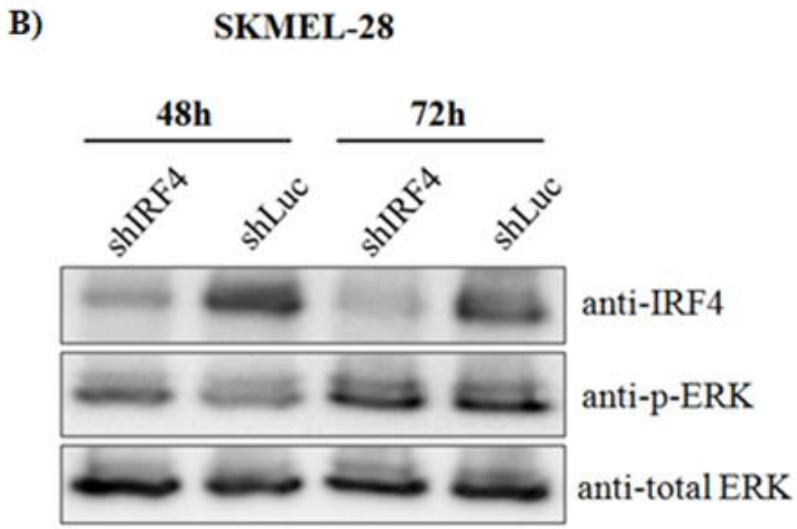

Figure 5.24. Phospho-ERK (p-ERK) protein levels upon IRF4 knock-down in A) SKMEL-5 and B) SKMEL-28 cell lines (cont.). Anti-total ERK is used as loading control in Figure B.

Although we did not observe any regulatory effect of IRF4 on p-ERK1/2 levels, western blotting results of IRF4 down-regulated SKMEL-28 cells show decreased phosphorylated AKT (p-AKT (Ser473) and p-AKT (Thr308)) levels compared to control (Figure 5.25B and U.1B). However, in SKMEL-5, results were inconclusive as alteration is not stable (Figure 5.25A) or could not be replicated at IRF4 knock-down experiments (Figure U.1A). It should also be noted that alteration in NRAS mRNA expression in SKMEL-5 cell line is relatively modest compared to SKMEL-28 (Figure 5.16) which might be a reason for undetectable change in p-AKT protein level.

In A2058 and G-361 cell lines with IRF4 knock-down, when compared to shLuc (control) transduced counterparts, we did not observed p-AKT level change for either of the cell lines (Figure R.1A and R.1B).

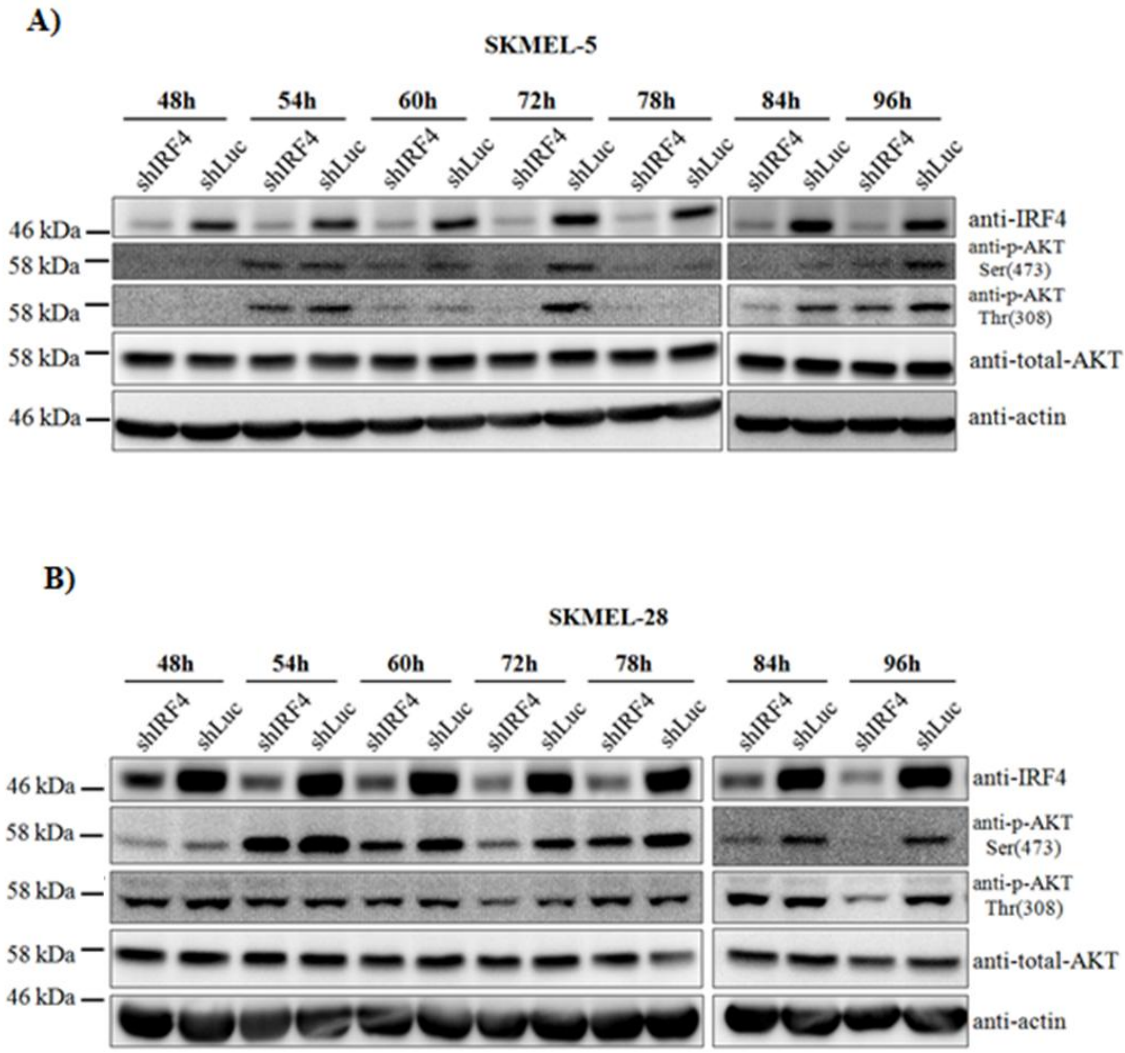

Figure 5.25. Phospho-AKT protein levels upon IRF4 knock-down in A) SKMEL-5 and B) SKMEL-28 cell lines.

In order to verify the effect of IRF4 on p-AKT regulation in a complementary assay, we checked p-AKT (Ser473 and Thr308) levels by western blotting in IRF4 over-expressed SKMEL-5 and SKMEL-28 cell lines. SKMEL-28 cell line shows p-AKT (Ser473 and Thr308) increase compared to control when IRF4 is over-expressed (Figure 5.26B), except of 66h time point. Figure V.1A, as a repeat experiment for SKMEL-28, also verifies the regulatory role of IRF4 on AKT phosphorylation in this cell line. However, p-AKT levels in SKMEL-5 did not change upon IRF4 over-expression (Figure 5.26A). Over-expression of IRF4 in MEL-ST cell line, an immortalized melanocyte line lacking IRF4

expression, also shows IRF4-activated characteristic of AKT phosphorylation as in the case of SKMEL-28 (Figure V.1B).

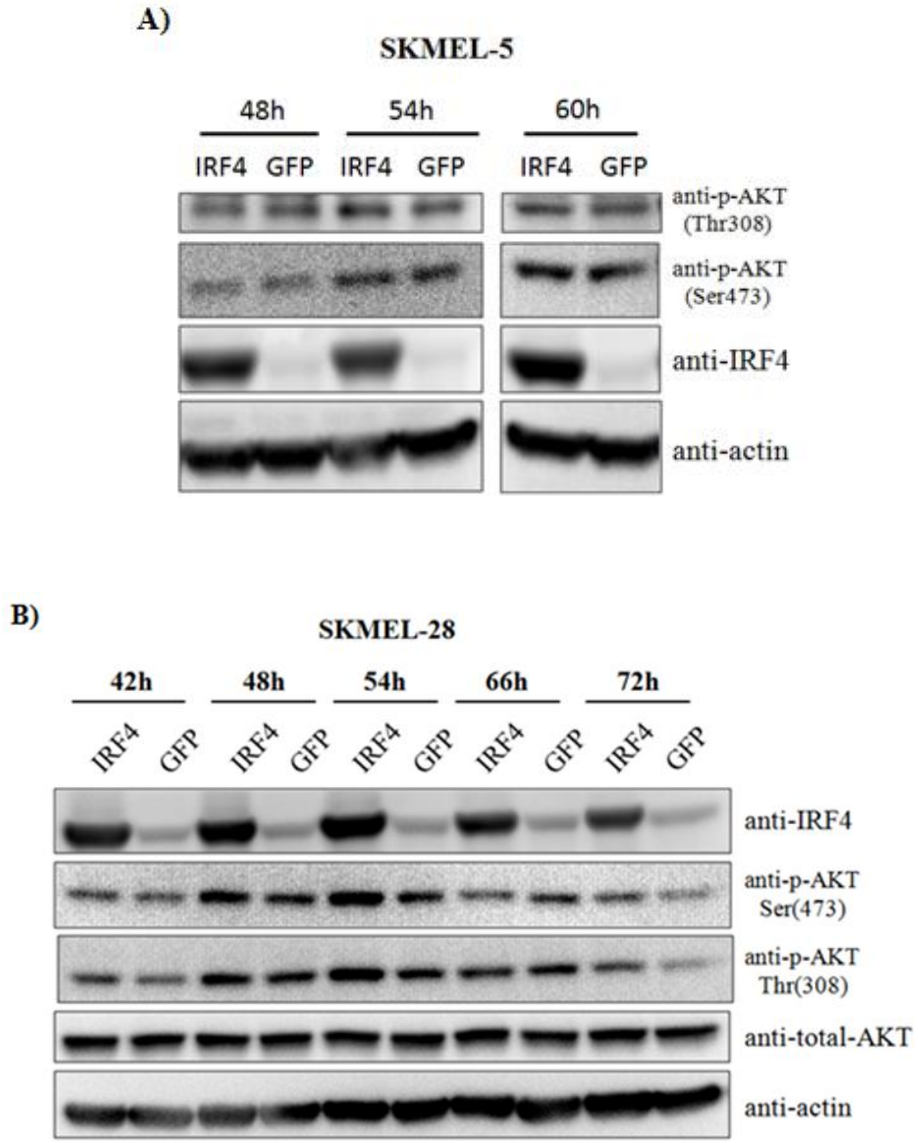

Figure 5.26. Phospho-AKT protein levels upon IRF4 over-expression in A) SKMEL-5 and B) SKMEL-28 cell lines.

Overall, p-AKT levels in SKMEL-28 and MEL-ST cell line increases upon IRF4 over-expression but, SKMEL-5 cell line didn't show a detectable change. However, when IRF4 was down-regulated, p-AKT levels decreased at certain time points for both of the cell lines, SKMEL-5 and SKMEL-28.

6. DISCUSSION

IRF4 has been extensively studied in immune cells, especially in lymphocytes, as it has critical roles in lymphocyte development and function. In addition to its roles in normal cells, previous studies also linked IRF4 to immune cell related malignancies, such as activated B-cell-like diffuse large lymphoma (ABC-DLBCL) and multiple myeloma (MM). Shaffer *et al.* showed that ABC-DLBCL and MM cells have a non-oncogenic addiction to IRF4 expression, and its expression level in these cell lines are important for the viability of the cancer cells (Shaffer *et al.*, 2008, Yang *et al.*, 2012). Previously, we realized that IRF4 expression was also present in melanoma cells, not necessarily as high as in hematological cancer types but also distinctly higher than other types of cancer cells, which presumably have low or absent levels of IRF4 expression (Ayhan, 2014). Furthermore, several genome-wide association studies linking a particular SNP in IRF4 locus to melanoma predisposition (Duffy at al., 2010, Han *et al.*, 2011, Pena-Chilet, 2013) aroused interest to reveal its functional role in melanoma. Preliminary studies in melanoma cell lines, performed by our group, showed a similar non-oncogenic addiction of these cells to IRF4 suggesting that viability loss upon down-regulation of IRF4 expression in IRF4-positive melanoma cell lines might be due to a cell cycle arrest at G2/M checkpoint (Ayhan, 2014).

We checked several published melanoma gene expression studies with patient survival data in order to find out if there is any correlation between overall survival and IRF4 expression. As another supportive evidence on critical role of IRF4 in melanoma, we observed that in two of the studies performed with melanoma patients, IRF4 expression is inversely correlated ($p < 0.05$) with patient survival (Bogunovic *et al.*, 2009, Journe *et al.*, 2011) (Figure A.1, Table 1.2). On the contrary, in one of the studies IRF4 expression correlated ($p < 0.05$) with patient survival (Jonsson *et al.*, 2010) (data not shown). All the patients in this study were subjected to DTIC (chemotheraphy drug used in the treatment of malignant melanoma) treatment after biopsies were taken. Hence, different outcomes between these studies might be related to high benefit rate in response to DTIC treatment in the study of Jonsson *et al.*

Data supporting critical role of IRF4 in melanoma cell lines encouraged us for further studies, one of which is to reveal its downstream transcriptional gene targets and therefore, to get insight about its roles in melanoma.

In order to find out IRF4 regulated genes, we decided to perform whole transcriptome expression profiling between two conditions which are IRF4 down-regulated (shIRF4 transduced) and control (shLuc transduced) melanoma cells. Expression profiling was performed using whole transcriptome sequencing (RNA-seq), which is a frequently used method alongside expression microarrays.

As a first step, we evaluated the expression of IRF4 in melanoma cell lines, as a replication study of Ayhan, 2014, by reverse transcriptase quantitative PCR (RT-qPCR) (Figure B.1) and western blotting (Figure B.2). Additionally, we used intracellular flow cytometry as another method to measure IRF4 levels (Figure 5.1). We observed that in protein level, SKMEL-5 and A2058 cell lines have moderate, and SKMEL-28 and G-361 cell lines have relatively higher level of expression (Figure B.2). This phenotype, having divergent level of IRF4 expression, was one of the reasons for the selection of SKMEL-28 and SKMEL-5 cell lines for RNA-seq study. SKMEL-5 and SKMEL-28 cell lines also differ in the gender (SKMEL-28, male origin; SKMEL-5, female origin) and the tissues the cell lines were derived from (SKMEL-28, skin; SKMEL-5, axillary node metastasis) which are additional points satisfying our criteria of displaying divergent characteristics, so that results would be more global in terms of melanoma biology.

In order to compare gene expression profiles of shIRF4 and shLuc transduced cells, we decided to select a suitable time point after transduction. After we realized that down-regulation of IRF4 happens at early time-points in SKMEL-28 cell line (Figure 5.4), we focused on the first 4 days after transduction. Analysis on SKMEL-28 and G-361 cell lines either by western blotting or intracellular flow cytometry verified a satisfactory down-regulation at 72h time point (Figure 5.5, Figure 5.6). It should also be noted that we have not been able to eliminate IRF4 expression completely, similar to the previous studies (Shaffer *et al.*, 2008; Yang *et al.*, 2012). Although down-regulation of IRF4 in protein level is detectable at 48h time point, it was lower in 72h time point. Other parameter we tried

to optimize was transduction efficiency due to an observation of viability loss in control cells (shLuc transduced) observed in GFP competition assay resulting from high level of transduction. Assuming that high level of transduction also indicates more virus introduction and integration to most cells in the population, we hypothesized that this could induce additional stress on excessively transduced cells, which may lead to death or senescence. Although we encountered this effect after relatively longer period of time than 72 hours with 97% transduction efficiency on shLuc transduced cells (Figure 5.2), to keep away from the effects of high efficiency transduction, we aimed not to exceed 90% of transduction efficiency for RNA-seq experiments, as we have also seen satisfactory results with 86% transduction efficiency (Figure C.1A).

In order to avoid experimental bias at the step of library preparation, all the total RNA samples isolated should be as intact (i.e., not degraded) as possible. As the first step in library preparation is the purification by poly-A tail selection, degraded RNAs are prone to resulting in relatively more hits near to poly-A site. In this regard, our samples were very close to be fully intact since nearly all of them has an RNA integrity number (RIN) very close to 10 as determined by Agilent Bioanalyzer 2100 (Table 5.1).

Upon completion of RNA-seq experiments, we started our bioinformatics pipeline by quantifying per base read qualities which were in satisfactory range for all samples (Figure H.1 and H.2). As a result, we did not perform any manipulation on the reads before mapping step.

In the mapping step of reads to the reference genome, we preferred to use transcriptome mapping rather than genome mapping as we are only interested in differential expression analysis of known genes, not in transcript discovery. In order to identify novel transcripts, genome mapping can be used in further studies. We also selected the reads which maps only once to the transcriptome to avoid the uncertainty about the source of individual sequencing reads (Table 5.2). Mapped reads can be visualized by Integrated Genome Viewer as shown in Figure I.1 for the IRF4 locus for all the samples in SKMEL-28 as an example. Reduction in the read number can be observed even by eye when shIRF4 transduced samples are compared to shLuc transduced samples.

Following mapping of reads onto transcriptome, we performed differential expression analysis by Cuffdiff. When we observed a lower number of significant DEGs in SKMEL-5 dataset compared to SKMEL-28, we questioned if this could be a result of lower number of sequencing reads used in the SKMEL-5 analysis which may lower the power of Cuffdiff to detect DEGs (Table 5.2). To test this, we lowered the number of SKMEL-28 mapped reads approximately to SKMEL-5 dataset level, and compared the number of DEGs with the original value (Table J.1 and Figure 5.13). We detected a slight difference which cannot be accounted for the difference between SKMEL-28 and SKMEL-5 DEGs. Therefore, difference in DEG number can likely be explained by our criteria of selecting the cell lines (i.e., cell lines being different in IRF4 expression levels, gender and tissue origin).

In order to understand how variable (in terms of FPKM) is the biological replicates between each other, we applied pair-wise Spearman correlation test. All correlation values were around 0.95 and 0.96 (Table 5.5) which are in acceptable range. Moreover, dendrograms generated based on sample distances (Jensen-Shannon distance) shows clustering of biological replicates between conditions (i.e., shIRF4 vs. control) as expected (Figure 5.14). These results provide evidence for the reproducibility of sample and library preparation.

As a verification of RNA-seq, we compared the fold change results of RNA-seq with RT-qPCR for eight of the genes (*IRF4*, *MITF*, *BRCA2*, *NRAS*, *CDKN2A*, *MYC*, *SQLE* and *TYR*) (Figure 5.16 and Table 5.6) which were selected based on various level of expression and their relation to melanoma or IRF4. *MITF* and *TYR* are genes related to pigmentation; *NRAS* and *CDKN2A* are genes contributing to melanomagenesis; *BRCA2* and *MYC* are genes deregulated in most of the cancers; and *SQLE* is a known IRF4 target in multiple myeloma. With a few exceptions, there is a high correlation between these two different methods.

Although our analysis with Tophat and Cuffdiff pipeline shows reproducibility in general (Figure 5.16), we wanted to use another software to find DEGs and compare the results with Cuffdiff in order to see the difference in output between two widely-used dif-

ferential expression analysis software. For this purpose, we used another commonly used tool, DESeq, to define DEGs (Figure 5.20). DESeq uses raw counts for each gene to find DEGs. In order to do this, after using Tophat for mapping, HTSeq is used for generating a table of genes and corresponding read counts. At this step, we used "intersection-strict" method to eliminate reads mapping ambiguously (onto two or more different genes). When we compared the results (Figure 5.21) we did not observe a high enough difference to conclude that they produced fundamentally divergent results suggesting that both programs are working properly. We chose to do our analysis via Cuffdiff as it has a more established background with protocol papers and integrated diagnostic programs, such as cummeRbund, allowing user friendly utilization.

After we determined significantly DEGs, we split them up as IRF4-activated (down-regulated genes upon IRF4 knock-down) and IRF4-repressed (up-regulated upon IRF4 knock-down). These lists were analyzed using gene enrichment analysis to find over-represented Gene Ontology terms in biological process domain (GO_BP). Among several alternatives we chose GOrilla for this purpose, as it has an up-to-date database (Eden *et al.*, 2009). As a result of the GOrilla analysis and its graphical output, enriched GO_BP terms of IRF4-activated genes in SKMEL-28 suggest an association to mitotic activity alongside with an increased transcription and translation. In the DAG of activated GO term list of SKMEL-5, nearly all of the GO_BP terms at the bottom of branches are related to proliferative characteristic.

Gene ontology enrichment analysis with IRF4-repressed gene lists, for SKMEL-5 and SKMEL-28, we observe GO terms mainly related to lipids, such as sterol biosynthetic process, which might be related to cellular membrane structures. Additionally, in SKMEL-28, as distinct from SKMEL-5, "vesicle mediated transport" and "melanin synthesis" (not shown in DAG but in Table N.2) might be a link to melanocyte-specific vesicles, melanosomes.

Common genes shared between SKMEL-28 and SKMEL-5 for IRF4-activated and IRF4-repressed lists were also analyzed to find enriched GO_BP terms by GOrilla. In Figure 5.18, GO terms very significantly enriched ($p < 10^{-9}$) for IRF4-activated genes are

shown. It could be deduced that proliferation related terms including "cell cycle" (i.e., *E2F2*, e2f transcription factor 2) and "mitotic division" (i.e., *BRCA2*, breast cancer 2) are dominators for IRF4-activated genes. This result is consistent with the effect of IRF4 on cell viability we observed in GFP competition assays. Highest ranked enriched GO terms for IRF4-repressed genes ($p < 10^{-9}$) are shown in Figure 5.19. Related DAG contains "lipid biosynthetic process" as the "child" term, but in Table P.1 "lipid" related terms like sterol, cholesterol, steroid, glycolipid, membrane lipid biosyntheses can also be observed. It is convincing that IRF4 represses biological processes related with lipid synthesis in melanoma cells (i.e., *SQLE*, squalene monooxygenase). This regulation could be related to membrane or more specifically melanosome synthesis as we have also seen related enriched terms ("vesicle mediated transport" and "melanin synthesis") in over-represented GO terms of IRF4-repressed genes in SKMEL-28. In further experiments, melanosome transfer assay can be performed to evaluate the effect of IRF4 on melanosome formation and transport.

We sorted significantly differentially expressed genes according to their fold change in differential expression between two conditions. Highest ranked (the first 100 genes) differentially expressed genes which are common in both cell lines are shown in Table 5.3 (IRF4-activated list) and Table 5.4 (IRF4-repressed list). Among IRF4-activated genes, *EPHB3* is a gene encoding an ephrin receptor (a receptor tyrosine kinase) which binds ephrin-B family ligands and functions in axon guidance during development. It has been reported that EPHB3 is over-expressed in melanoma cells compared to normal melanocytes (in 94% of melanoma lines) so it may promote tumor progression (Easty *et al.*, 2011). In non small-cell lung cancer (NSCLC), its over-expression induces cell growth and migration, and repression leads to inhibition of cell proliferation, migration, tumor growth and metastasis (Ji *et al.*, 2011). Also in prostate cancer cell line, it stimulates invasive migration (Wang, 2011). Another ephrin receptor, EPHA2, although not in the highest ranked DEGs, is significantly differentially expressed (IRF4-activated characteristics) in both cell lines. EPHA2 expression was linked to melanoma thickness, increased cell proliferation and vascular mimicry so it has been verified as an important oncogene in melanoma (Udayakumar *et al.*, 2011). One of the top IRF4-activated genes, *ECE1*, encoding an enzyme to convert big endothelin-1 to endothelin-1, was also shown to induce invasiveness in prostate and breast cancer cell lines (Smollich *et al.*, 2007, Whyteside *et al.*, 2010).

MTFP1, encoding a mitochondrial protein, and *PON2* which encodes a membrane-bound protein acting as a cellular antioxidant, in Table 5.3, have anti-apoptotic characteristics (Tondera *et al.*, 2004, Witte *et al.*, 2011). *PON2* is accepted as an oncogene which provides resistance against different chemotherapeutics in human cancer cell culture models (Witte *et al.*, 2011). ADAM9, a metallopeptidase mediating cell-cell or cell-matrix interaction, and LAMP1 which presents carbonhydrate ligands to selectins, were also linked to metastasis in certain cancer cell lines (Agarwal *et al.*, 2014, Lin *et al.*, 2014). LAMP1 was also shown to facilitate metastatis of melanoma cells to lungs (Agarwal *et al.*, 2014). In Table 5.3, there are 2 genes belonging to solute carrier family, *SLC2A3* and *SLC44A1*, which are responsible for glucose and choline transport, respectively. It has been demonstrated that SLC2A3 regulates energy metabolism in cancer cells (such as breast and lung cancers) and it is up-regulated due to accelerated metabolism and high glucose requirements (Macheda *et al.*, 2005). Choline transporter, SLC44A1, is also important for cancer cells because choline plays role in structure and function of cell membranes and it is required for new membrane synthesis. Cancer cells require a fast membrane biosynthesis as they proliferate frequently. Choline metabolite is used as cancer biomarker and its metabolism is strongly correlated with malignant progression (Inazu *et al.*, 2013). Although not in the highest ranked DEG list in Table 5.3, *E2F2*, which was discovered for its critical role in cell cycle progression, is also a significant IRF4-activated gene in both cell lines. Upregulation of E2F2 activity induces proliferation in melanoma cells (Halaban *et al.*, 2000). Activity of E2F family proteins are regulated by cyclins and cyclin dependent kinases (CDKs). Increase in CDK activity due to up-regulated cyclin concentration leads to phosphorylation of Retinablastoma (Rb) protein which is the inhibitor of E2F family (Duronio and Xiong, 2013). Consistently, expression of certain cyclin family members, including *CCNA2* (cyclin A2), *CCNB1* (cyclin B1), *CCNC* (cyclin C), *CCND1* (cyclin D1), *CCND3* (cyclin D3), *CCNE1* (cyclin E1), *CCNF* (cyclin F) are downregulated significantly in both cell lines upon IRF4 depletion (not shown in Table 5.3). Overall, there are numerous genes, having roles in proliferation, tumor growth, migration and invasion, whose expression is repressed upon IRF4 depletion, suggesting a diverse role for IRF4 in melanoma biology.

In IRF4-repressed gene list, *CEND1*, which is an integral membrane protein and neuronal lineage-specific regulator, is one of the most affected gene in both cell lines upon

IRF4 knock-down (Table 5.4). It has been demonstrated that CEND1 mediates cyclin D1/Rb signaling pathway and negatively regulates proliferation in neurons, and its over-expression leads to inhibition of proliferation in a neuroblastoma cell line (Tsioras *et al.*, 2013). Attenuation of calcium release upon CEND1 upregulation and consequent effect on regulators of cell cycle proteins was demonstrated (Georgopoulou *et al.*, 2006). CEND1 has also anti-apoptotic properties besides anti-proliferative effects (Masgrau *et al.*, 2009). Another high ranked IRF4-repressed gene *LEPREL1,* encoding an enzyme important for collagen chain assembly, is also accounted as a potential tumor suppressor gene because it has an anti-proliferative effect in breast cancer and hepatocellular carcinoma cells via downregulation of cell cycle regulatory proteins (Shah *et al.*, 2009, Wang *et al.*, 2013). Another high ranked IRF4-repressed factor, 4E-BP2 (encoded from *ElF4EBP2*) binds to mRNA cap-binding protein elF4E and inhibits translation, leading to attenuation of cell growth and proliferation. It has been suggested that activation of PI3K-AKT-mTOR pathway induces 4E-BP2 phosphorylation leading to disassociation from elF4E protein so its translation inhibitory capacity is suppressed in most tumors (Martineau *et al.*, 2013). Additionally, elevated levels of elF4E are shown in 30% of cancer cells and it has been linked to tumorigenic transformation, proliferation and survival (Alain *et al.*, 2012, Lazaris-Karatzas *et al.*, 1990). *MAP2,* encoding a protein playing role in microtubule assembly, is one of the highest ranked IRF4-repressed gene, has been linked to cell death and cell cycle arrest in human melanoma cell lines (Song *et al.*, 2010). It has been shown that MAP2 expression inhibits melanoma progression via microtubule stabilization, cell cycle arrest in G2-M phase and growth inhibition (Soltani *et al.*, 2005). Overall, IRF4-repressed genes in highest ranks in both cell lines includes factors which inhibits proliferation, tumor growth or progression.

RNA-seq and RT-qPCR results showed the regulatory role of IRF4 on MITF which is an important player in melanoma as it is involved in cell cycle, proliferation, survival, pigmentation, metastasis and invasion (Levy *et al.*, 2006). In order to verify the effect of IRF4 on MITF at protein level, we performed western blotting assays. We observed IRF4-repressed characteristic of MITF protein expression (i.e., increases upon IRF4 down-regulation and decreases upon IRF4 over expression) in SKMEL-5 and SKMEL-28 cell lines both by IRF4 down-regulation (Figure 5.21 and Q.1) and over expression (Figure 5.22 and S.1). Interestingly, it was previously shown that when MITF was over-expressed,

IRF4 was up-regulated in SKMEL-28 cell line (Hoek *et al.*, 2008b). Moreover, previous study linking IRF4 to pigmentation (Praetorius *et al.*, 2013), demonstrated that when MITF was down-regulated by shMITF, IRF4 decreased both in mRNA and protein levels in 501mel, a human melanoma cell line. MITF binding to intron 4 of IRF4 was shown by ChIP analysis, indicating a direct regulation. This study also showed that MITF levels were unaffected by reduction in IRF4 in the same cell line (Praetorius *et al.*, 2013), as opposed to our observations in SKMEL-5 and SKMEL-28 cell lines. As MITF in protein and mRNA levels in G-361 (Figure 5.17 and R.1B) and in protein level in A2058 (Figure R.1A) was also not affected by shIRF4 transduction, we can conclude that regulatory role of IRF4 on MITF expression is not universal for melanoma cell lines. This may be due to epigenetic factors or other transcriptional cofactors present in different melanoma cell lines. Additionally, our results indicate that *POU3F2* is an IRF4-activated gene and its product BRN-2 is a transcriptional repressor of MITF (Goodall *et al.*, 2008). This protein could be acting as an intermediary on IRF4's repressive effect on *MITF* transcription. Our results from SKMEL-5 and SKMEL-28 suggest a model of MITF and IRF4 regulation as shown in Figure 6.1. MITF induces transcriptional activation of IRF4 (Praetorius *et al.*, 2013) and in turn, IRF4 represses the MITF expression and BRN-2 might be a potential link in-between. This regulation could be a control mechanism on MITF levels through IRF4.



Figure 6.1. A model for IRF4 and MITF cross regulation. MITF directly activates IRF4 expression (solid line) (Praetorius *et al.*, 2013). On the other hand repressive effect of IRF4 on MITF expression could be direct or indirect (dashed line).

One of the other important downstream effectors of IRF4 is NRAS according to RNA-seq and RT-qPCR results (Figure 5.16). NRAS is an important protein in melanoma, as a mediator of MAPK/ERK and PI3K/AKT pathways which are over-activated in most of the melanoma cells. In this regard, we checked the NRAS downstream elements, phospho-ERK1/2 and phospho-AKT (Section 5.10). ERK1/2 in MAPK pathway, and AKT in PI3K pathway, are activated upon phosphorylation upon NRAS activation (Dahl *et al.*, 2007), so we hypothesized that NRAS decrease upon IRF4 knock-down could influence phosphorylation status of these proteins. Western blotting assays showed unaffected levels of p-ERK1/2 in shIRF4 transduced SKMEL-5 (Figure 5.24A and T.1A) and SKMEL-28 (Figure 5.24B and T.1B) cell lines, suggesting that IRF4 does not have a regulatory effect on ERK phosphorylation. This might be due to constant hyperactivity of MAPK/ERK pathway as both of the cell lines carries $BRAF^{V600E}$ mutation. On the other hand, p-AKT levels (p-AKT (Ser473) and p-AKT (Thr308), two sites phosphorylated by mTORC2 and PDK1, respectively) in SKMEL-28 are reduced upon IRF4 knock-down (Figure 5.25B and U.1B) and increased in IRF4 over-expression (Figure 5.26B and V.1A) suggesting that IRF4 has effect on AKT activation. However, if regulation is through NRAS or not should be also investigated as AKT has other upstream regulators such as mTORC2. In SKMEL-5, results were inconclusive in a way that alteration is not stable over time-series in IRF4 knock-down experiments (Figure 5.25A and U.1A) and shows no alteration in IRF4 over-expression study (Figure 5.26A). It should also be noted that in SKMEL-5, alteration in NRAS mRNA levels were significant but relatively lower compared to SKMEL-28 in both RNA-Seq and RT-qPCR assays. We also applied IRF4 over expression experiment in MEL-ST, which is an immortalized melanocyte cell line and has no observable expression of IRF4 (Figure 5.1, B.1 and B.2). In this cell line, we detected p-AKT level increase upon IRF4 expression, especially at 60h time point very convincingly (Figure V.1B). If IRF4 is at the upstream of NRAS, affecting p-AKT levels, and MITF, because these players have important roles in melanoma, critical role of IRF4 in melanoma cell lines could be deduced that we have demonstrated also in previous studies (Ayhan, 2014).

In summary, after performing a comprehensive analysis of RNA-seq experiments and the following GO enrichment analysis, we suggest IRF4 positively regulates proliferative phenotype. On the other hand, its activity represses lipid biosynthesis, in a general manner. Effect of IRF4 on proliferation is a supportive factor for the hypothesis that IRF4

knock down leads to viability loss in melanoma cells (Ayhan, 2014). Repressive effect of IRF4 on "lipid synthesis" alongside with "membrane" and "transport" related GO terms and "melanin biosythesis" suggest that it might have a regulatory effect on melanosome production and transport. Furthermore, ongoing ChIP-Seq experiment to reveal IRF4 direct targets will help to gain more insight about its transcriptional regulatory role and to develop more accurate hypotheses. In general, high-throughput analyses should be combined with other methods, both for accuracy and replication of the results, as certain significant changes might also be related to secondary factors, such as off-target effects of shRNAs.

APPENDIX A: KAPLAN MEIER PLOTS OF PATIENTS WITH LOW AND HIGH IRF4 EXPRESSION PROFILES

A)

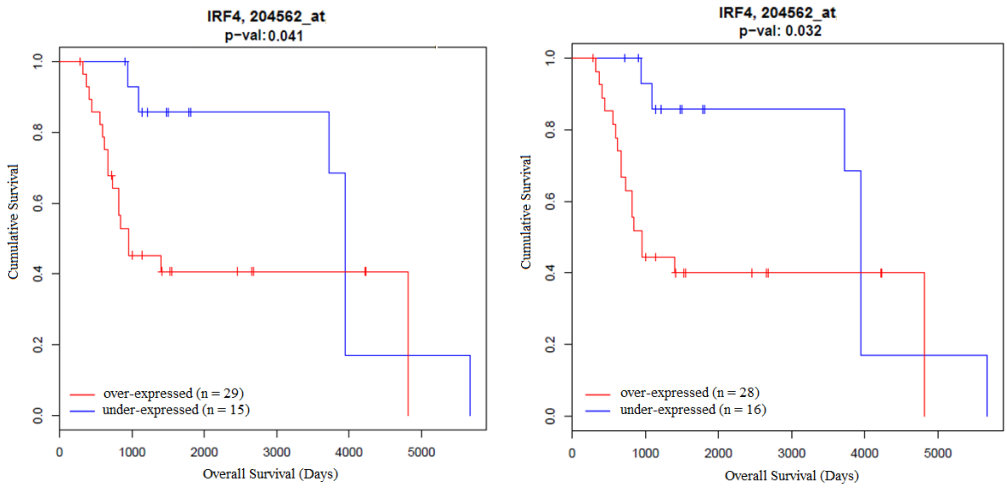

B)

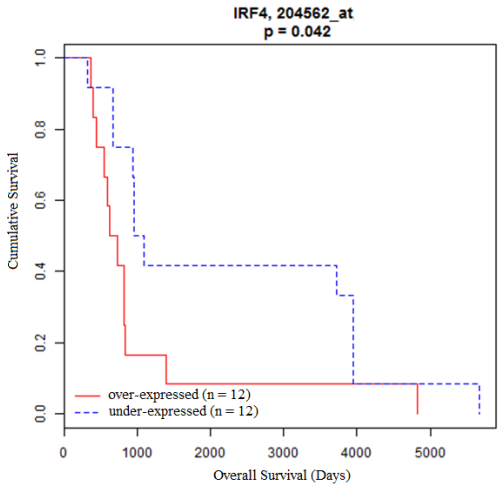

Figure A.1. Patient survival plots from Bogunovic *et al.* dataset. All the samples taken from patients were subjected to microarray analysis, and here in the plots, survival of patients with low IRF4-expressing samples are compared to survival of patients with high IRF4-expressing samples. A) All the patients (n=44), but sub-grouped in different sizes B) Censored patients are excluded (n=24).

APPENDIX B: REPLICATION OF ENDOGENOUS IRF4 LEVEL DETERMINATION BY WESTERN BLOTTING AND RT-qPCR

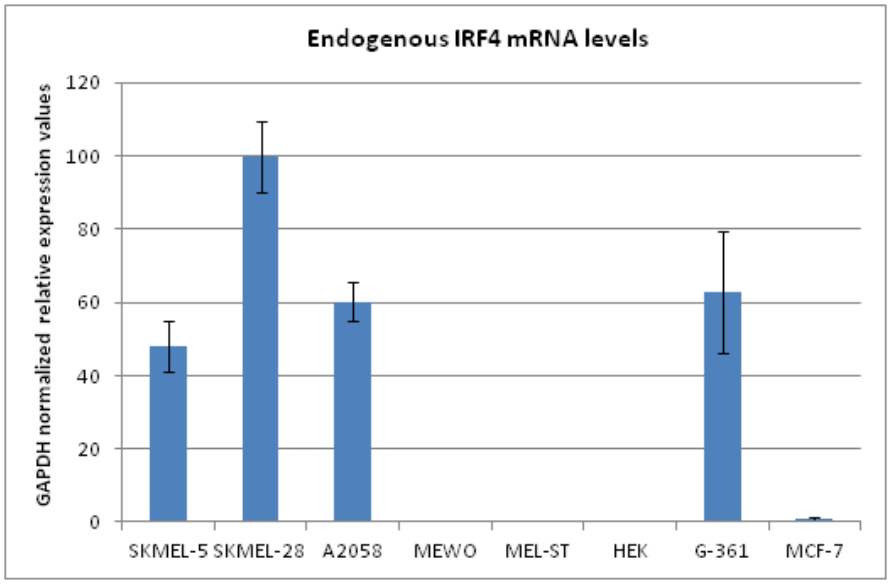

Figure B.1. qRT-PCR result showing endogenous IRF4 mRNA levels at indicated human cell lines. SKMEL-5, SKMEL-28, A2058, G-361 and MEWO are melanoma cell lines. MEL-ST is an immortalized melanocyte, HEK is an embryonic kidney, MCF-7 is a breast cancer cell line.

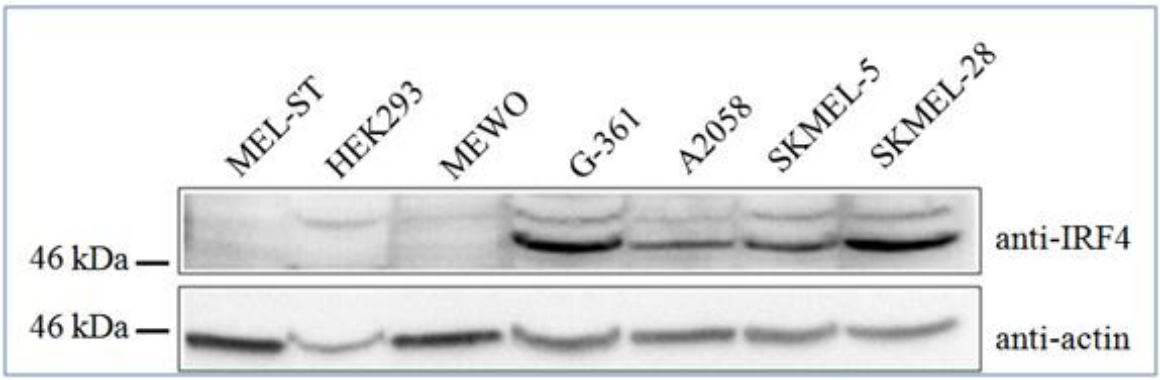

Figure B.2. Western blotting result showing endogenous IRF4 protein levels at indicated cell lines.

APPENDIX C: REPLICATION OF GFP COMPETITIONS

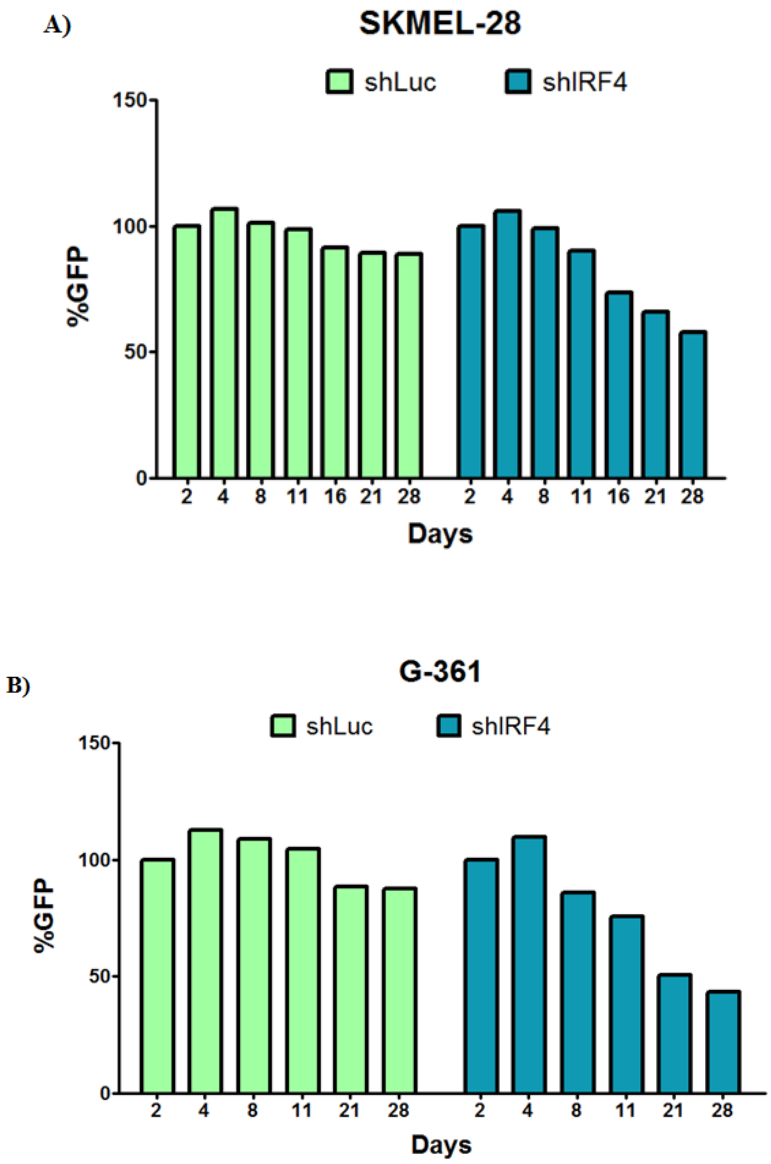

Figure C.1. GFP competition experiments without shLuc normalization. All the time points were normalized to only the untransduced cells' data. Error bars represent SEM of replicates. Transduction efficiencies are A) shLuc, 86%; shIRF4, 83% B) shLuc, 51%; shIRF4, 59% C) shLuc, 70%; shIRF4, 82% D) shLuc, 62%; shIRF4, 50%.

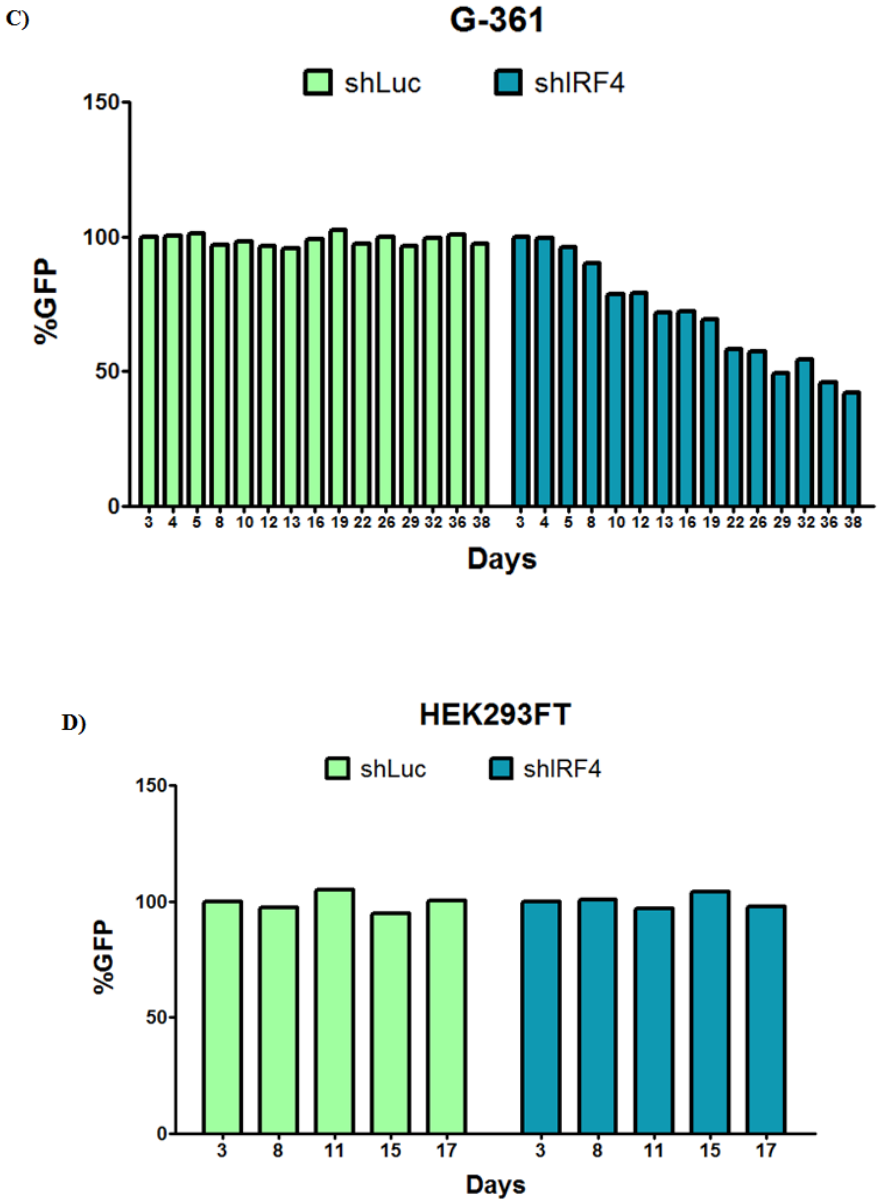

Figure C.1. GFP competition time points without shLuc normalization (cont.). All the time points were normalized to only the untransduced cells' data. Error bars represent SEM of replicates. Transduction efficiencies are A) shLuc, 86%; shIRF4, 83% B) shLuc, 51%; shIRF4, 59% C) shLuc, 70%; shIRF4, 82% D) shLuc, 62%; shIRF4, 50%.

APPENDIX D: INTRACELLULAR FLOW CYTOMETRY RESULTS FOR GOAT SERUM TREATED SKMEL-28 CELLS

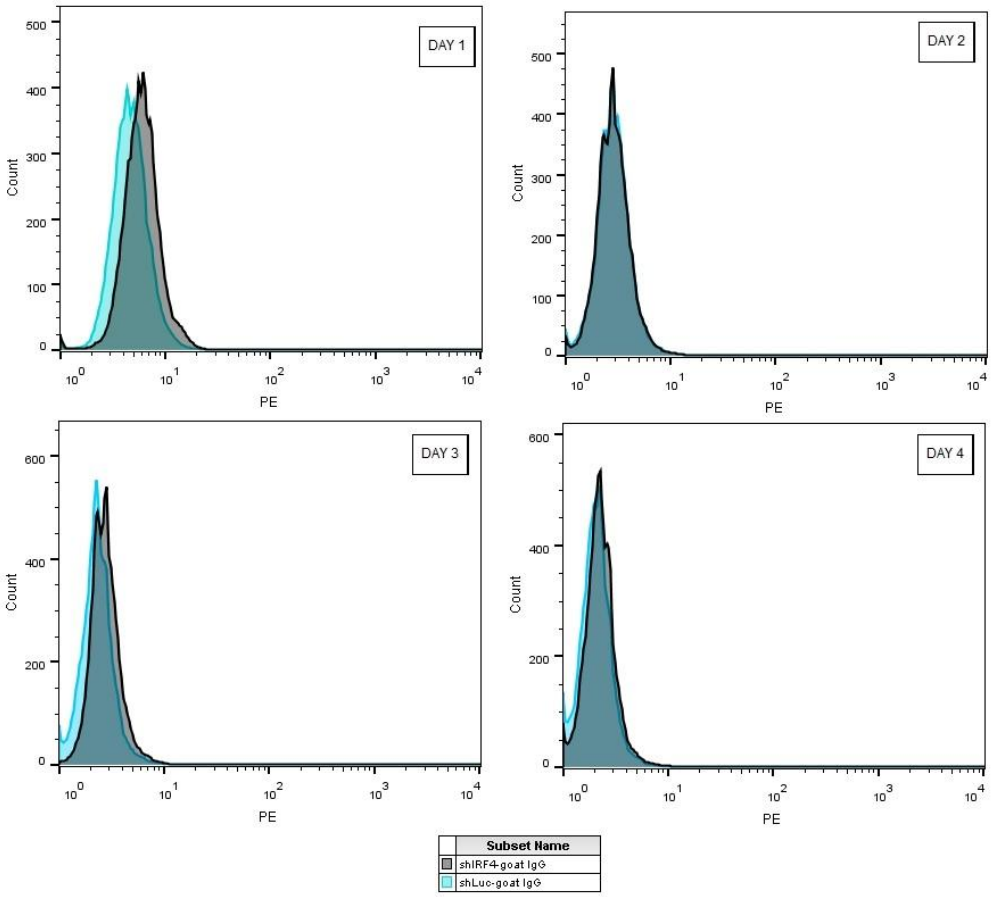

Figure D.1. Intracellular flow cytometry results of goat serum IgG treated SKMEL-28 cell line as negative controls of samples in Figure 5.6. Intensity of fluorescence emitted from phycoerythrin (PE) which is conjugated to secondary antibodies are shown on the x-axis and cell counts are shown on the y-axis.

APPENDIX E: INTRACELLULAR FLOW CYTOMETRY RESULTS OF shIRF4 AND shLUC TRANSDUCED SKMEL-28 CELL LINE

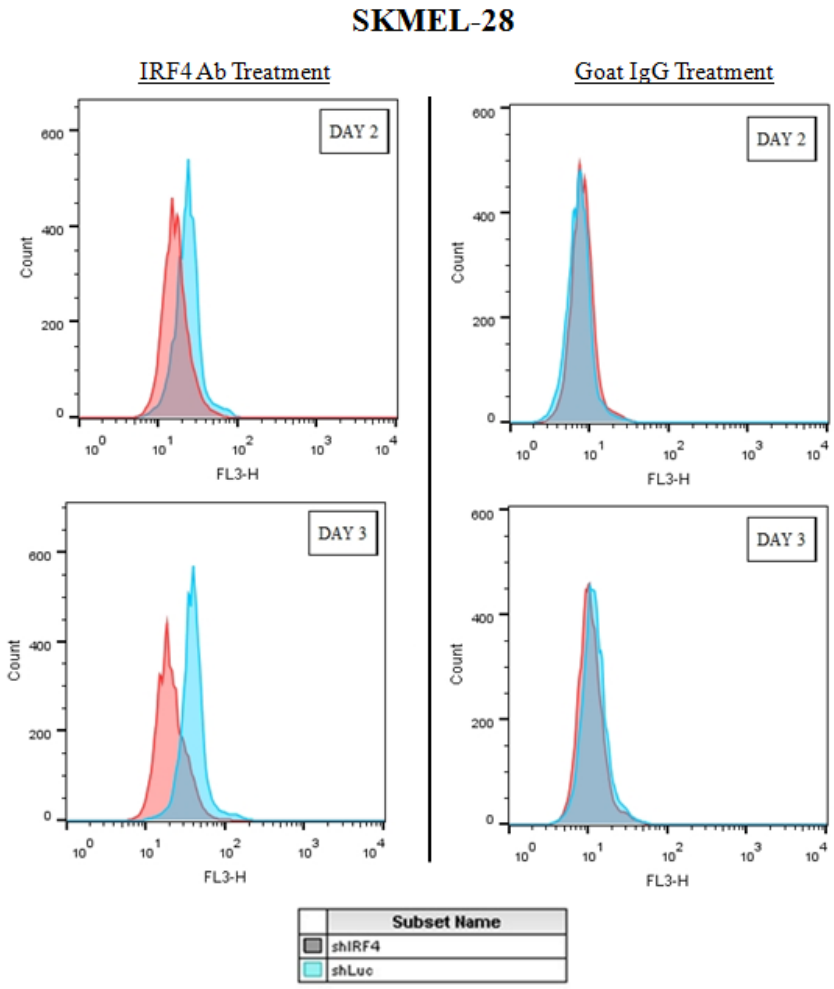

Figure E.1. Intracellular flow cytometry results with SKMEL-28 cells, transduced either by shIRF4 or shLuc, for optimal time point selection. Intensities of fluorescence emitted from peridinin chlorophyll protein complex (PerCP)-conjugated secondary antibody are shown on the x-axis and cell counts are shown on the y-axis.

APPENDIX F: AGILENT BIOANALYZER ANALYSES

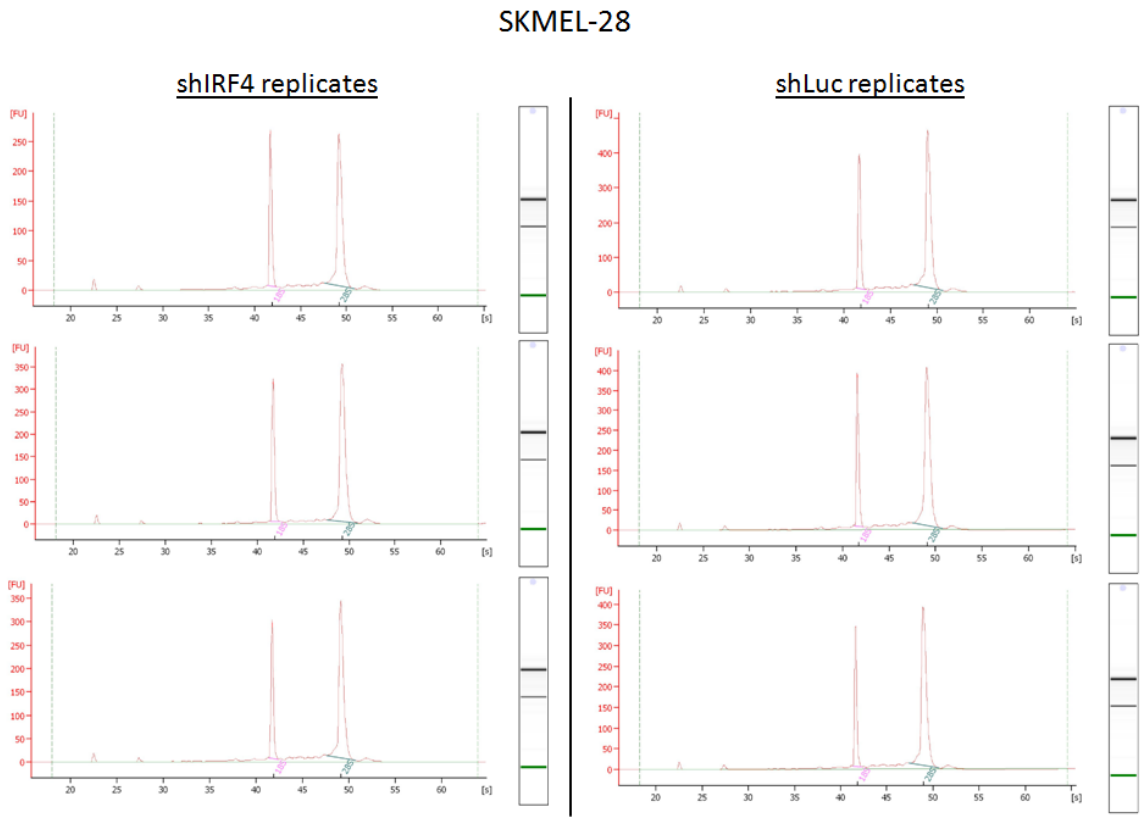

Figure F.1. Agilent Bioanalyzer results of total RNA extractions for SKMEL-28 cell line.

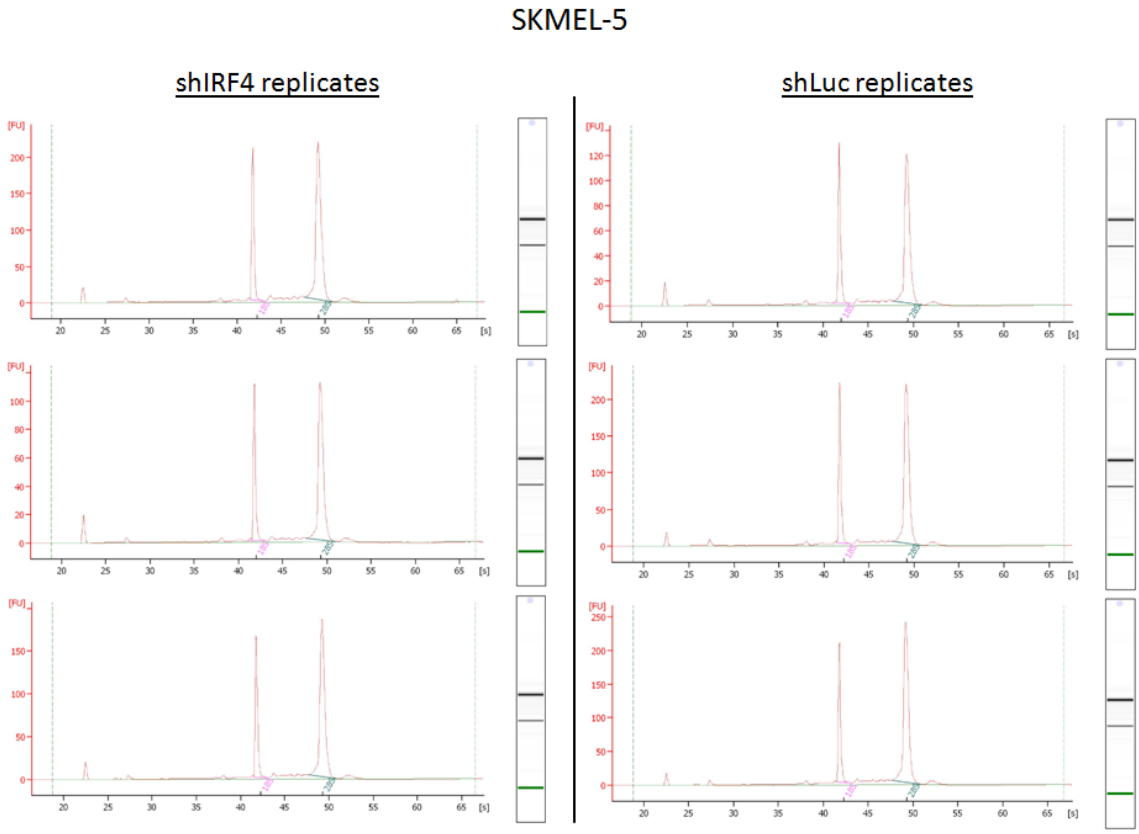

Figure F.2. Agilent Bioanalyzer results of total RNA extractions for SKMEL-5 cell line.

APPENDIX G: QUALITY CHECK FOR RNA-STABLE TREATED SAMPLES

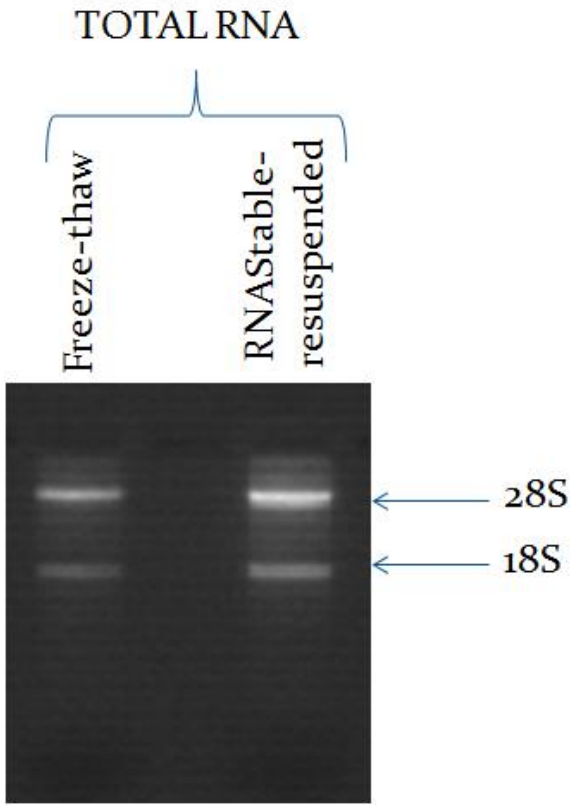

Figure G.1. Comparison of RNA integrity on agarose gel electrophoresis for RNAstable kit treated (stored at room temperature) and frozen (stored at -150°C) RNA samples.

APPENDIX H: PER BASE QUALITY GRAPHS



Figure H.1. Per base quality graphs for shIRF4 and shLuc transduced replicates of SKMEL-5. x-axis shows base position and y-axis indicates a Phred quality score.

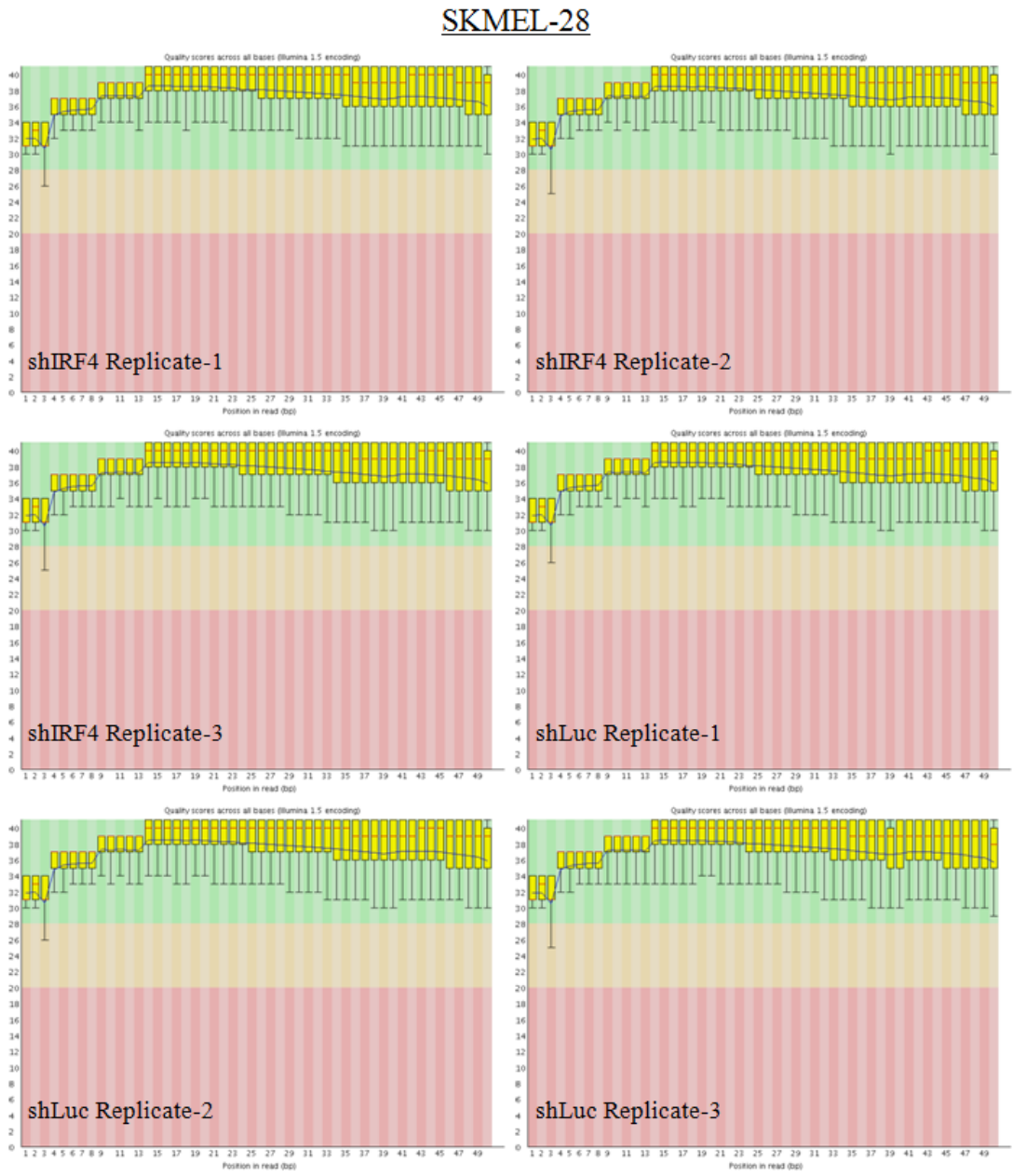

Figure H.2. Per base quality graphs for shIRF4 and shLuc transduced replicates of SKMEL-28. x-axis shows base position and y-axis indicates a Phred quality score.

APPENDIX I: INTEGRATIVE GENOME VIEWER VISUALIZATION FOR IRF4 LOCUS IN SKMEL-28

SKMEL-28

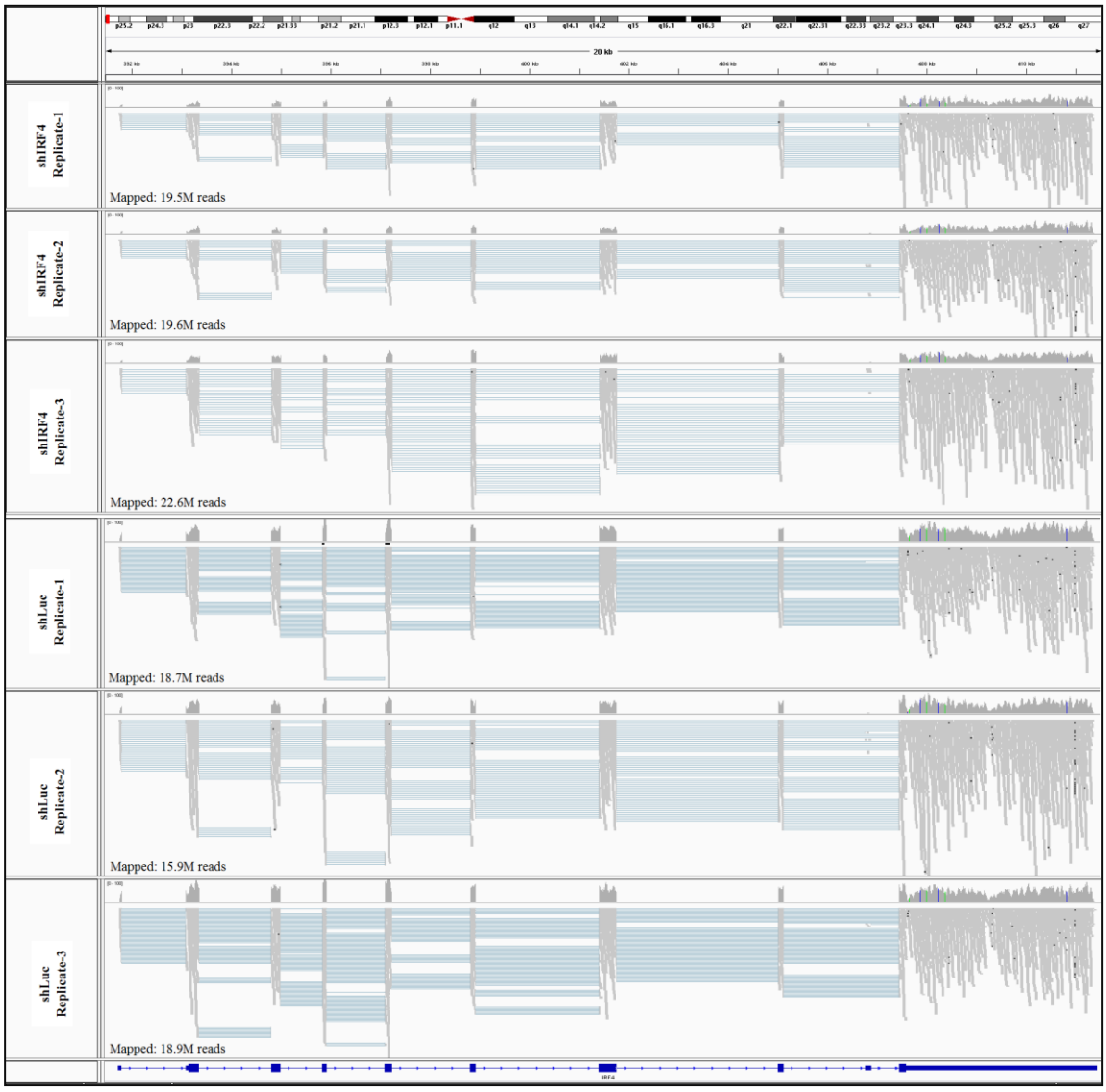

Figure I.1. IGV (Integrative Genome Viewer) visualization at IRF4 locus with the mapped reads for each of biological replicates of SKMEL-28. First three show shIRF4 replicates and last three show shLuc replicates. Visualizations were performed with mapped reads without read number normalization between samples.

APPENDIX J: COMPARISON OF UNIQUELY MAPPED READ NUMBERS OF SKMEL-5 AND SKMEL-5-ADJUSTED SKMEL-28

Table J.1. Number of the reads when SKMEL-28 mapped number decreased to the level of SKMEL-5 mapped number.

	Uniquely Mapped SKMEL-5	**Uniquely mapped SKMEL-28-adjusted**
shIRF4 Replicate-1	12,761,453	12,733,398
shIRF4 Replicate-2	12,058,698	11,964,300
shIRF4 Replicate-3	11,117,188	11,075,851
shLuc Replicate-1	12,979,486	12,890,874
shLuc Replicate-2	12,779,152	12,808,957
shLuc Replicate-3	12,313,966	12,274,444
TOTAL	74,009,943	73,747,824

APPENDIX K: GLOBAL STATISTICS FOR RNA-SEQ DATA

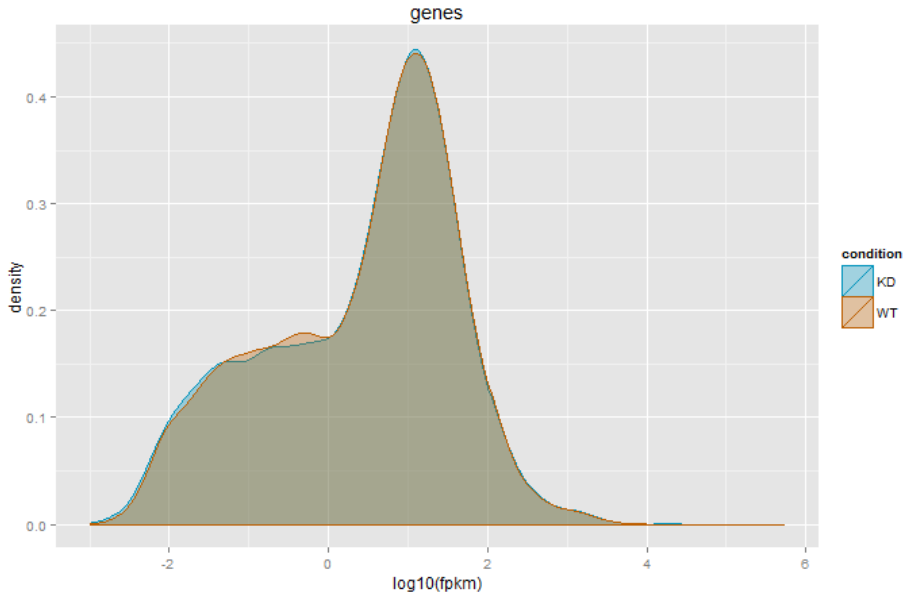

Figure K.1. Expression distribution (density) graph of SKMEL-28 (KD: shIRF4 transduced samples, WT: shLuc transduced samples).

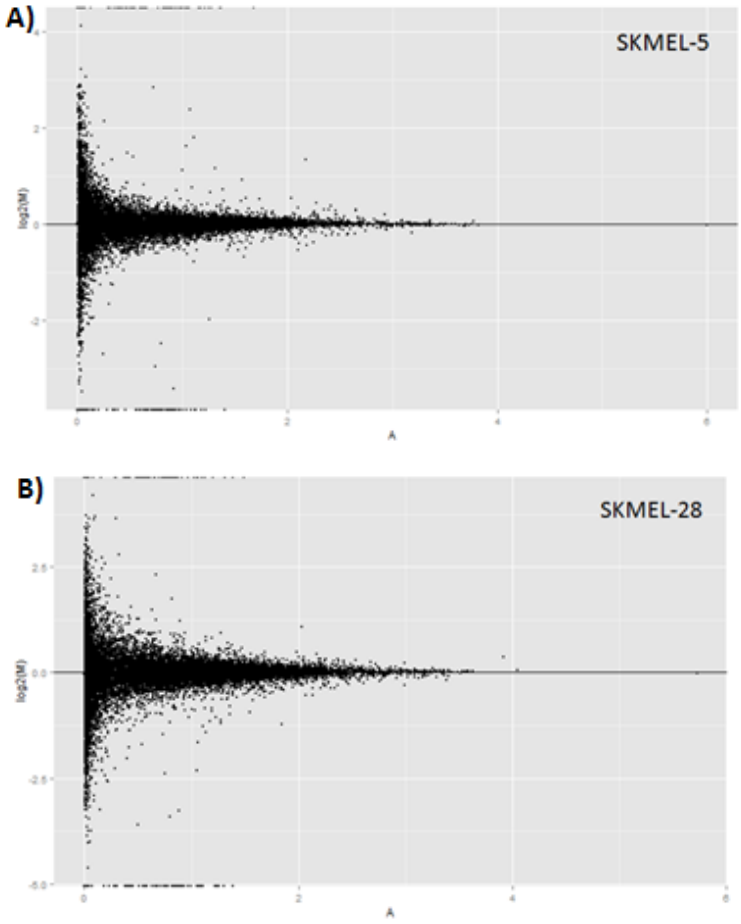

Figure K.2. M vs A plots for A) SKMEL-5 and B) SKMEL-28.

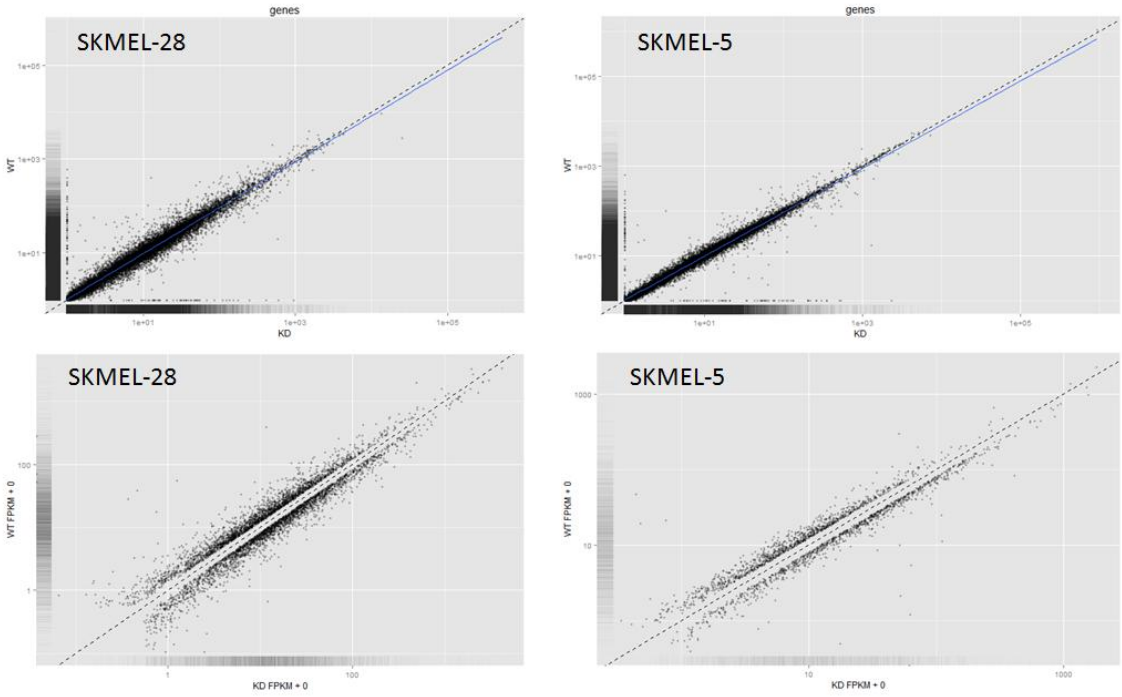

Figure K.3. Scatterplots comparing the FPKM values from each condition. Upper pictures depict all the genes, lower pictures depict only significantly DEGs.

APPENDIX L: CORRELATION GRAPHS OF FPKM VALUES OF SAME CONDITION'S BIOLOGICAL REPLICATES

SKMEL-28

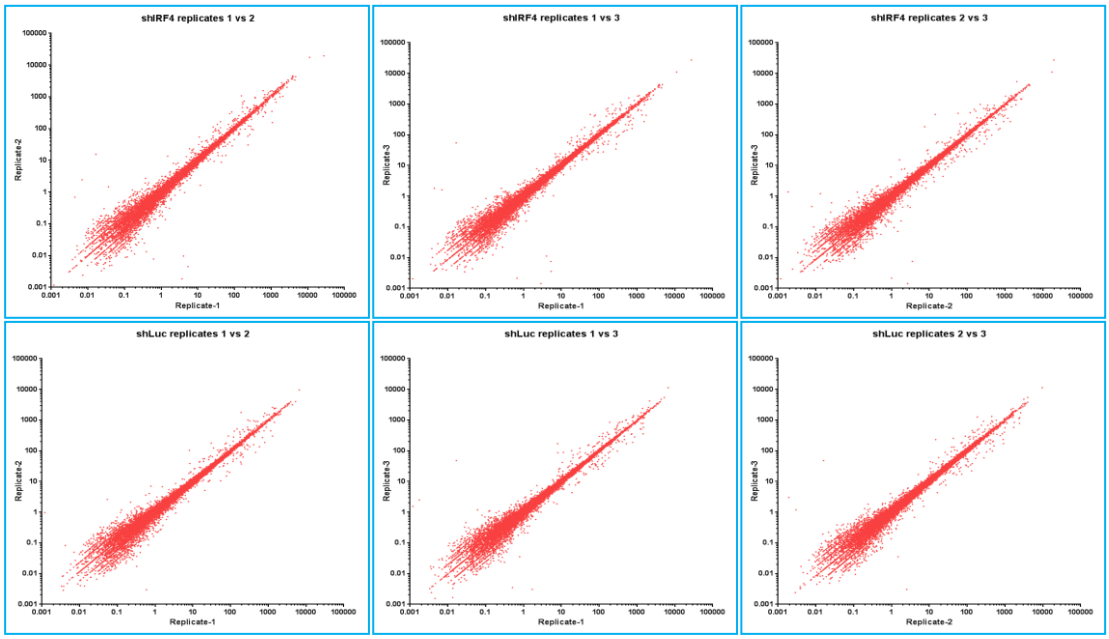

Figure L.1. FPKM values of each gene were compared between each biological replicate of each condition. A high correlation is expected for further analysis.

SKMEL-5

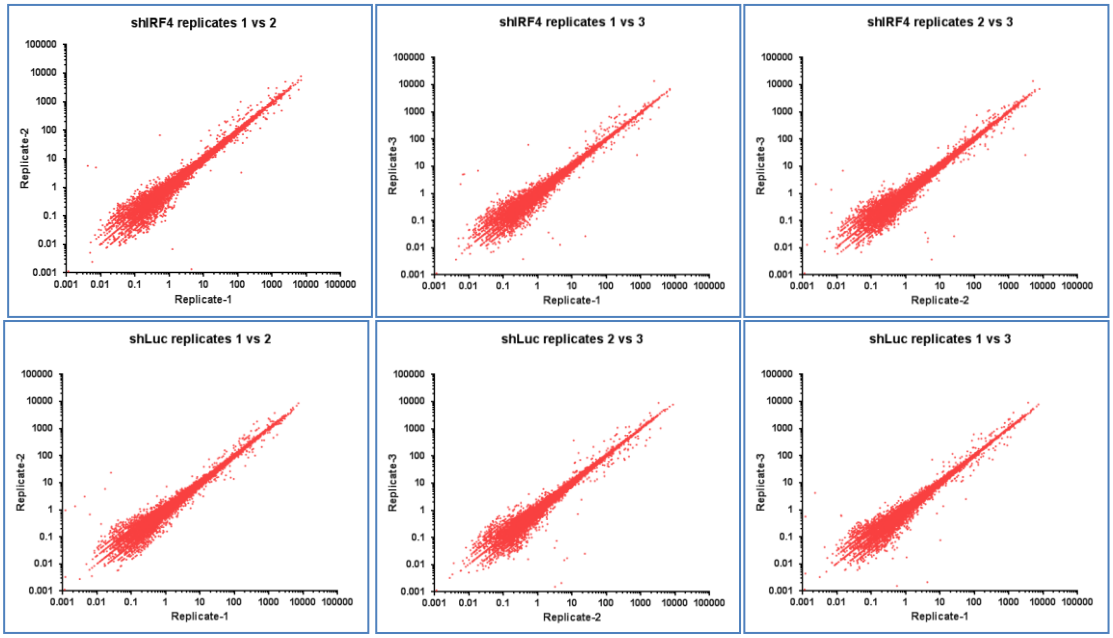

Figure L.1. FPKM values of each gene were compared between each biological replicate of each condition (cont.). A high correlation is expected for further analysis.

APPENDIX M: GENE ENRICHMENT ANALYSIS OF IRF4 ACTIVATED GENES FOR GO_BP TERMS BY GORILLA

Table M.1. GO enrichment analysis (Biological Process) for IRF4-activated genes in SKMEL-5 ($q<10^{-3}$).

Description	P-value	FDR q-value	Enrichment
cell cycle process	8.03E-63	1.00E-58	3.65
mitotic cell cycle process	6.76E-61	4.21E-57	4.31
mitotic cell cycle	4.74E-53	1.97E-49	5.15
cell cycle	4.25E-50	1.32E-46	4.09
single-organism organelle organization	1.98E-40	4.93E-37	2.7
organelle organization	6.32E-40	1.31E-36	2.27
cellular component organization	7.56E-32	1.35E-28	1.71
cellular component organization or biogenesis	1.95E-31	3.04E-28	1.7
chromosome organization	1.24E-29	1.71E-26	2.98
DNA metabolic process	2.31E-28	2.87E-25	2.98
mitotic nuclear division	1.86E-27	2.11E-24	4.76
organelle fission	2.62E-26	2.71E-23	3.9
nuclear division	1.11E-25	1.07E-22	3.99
DNA replication	4.36E-25	3.88E-22	5.19
cellular macromolecule metabolic process	6.14E-25	5.10E-22	1.45
regulation of cell cycle	5.16E-24	4.01E-21	2.68
macromolecule metabolic process	1.74E-20	1.28E-17	1.36
cell cycle phase transition	1.63E-19	1.13E-16	3.73
single-organism cellular process	3.69E-19	2.42E-16	1.27
mitotic cell cycle phase transition	4.40E-19	2.74E-16	3.71
nucleic acid metabolic process	1.42E-18	8.43E-16	1.54
regulation of cell cycle process	1.78E-18	1.01E-15	2.96
cellular metabolic process	2.28E-18	1.24E-15	1.29
metabolic process	4.85E-18	2.52E-15	1.24
regulation of mitotic cell cycle	8.78E-18	4.37E-15	3.19
microtubule-based process	1.14E-17	5.47E-15	3.05
primary metabolic process	2.24E-17	1.03E-14	1.27
nucleobase-containing compound metabolic process	6.57E-17	2.92E-14	1.45
cellular response to stress	6.65E-17	2.86E-14	2.08
cellular process	3.14E-16	1.30E-13	1.14
organic substance metabolic process	1.11E-15	4.47E-13	1.25
cellular response to DNA damage stimulus	2.54E-15	9.89E-13	2.45
cellular aromatic compound metabolic process	3.70E-15	1.39E-12	1.41

Table M.1. GO enrichment analysis (Biological Process) for IRF4-activated genes in SKMEL-5 ($q<10^{-3}$) (cont.).

Description	P-value	FDR q-value	Enrichment
heterocycle metabolic process	3.75E-15	1.37E-12	1.41
microtubule cytoskeleton organization	4.49E-15	1.60E-12	3.62
cell cycle checkpoint	1.26E-14	4.34E-12	4.26
chromatin modification	1.65E-14	5.56E-12	2.67
cellular nitrogen compound metabolic process	2.39E-14	7.85E-12	1.39
cellular macromolecule biosynthetic process	1.10E-13	3.52E-11	1.54
chromatin organization	1.40E-13	4.37E-11	2.42
chromosome segregation	1.92E-13	5.84E-11	5.39
single-organism process	2.87E-13	8.52E-11	1.18
macromolecule biosynthetic process	6.47E-13	1.87E-10	1.5
G1/S transition of mitotic cell cycle	1.01E-12	2.80E-10	4.01
cell cycle G1/S phase transition	1.01E-12	2.86E-10	4.01
DNA repair	1.76E-12	4.77E-10	2.7
organic cyclic compound metabolic process	2.57E-12	6.82E-10	1.35
regulation of mitotic cell cycle phase transition	3.81E-12	9.89E-10	3.18
DNA strand elongation involved in DNA replication	7.13E-12	1.81E-09	8.33
regulation of cellular metabolic process	7.55E-12	1.88E-09	1.32
regulation of organelle organization	8.67E-12	2.12E-09	2.16
regulation of cell cycle phase transition	1.39E-11	3.33E-09	3.07
DNA strand elongation	2.22E-11	5.22E-09	7.85
mitotic cell cycle checkpoint	2.34E-11	5.39E-09	4.65
nitrogen compound metabolic process	3.37E-11	7.64E-09	1.32
regulation of microtubule-based process	4.09E-11	9.09E-09	4.25
regulation of primary metabolic process	4.50E-11	9.83E-09	1.31
regulation of macromolecule metabolic process	4.77E-11	1.02E-08	1.33
sister chromatid segregation	5.45E-11	1.15E-08	9.71
regulation of microtubule cytoskeleton organization	6.75E-11	1.40E-08	4.62
cytoskeleton organization	8.55E-11	1.74E-08	2.2
negative regulation of mitotic cell cycle phase transition	9.36E-11	1.88E-08	3.38
negative regulation of cell cycle process	1.13E-10	2.24E-08	3.02
mitotic sister chromatid segregation	1.17E-10	2.27E-08	10.3
cellular protein modification process	1.34E-10	2.57E-08	1.54
protein modification process	1.34E-10	2.53E-08	1.54
regulation of cell division	1.90E-10	3.54E-08	3.07
regulation of transcription involved in G1/S transition of mitotic cell cycle	2.22E-10	4.07E-08	8.93
negative regulation of cell cycle phase transition	2.42E-10	4.36E-08	3.27
regulation of transcription from RNA polymerase II promoter	2.84E-10	5.06E-08	1.68
spindle organization	4.31E-10	7.55E-08	5.01
regulation of metabolic process	5.86E-10	1.01E-07	1.27

Table M.1. GO enrichment analysis (Biological Process) for IRF4-activated genes in SKMEL-5 ($q<10^{-3}$) (cont.).

Description	P-value	FDR q-value	Enrichment
regulation of mitosis	8.98E-10	1.53E-07	4.13
macromolecule modification	1.74E-09	2.92E-07	1.48
spindle checkpoint	1.82E-09	3.03E-07	6.6
regulation of nucleobase-containing compound metabolic process	2.39E-09	3.92E-07	1.33
G2/M transition of mitotic cell cycle	2.52E-09	4.02E-07	3.51
cell cycle G2/M phase transition	2.52E-09	4.08E-07	3.51
cytokinesis	3.60E-09	5.68E-07	4.51
positive regulation of cell cycle	5.43E-09	8.46E-07	3.69
centrosome organization	5.44E-09	8.36E-07	5.41
regulation of macromolecule biosynthetic process	5.70E-09	8.66E-07	1.35
regulation of cellular macromolecule biosynthetic process	7.73E-09	1.16E-06	1.36
phosphorylation	8.84E-09	1.31E-06	1.79
regulation of RNA biosynthetic process	8.98E-09	1.32E-06	1.38
DNA replication-independent nucleosome assembly	1.01E-08	1.45E-06	6.98
DNA replication-independent nucleosome organization	1.01E-08	1.47E-06	6.98
cell proliferation	1.02E-08	1.44E-06	2.03
regulation of transcription, DNA-templated	1.06E-08	1.48E-06	1.38
covalent chromatin modification	1.09E-08	1.51E-06	2.57
regulation of RNA metabolic process	1.16E-08	1.59E-06	1.37
positive regulation of macromolecule metabolic process	1.17E-08	1.59E-06	1.49
regulation of nitrogen compound metabolic process	1.20E-08	1.60E-06	1.31
chromatin assembly or disassembly	1.36E-08	1.81E-06	5.12
cellular biosynthetic process	1.47E-08	1.93E-06	1.33
protein phosphorylation	1.56E-08	2.02E-06	1.95
microtubule organizing center organization	1.83E-08	2.34E-06	5.03
negative regulation of macromolecule biosynthetic process	2.08E-08	2.64E-06	1.72
regulation of nuclear division	2.22E-08	2.80E-06	3.46
regulation of cyclin-dependent protein serine/threonine kinase activity	2.27E-08	2.80E-06	4.1
negative regulation of cellular process	2.27E-08	2.83E-06	1.37
DNA conformation change	2.34E-08	2.86E-06	3.94
negative regulation of biological process	2.72E-08	3.29E-06	1.34
negative regulation of cellular macromolecule biosynthetic process	2.76E-08	3.31E-06	1.73
chromatin remodeling at centromere	3.07E-08	3.64E-06	7.87
regulation of biosynthetic process	3.51E-08	4.12E-06	1.32
cellular protein metabolic process	4.59E-08	5.34E-06	1.39
regulation of chromosome segregation	4.65E-08	5.36E-06	6.87
DNA integrity checkpoint	5.10E-08	5.83E-06	4.09
kinetochore organization	5.17E-08	5.85E-06	11.45
regulation of mitotic metaphase/anaphase transition	5.38E-08	6.04E-06	5.72

Table M.1. GO enrichment analysis (Biological Process) for IRF4-activated genes in SKMEL-5 ($q<10^{-3}$) (cont.).

Description	P-value	FDR q-value	Enrichment
regulation of cellular biosynthetic process	5.49E-08	6.10E-06	1.32
regulation of protein modification process	5.72E-08	6.30E-06	1.65
negative regulation of transcription, DNA-templated	6.17E-08	6.74E-06	1.76
positive regulation of cell cycle process	6.24E-08	6.76E-06	2.72
histone modification	6.91E-08	7.42E-06	2.48
negative regulation of nucleobase-containing compound metabolic process	7.23E-08	7.70E-06	1.69
regulation of metaphase/anaphase transition of cell cycle	7.56E-08	7.97E-06	5.59
organic substance biosynthetic process	8.79E-08	9.20E-06	1.31
negative regulation of nitrogen compound metabolic process	9.89E-08	1.03E-05	1.68
negative regulation of gene expression	1.08E-07	1.11E-05	1.7
negative regulation of RNA metabolic process	1.12E-07	1.14E-05	1.72
centromere-specific nucleosome assembly	1.46E-07	1.48E-05	7.81
negative regulation of RNA biosynthetic process	1.54E-07	1.54E-05	1.72
negative regulation of biosynthetic process	2.29E-07	2.28E-05	1.63
DNA replication initiation	2.45E-07	2.38E-05	7.47
regulation of cellular protein metabolic process	2.45E-07	2.42E-05	1.54
protein localization to chromosome	2.45E-07	2.40E-05	7.47
DNA recombination	2.83E-07	2.73E-05	2.8
positive regulation of metabolic process	3.32E-07	3.18E-05	1.41
negative regulation of macromolecule metabolic process	3.37E-07	3.20E-05	1.52
mitotic spindle checkpoint	3.42E-07	3.22E-05	5.89
nucleobase-containing compound biosynthetic process	4.04E-07	3.78E-05	1.37
protein complex subunit organization	4.63E-07	4.30E-05	1.61
biosynthetic process	5.08E-07	4.68E-05	1.28
regulation of gene expression	5.51E-07	5.04E-05	1.28
positive regulation of protein modification process	6.24E-07	5.67E-05	1.73
negative regulation of cellular biosynthetic process	6.39E-07	5.77E-05	1.61
phosphorus metabolic process	6.84E-07	6.12E-05	1.41
histone exchange	7.13E-07	6.34E-05	6.09
cell division	7.99E-07	7.05E-05	3.26
regulation of cellular component organization	8.71E-07	7.64E-05	1.5
positive regulation of cellular protein metabolic process	1.02E-06	8.86E-05	1.67
regulation of protein kinase activity	1.02E-06	8.85E-05	1.8
positive regulation of cellular metabolic process	1.07E-06	9.19E-05	1.4
phosphate-containing compound metabolic process	1.14E-06	9.76E-05	1.41
heterocycle biosynthetic process	1.21E-06	1.03E-04	1.34
negative regulation of cell cycle	1.29E-06	1.09E-04	2.4
regulation of transferase activity	1.31E-06	1.10E-04	1.71
spindle assembly checkpoint	1.46E-06	1.21E-04	5.72

Table M.1. GO enrichment analysis (Biological Process) for IRF4-activated genes in SKMEL-5 ($q<10^{-3}$) (cont.).

Description	P-value	FDR q-value	Enrichment
positive regulation of protein metabolic process	1.60E-06	1.32E-04	1.62
telomere maintenance via semi-conservative replication	1.86E-06	1.52E-04	7.02
regulation of DNA metabolic process	1.87E-06	1.53E-04	2.37
transcription, DNA-templated	1.89E-06	1.53E-04	1.38
aromatic compound biosynthetic process	1.95E-06	1.57E-04	1.34
negative regulation of mitotic metaphase/anaphase transition	2.05E-06	1.64E-04	5.56
negative regulation of cellular metabolic process	2.07E-06	1.64E-04	1.47
biological_process	2.15E-06	1.69E-04	1.05
RNA biosynthetic process	2.20E-06	1.73E-04	1.36
negative regulation of metabolic process	2.25E-06	1.75E-04	1.45
regulation of kinase activity	2.25E-06	1.74E-04	1.75
cell cycle phase	2.34E-06	1.80E-04	5.03
positive regulation of cellular process	2.43E-06	1.86E-04	1.28
mitotic G2 phase	2.77E-06	2.09E-04	11.45
G2 phase	2.77E-06	2.11E-04	11.45
mitotic chromosome condensation	2.80E-06	2.10E-04	9.25
negative regulation of metaphase/anaphase transition of cell cycle	2.83E-06	2.11E-04	5.4
chromosome condensation	3.11E-06	2.31E-04	5.92
telomere maintenance via telomere lengthening	3.86E-06	2.85E-04	5.25
negative regulation of mitosis	4.07E-06	2.98E-04	4.79
nucleotide-excision repair	4.28E-06	3.12E-04	3.71
regulation of centrosome cycle	4.39E-06	3.18E-04	6.44
cellular nitrogen compound biosynthetic process	4.55E-06	3.28E-04	1.32
regulation of cytoskeleton organization	4.98E-06	3.57E-04	2.13
mitotic cytokinesis	5.47E-06	3.89E-04	7.23
nucleotide-excision repair, DNA gap filling	5.47E-06	3.87E-04	7.23
mitotic recombination	6.19E-06	4.36E-04	5.54
nuclear envelope organization	6.22E-06	4.35E-04	4.29
mitotic spindle organization	6.51E-06	4.53E-04	6.18
kinetochore assembly	6.59E-06	4.54E-04	10.3
regulation of attachment of spindle microtubules to kinetochore	6.59E-06	4.56E-04	10.3
protein metabolic process	7.71E-06	5.28E-04	1.27
telomere maintenance	8.11E-06	5.52E-04	3.94
negative regulation of organelle organization	8.53E-06	5.77E-04	2.38
mitotic spindle assembly checkpoint	8.54E-06	5.75E-04	5.37
negative regulation of microtubule depolymerization	8.64E-06	5.79E-04	6.87
telomere maintenance via recombination	9.44E-06	6.28E-04	5.94
telomere organization	9.92E-06	6.57E-04	3.88
macromolecular complex subunit organization	1.11E-05	7.33E-04	1.48
regulation of microtubule polymerization or depolymerization	1.12E-05	7.32E-04	4.38

Table M.1. GO enrichment analysis (Biological Process) for IRF4-activated genes in SKMEL-5 ($q<10^{-3}$) (cont.).

Description	P-value	FDR q-value	Enrichment
regulation of protein serine/threonine kinase activity	1.12E-05	7.29E-04	1.95
negative regulation of transcription from RNA polymerase II promoter	1.14E-05	7.41E-04	1.75
positive regulation of mitotic cell cycle	1.20E-05	7.74E-04	4.72
metaphase/anaphase transition of mitotic cell cycle	1.26E-05	8.06E-04	12.27
metaphase/anaphase transition of cell cycle	1.26E-05	8.10E-04	12.27
attachment of spindle microtubules to kinetochore	1.38E-05	8.76E-04	9.37
positive regulation of transferase activity	1.45E-05	9.18E-04	1.78

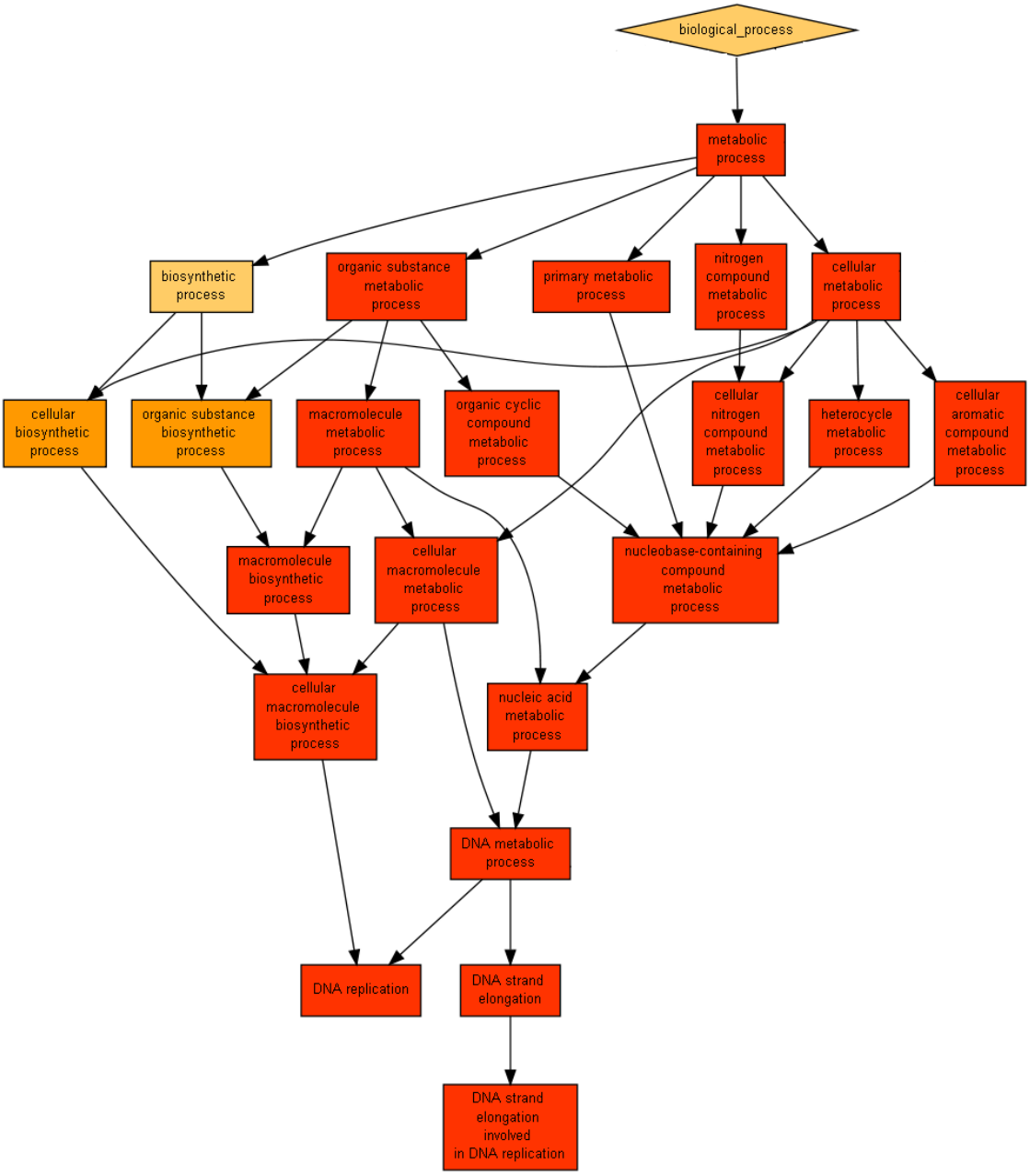

Figure M.1. Hierarchical visualization of over-represented GO_ BP terms ($q<10^{-11}$) in IRF4-activated genes in SKMEL-5 cell line (Part I).

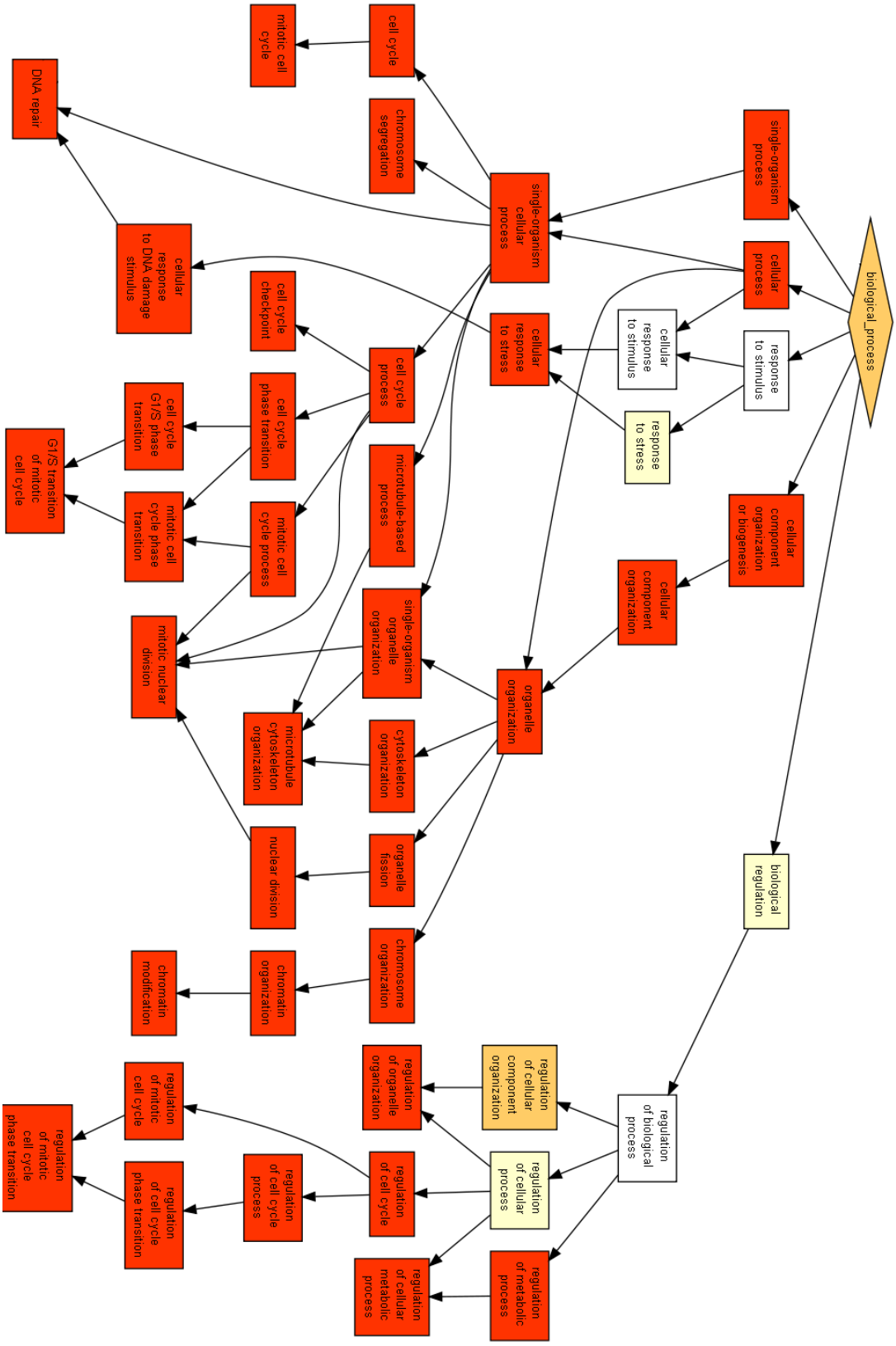

Figure M.2. Hierarchical visualization of over-represented GO_ BP terms ($q<10^{-11}$) in IRF4-activated genes in SKMEL-5 cell line (Part II).

Table M.2. GO enrichment analysis (Biological Process) for IRF4-activated genes in SKMEL-28 ($q<10^{-3}$).

Description	P-value	FDR q-value	Enrichment
cellular macromolecule metabolic process	5.26E-46	6.55E-42	1.4
macromolecule metabolic process	6.37E-42	3.97E-38	1.35
cellular metabolic process	1.32E-37	5.48E-34	1.27
organic substance metabolic process	7.34E-35	2.29E-31	1.25
primary metabolic process	9.64E-35	2.40E-31	1.26
metabolic process	5.65E-34	1.17E-30	1.22
nucleic acid metabolic process	1.16E-30	2.06E-27	1.46
regulation of macromolecule metabolic process	4.65E-30	7.23E-27	1.37
nucleobase-containing compound metabolic process	5.73E-30	7.92E-27	1.4
heterocycle metabolic process	1.95E-28	2.43E-25	1.38
cellular aromatic compound metabolic process	2.98E-27	3.38E-24	1.37
regulation of primary metabolic process	3.30E-26	3.42E-23	1.32
regulation of cellular metabolic process	4.73E-26	4.53E-23	1.32
regulation of metabolic process	9.82E-26	8.74E-23	1.3
RNA metabolic process	1.94E-25	1.61E-22	1.45
cellular nitrogen compound metabolic process	5.70E-25	4.43E-22	1.34
organic cyclic compound metabolic process	1.49E-24	1.09E-21	1.34
single-organism organelle organization	2.85E-24	1.97E-21	1.78
regulation of gene expression	9.80E-24	6.42E-21	1.37
nitrogen compound metabolic process	3.93E-23	2.45E-20	1.31
organelle organization	4.37E-21	2.59E-18	1.55
regulation of cellular macromolecule biosynthetic process	4.50E-21	2.55E-18	1.38
macromolecule biosynthetic process	7.74E-21	4.19E-18	1.42
cellular process	1.42E-20	7.34E-18	1.11
regulation of macromolecule biosynthetic process	2.10E-20	1.05E-17	1.37
regulation of nucleobase-containing compound metabolic process	2.37E-20	1.14E-17	1.34
cellular macromolecule biosynthetic process	9.83E-20	4.54E-17	1.43
regulation of nitrogen compound metabolic process	1.40E-19	6.21E-17	1.33
regulation of RNA metabolic process	1.87E-19	8.04E-17	1.38
regulation of transcription, DNA-templated	1.24E-18	5.14E-16	1.38
regulation of RNA biosynthetic process	1.81E-18	7.27E-16	1.37
cellular biosynthetic process	3.19E-18	1.24E-15	1.34
cellular protein metabolic process	7.10E-18	2.68E-15	1.41
regulation of cellular biosynthetic process	1.24E-17	4.54E-15	1.33
regulation of biosynthetic process	1.47E-17	5.22E-15	1.33
heterocycle biosynthetic process	1.92E-17	6.65E-15	1.4
transcription, DNA-templated	2.23E-17	7.51E-15	1.45
nucleobase-containing compound biosynthetic process	2.54E-17	8.33E-15	1.4
organic substance biosynthetic process	3.30E-17	1.05E-14	1.32
cellular component organization or biogenesis	5.90E-17	1.84E-14	1.31

Table M.2. GO enrichment analysis (Biological Process) for IRF4-activated genes in SKMEL-28 ($q<10^{-3}$) (cont.).

Description	P-value	FDR q-value	Enrichment
aromatic compound biosynthetic process	6.25E-17	1.90E-14	1.39
cellular nitrogen compound biosynthetic process	6.76E-17	2.01E-14	1.39
mitotic cell cycle process	8.26E-17	2.39E-14	1.92
negative regulation of macromolecule metabolic process	8.53E-17	2.42E-14	1.55
RNA biosynthetic process	1.01E-16	2.79E-14	1.42
biosynthetic process	1.94E-16	5.26E-14	1.31
regulation of cellular protein metabolic process	2.45E-16	6.50E-14	1.56
cell cycle process	7.27E-16	1.89E-13	1.71
cellular component organization	9.77E-16	2.48E-13	1.3
positive regulation of cellular process	1.33E-15	3.31E-13	1.32
organic cyclic compound biosynthetic process	1.36E-15	3.33E-13	1.36
positive regulation of macromolecule metabolic process	1.66E-15	3.97E-13	1.44
chromosome organization	2.83E-15	6.66E-13	1.81
macromolecule modification	1.33E-14	3.07E-12	1.4
regulation of protein metabolic process	1.54E-14	3.49E-12	1.46
protein modification process	6.54E-14	1.43E-11	1.4
cellular protein modification process	6.54E-14	1.45E-11	1.4
positive regulation of biological process	9.32E-14	2.00E-11	1.27
regulation of cell cycle	1.45E-13	3.05E-11	1.73
cellular response to stress	1.65E-13	3.43E-11	1.58
negative regulation of metabolic process	1.78E-13	3.64E-11	1.46
positive regulation of cellular metabolic process	5.83E-13	1.17E-10	1.39
positive regulation of metabolic process	6.48E-13	1.28E-10	1.37
negative regulation of cellular process	1.18E-12	2.30E-10	1.3
chromatin modification	1.55E-12	2.98E-10	1.93
negative regulation of biological process	1.68E-12	3.16E-10	1.28
protein metabolic process	1.80E-12	3.35E-10	1.28
cell cycle	1.92E-12	3.52E-10	1.8
positive regulation of RNA metabolic process	4.86E-12	8.77E-10	1.53
regulation of protein modification process	8.49E-12	1.51E-09	1.53
negative regulation of cellular metabolic process	1.70E-11	2.99E-09	1.44
RNA processing	1.95E-11	3.37E-09	1.72
regulation of transcription from RNA polymerase II promoter	2.02E-11	3.44E-09	1.46
covalent chromatin modification	3.60E-11	6.05E-09	2.13
chromatin organization	4.77E-11	7.92E-09	1.76
histone modification	5.44E-11	8.92E-09	2.12
regulation of cellular process	5.50E-11	8.90E-09	1.12
positive regulation of RNA biosynthetic process	6.48E-11	1.04E-08	1.51
regulation of molecular function	9.00E-11	1.42E-08	1.33
biological_process	1.69E-10	2.63E-08	1.04

Table M.2. GO enrichment analysis (Biological Process) for IRF4-activated genes in SKMEL-28 ($q<10^{-3}$) (cont.).

Description	P-value	FDR q-value	Enrichment
positive regulation of nucleobase-containing compound metabolic process	1.94E-10	2.99E-08	1.46
positive regulation of macromolecule biosynthetic process	3.33E-10	5.05E-08	1.45
regulation of protein kinase activity	4.45E-10	6.68E-08	1.65
regulation of transferase activity	4.58E-10	6.79E-08	1.58
mitotic nuclear division	4.58E-10	6.71E-08	2.17
positive regulation of gene expression	5.10E-10	7.39E-08	1.47
negative regulation of gene expression	5.87E-10	8.40E-08	1.52
positive regulation of nitrogen compound metabolic process	5.89E-10	8.33E-08	1.44
mitotic cell cycle	5.90E-10	8.26E-08	1.87
regulation of protein phosphorylation	6.92E-10	9.58E-08	1.54
regulation of biological process	1.06E-09	1.44E-07	1.11
single-organism cellular process	1.12E-09	1.52E-07	1.12
regulation of kinase activity	1.30E-09	1.74E-07	1.61
regulation of catalytic activity	1.35E-09	1.78E-07	1.34
negative regulation of cellular macromolecule biosynthetic process	1.63E-09	2.14E-07	1.5
negative regulation of macromolecule biosynthetic process	1.90E-09	2.46E-07	1.48
cell death	1.93E-09	2.48E-07	1.54
DNA metabolic process	2.03E-09	2.58E-07	1.61
positive regulation of transcription, DNA-templated	2.08E-09	2.62E-07	1.47
biological regulation	2.70E-09	3.36E-07	1.1
death	2.74E-09	3.38E-07	1.53
programmed cell death	4.41E-09	5.39E-07	1.61
positive regulation of cellular biosynthetic process	6.10E-09	7.37E-07	1.4
positive regulation of biosynthetic process	7.91E-09	9.47E-07	1.39
regulation of phosphorylation	8.53E-09	1.01E-06	1.45
negative regulation of cellular protein metabolic process	1.18E-08	1.38E-06	1.69
organelle fission	1.85E-08	2.16E-06	1.84
cellular response to organic substance	2.30E-08	2.65E-06	1.36
negative regulation of protein phosphorylation	2.56E-08	2.93E-06	2
negative regulation of protein metabolic process	3.58E-08	4.05E-06	1.62
negative regulation of RNA metabolic process	3.72E-08	4.18E-06	1.47
response to endoplasmic reticulum stress	4.68E-08	5.21E-06	2.36
cellular response to chemical stimulus	5.42E-08	5.98E-06	1.32
regulation of cysteine-type endopeptidase activity	5.80E-08	6.34E-06	2.12
nuclear division	6.50E-08	7.04E-06	1.84
negative regulation of biosynthetic process	8.86E-08	9.51E-06	1.41
regulation of programmed cell death	8.91E-08	9.48E-06	1.39
negative regulation of nucleobase-containing compound metabolic process	9.04E-08	9.54E-06	1.43
regulation of mitotic cell cycle	9.26E-08	9.69E-06	1.77

Table M.2. GO enrichment analysis (Biological Process) for IRF4-activated genes in SKMEL-28 ($q<10^{-3}$) (cont.).

Description	P-value	FDR q-value	Enrichment
regulation of apoptotic process	9.74E-08	1.01E-05	1.39
negative regulation of phosphorylation	1.19E-07	1.23E-05	1.86
cellular response to growth factor stimulus	1.62E-07	1.64E-05	1.61
apoptotic process	1.62E-07	1.65E-05	1.55
regulation of cysteine-type endopeptidase activity involved in apoptotic process	1.66E-07	1.67E-05	2.1
negative regulation of cellular biosynthetic process	1.69E-07	1.69E-05	1.41
negative regulation of transcription, DNA-templated	1.77E-07	1.75E-05	1.46
regulation of cellular component organization	1.92E-07	1.89E-05	1.34
negative regulation of nitrogen compound metabolic process	2.29E-07	2.23E-05	1.41
cellular response to DNA damage stimulus	2.46E-07	2.37E-05	1.56
response to growth factor	2.54E-07	2.44E-05	1.59
negative regulation of RNA biosynthetic process	2.55E-07	2.40E-05	1.45
positive regulation of cellular protein metabolic process	2.55E-07	2.42E-05	1.45
negative regulation of protein modification process	2.55E-07	2.39E-05	1.72
regulation of cell death	2.66E-07	2.48E-05	1.37
ncRNA metabolic process	3.30E-07	3.04E-05	1.8
positive regulation of cell death	3.64E-07	3.33E-05	1.69
cytoskeleton organization	3.81E-07	3.47E-05	1.57
response to UV-C	3.86E-07	3.48E-05	6.4
ncRNA processing	4.01E-07	3.59E-05	1.95
regulation of cellular response to stress	4.31E-07	3.83E-05	1.73
intrinsic apoptotic signaling pathway	5.24E-07	4.63E-05	2.12
mRNA processing	5.62E-07	4.93E-05	1.7
positive regulation of transcription from RNA polymerase II promoter	6.87E-07	5.98E-05	1.46
regulation of developmental process	7.28E-07	6.30E-05	1.3
positive regulation of protein metabolic process	9.17E-07	7.88E-05	1.4
regulation of phosphorus metabolic process	9.66E-07	8.24E-05	1.29
regulation of phosphate metabolic process	1.01E-06	8.58E-05	1.29
positive regulation of programmed cell death	1.10E-06	9.16E-05	1.68
positive regulation of apoptotic process	1.10E-06	9.22E-05	1.68
histone lysine methylation	1.10E-06	9.15E-05	2.97
response to organic substance	1.15E-06	9.49E-05	1.26
single-organism process	1.37E-06	1.12E-04	1.08
peptidyl-amino acid modification	1.48E-06	1.20E-04	1.52
negative regulation of cell cycle	1.68E-06	1.36E-04	1.85
DNA conformation change	1.72E-06	1.38E-04	2.45
apoptotic signaling pathway	1.80E-06	1.44E-04	1.74
positive regulation of molecular function	1.83E-06	1.45E-04	1.33
response to UV	1.86E-06	1.47E-04	2.33

Table M.2. GO enrichment analysis (Biological Process) for IRF4-activated genes in SKMEL-28 ($q<10^{-3}$) (cont.).

Description	P-value	FDR q-value	Enrichment
positive regulation of cysteine-type endopeptidase activity	2.32E-06	1.82E-04	2.27
gene expression	2.58E-06	2.01E-04	1.48
negative regulation of intracellular signal transduction	2.79E-06	2.16E-04	1.74
positive regulation of catalytic activity	3.39E-06	2.61E-04	1.35
regulation of protein serine/threonine kinase activity	3.86E-06	2.95E-04	1.62
mammary gland epithelial cell proliferation	3.94E-06	2.99E-04	5.42
response to stress	4.06E-06	3.06E-04	1.22
positive regulation of cysteine-type endopeptidase activity involved in apoptotic process	4.44E-06	3.33E-04	2.28
negative regulation of signal transduction	4.95E-06	3.69E-04	1.41
centrosome organization	5.17E-06	3.84E-04	2.9
regulation of cell cycle process	5.49E-06	4.05E-04	1.57
response to abiotic stimulus	6.02E-06	4.41E-04	1.39
regulation of organelle organization	6.46E-06	4.68E-04	1.46
phosphate-containing compound metabolic process	6.46E-06	4.70E-04	1.24
transcription from RNA polymerase II promoter	6.61E-06	4.76E-04	1.57
intracellular signal transduction	6.65E-06	4.76E-04	1.3
histone methylation	6.90E-06	4.91E-04	2.57
regulation of cyclin-dependent protein serine/threonine kinase activity	8.20E-06	5.80E-04	2.4
phosphorus metabolic process	8.39E-06	5.90E-04	1.23
regulation of translation	8.96E-06	6.27E-04	1.77
DNA packaging	9.89E-06	6.88E-04	3.35
protein alkylation	1.06E-05	7.27E-04	2.29
protein methylation	1.06E-05	7.31E-04	2.29
positive regulation of endopeptidase activity	1.14E-05	7.80E-04	2.13
negative regulation of protein kinase activity	1.22E-05	8.28E-04	1.9
peptidyl-lysine modification	1.30E-05	8.81E-04	2.02
negative regulation of cell communication	1.45E-05	9.73E-04	1.38
organ morphogenesis	1.47E-05	9.85E-04	1.59

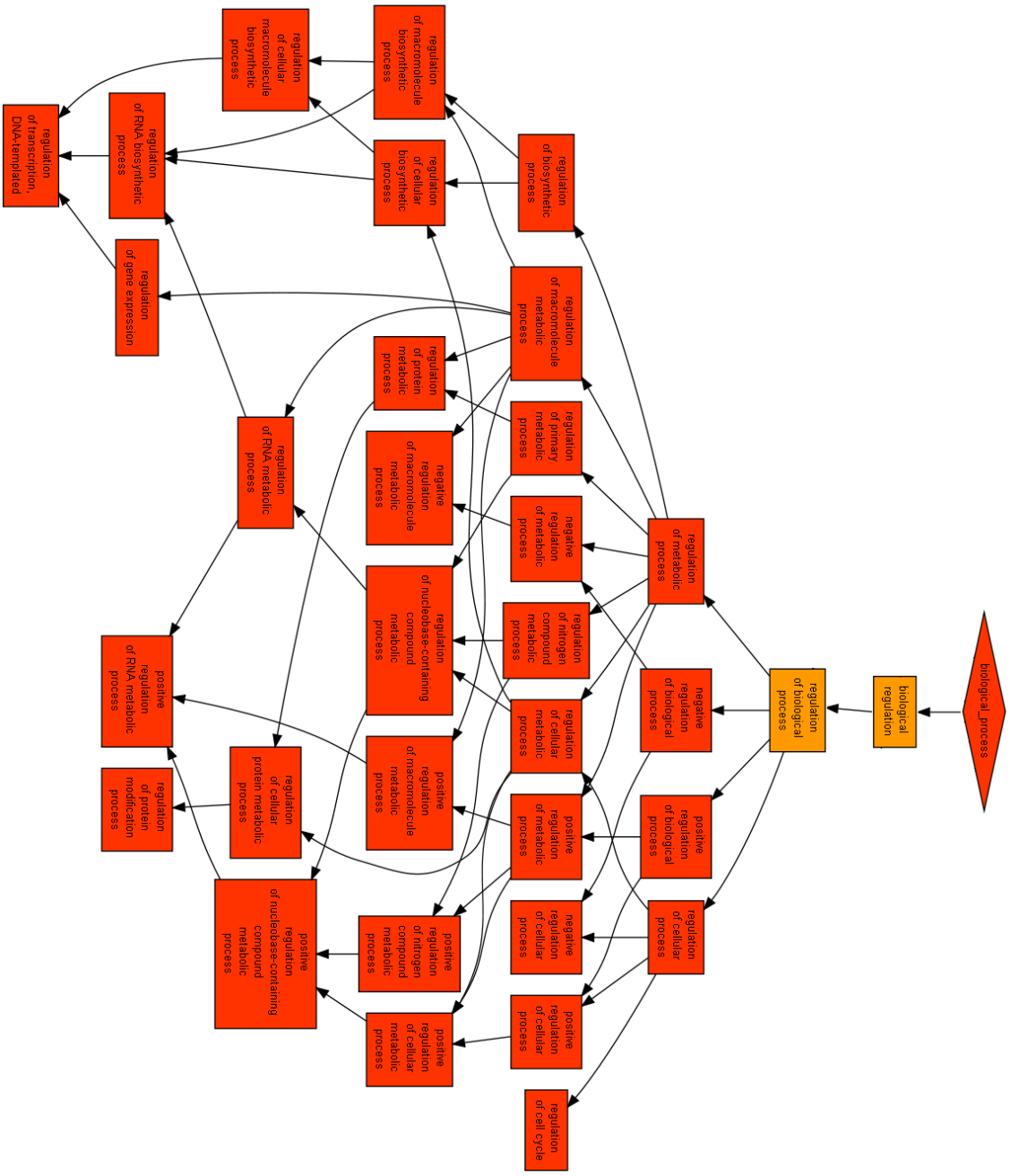

Figure M.3. Hierarchical visualization of over-repressented GO_ BP terms ($q<10^{-11}$) in IRF4-activated genes in SKMEL-28 cell line (Part I).

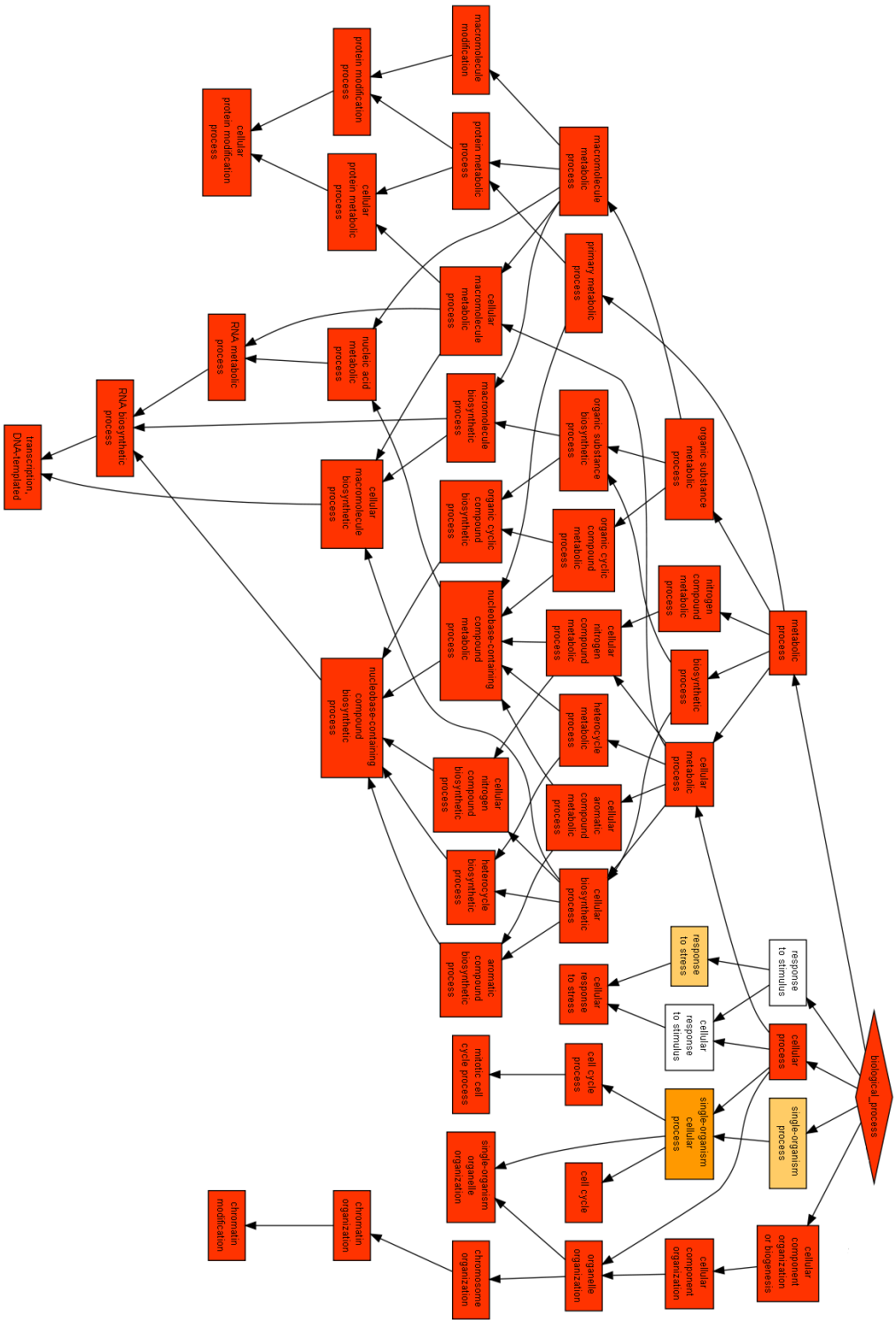

Figure M.4. Hierarchical visualization of over-repressented GO_ BP terms ($q<10^{-11}$) in IRF4-activated genes in SKMEL-28 cell line (Part II).

APPENDIX N: GENE ENRICHMENT ANALYSIS OF IRF4 REPRESSED GENES FOR GO_BP TERMS BY GORILLA

Table N.1. GO enrichment analysis (Biological Process) for IRF4-repressed genes in SKMEL-5 ($q<10^{-3}$).

Description	**P-value**	**FDR q-value**
single-organism biosynthetic process	3.79E-09	4.72E-05
aminoglycan metabolic process	8.65E-09	5.39E-05
lipid biosynthetic process	9.01E-09	3.74E-05
glycosaminoglycan metabolic process	9.97E-09	3.10E-05
sterol biosynthetic process	3.52E-08	8.78E-05
lipid metabolic process	4.95E-08	1.03E-04
carbohydrate metabolic process	1.71E-07	3.04E-04
membrane lipid metabolic process	4.85E-07	7.55E-04
sphingolipid metabolic process	5.96E-07	8.25E-04
response to unfolded protein	7.81E-07	9.73E-04

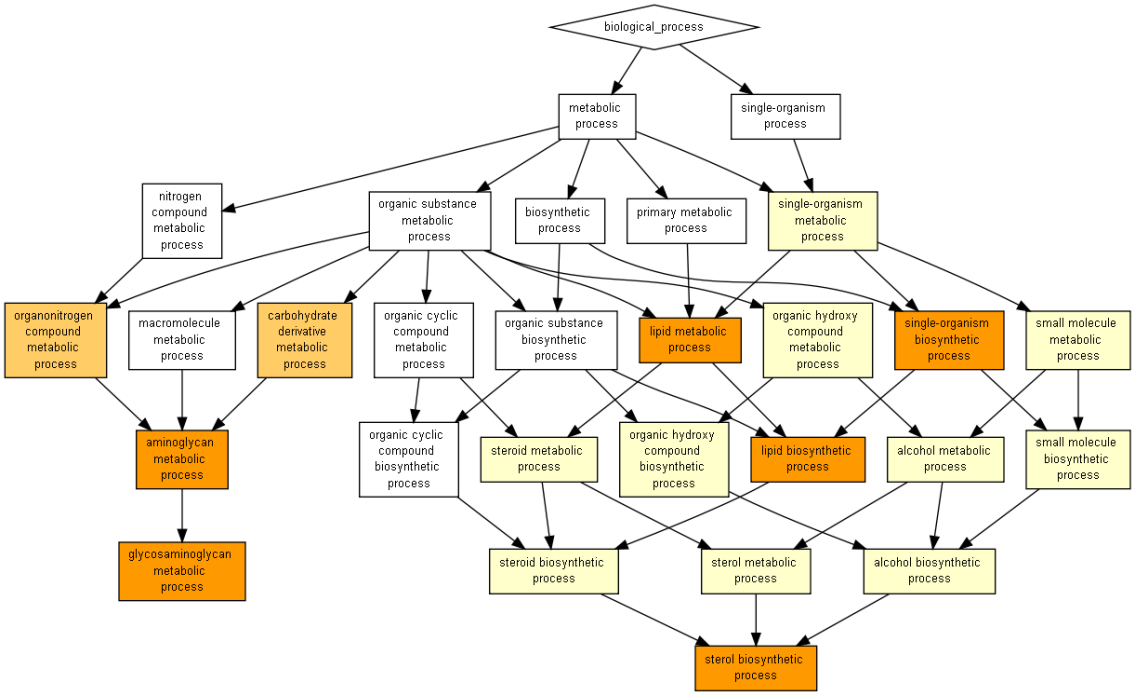

Figure N.1. Hierarchical visualization of over-represented GO_ BP terms ($q<10^{-11}$) for IRF4 repressed genes SKMEL-5 cell line.

Table N.2. GO enrichment analysis (Biological Process) for IRF4-repressed genes in SKMEL-28 ($q<10^{-3}$).

Description	**P-value**	**FDR q-value**
single-organism biosynthetic process	2.45E-17	3.05E-13
small molecule metabolic process	1.40E-14	8.71E-11
lipid biosynthetic process	2.55E-14	1.06E-10
lipid metabolic process	2.10E-13	6.54E-10
sterol biosynthetic process	1.89E-12	4.71E-09
cellular lipid metabolic process	2.10E-12	4.36E-09
protein transport	1.39E-11	2.48E-08
organic substance transport	2.67E-11	4.16E-08
cholesterol biosynthetic process	4.22E-11	5.84E-08
establishment of protein localization	6.43E-11	8.01E-08
organic hydroxy compound biosynthetic process	1.06E-10	1.20E-07
intracellular transport	3.68E-10	3.82E-07
single-organism intracellular transport	4.11E-10	3.93E-07
alcohol metabolic process	1.34E-09	1.19E-06
intracellular protein transport	2.15E-09	1.78E-06

Table N.2. GO enrichment analysis (Biological Process) for IRF4-repressed genes in SKMEL-28 ($q<10^{-3}$) (cont.).

Description	**P-value**	**FDR q-value**
transport	4.66E-09	3.63E-06
sterol metabolic process	4.83E-09	3.54E-06
alcohol biosynthetic process	6.15E-09	4.25E-06
cholesterol metabolic process	7.32E-09	4.80E-06
single-organism metabolic process	8.97E-09	5.58E-06
establishment of localization	1.23E-08	7.31E-06
organic hydroxy compound metabolic process	1.59E-08	8.98E-06
phosphorus metabolic process	3.26E-08	1.77E-05
small molecule biosynthetic process	3.83E-08	1.99E-05
sulfur compound metabolic process	4.09E-08	2.04E-05
oxoacid metabolic process	6.00E-08	2.87E-05
organonitrogen compound metabolic process	7.97E-08	3.68E-05
single-organism transport	9.53E-08	4.24E-05
phosphate-containing compound metabolic process	1.27E-07	5.44E-05
organic acid metabolic process	1.34E-07	5.55E-05
establishment of localization in cell	2.51E-07	1.01E-04
secondary metabolite biosynthetic process	2.79E-07	1.09E-04
glycerolipid biosynthetic process	3.03E-07	1.14E-04
steroid biosynthetic process	3.91E-07	1.43E-04
single-organism cellular process	3.95E-07	1.41E-04
melanin biosynthetic process	4.68E-07	1.62E-04
organophosphate metabolic process	6.16E-07	2.07E-04
membrane organization	6.38E-07	2.09E-04
phospholipid biosynthetic process	1.22E-06	3.90E-04
vesicle-mediated transport	1.41E-06	4.38E-04
glycerolipid metabolic process	1.50E-06	4.56E-04
vacuole organization	1.61E-06	4.79E-04
melanin metabolic process	1.65E-06	4.79E-04
phospholipid metabolic process	2.04E-06	5.77E-04
organophosphate biosynthetic process	2.20E-06	6.10E-04
carbohydrate metabolic process	3.36E-06	9.09E-04



Figure N.2. Hierarchical visualization of over-represented GO_ BP terms ($q<10^{-11}$) for IRF4 repressed genes SKMEL-28 cell line.

APPENDIX O: ENRICHED GENE ONTOLOGY (BIOLOGICAL PROCESS) TERMS IN IRF4-ACTIVATED GENE LIST SHARED BETWEEN SKMEL-5 AND SKMEL-28

Table O.1. GO enrichment analysis (Biological Process) for IRF4-activated genes in common ($q<10^{-3}$).

Description	P-value	FDR q-value	Enrichment
mitotic cell cycle process	9.20E-27	1.15E-22	3.63
cell cycle process	1.71E-25	1.07E-21	3.01
mitotic cell cycle	1.75E-22	7.25E-19	4.2
cell cycle	5.61E-22	1.75E-18	3.44
single-organism organelle organization	1.70E-21	4.23E-18	2.51
organelle organization	3.26E-21	6.77E-18	2.13
cellular component organization	1.59E-17	2.83E-14	1.64
cellular component organization or biogenesis	2.11E-17	3.28E-14	1.63
nuclear division	6.89E-17	9.53E-14	4.02
mitotic nuclear division	2.72E-16	3.39E-13	4.56
organelle fission	3.23E-16	3.65E-13	3.81
chromosome organization	7.72E-15	8.02E-12	2.68
cellular macromolecule metabolic process	7.22E-14	6.92E-11	1.4
regulation of cell cycle	1.23E-12	1.09E-09	2.46
macromolecule metabolic process	5.45E-12	4.53E-09	1.34
metabolic process	3.80E-11	2.96E-08	1.23
regulation of mitotic cell cycle	1.43E-10	1.05E-07	3.04
cellular metabolic process	4.23E-10	2.92E-07	1.26
single-organism cellular process	4.79E-10	3.14E-07	1.23
regulation of cell cycle process	5.13E-10	3.19E-07	2.72
primary metabolic process	5.73E-10	3.40E-07	1.25
organic substance metabolic process	1.76E-09	9.95E-07	1.24
cellular protein modification process	2.03E-09	1.10E-06	1.64
protein modification process	2.03E-09	1.05E-06	1.64
microtubule-based process	3.21E-09	1.60E-06	2.75
cellular process	3.41E-09	1.63E-06	1.13
macromolecule modification	6.30E-09	2.91E-06	1.59
regulation of protein modification process	6.94E-09	3.09E-06	1.9
regulation of cellular metabolic process	7.30E-09	3.14E-06	1.34
regulation of macromolecule metabolic process	7.46E-09	3.10E-06	1.36
DNA metabolic process	8.08E-09	3.25E-06	2.22
spindle checkpoint	1.17E-08	4.55E-06	8.15

Table O.1. GO enrichment analysis (Biological Process) for IRF4-activated genes in common ($q<10^{-3}$).

Description	P-value	FDR q-value	Enrichment
cellular protein metabolic process	1.60E-08	6.05E-06	1.52
regulation of primary metabolic process	2.12E-08	7.77E-06	1.33
regulation of cellular protein metabolic process	2.21E-08	7.86E-06	1.75
cellular response to stress	2.69E-08	9.30E-06	1.88
positive regulation of macromolecule metabolic process	2.71E-08	9.12E-06	1.61
mitotic spindle checkpoint	3.74E-08	1.23E-05	8.32
regulation of organelle organization	4.20E-08	1.34E-05	2.17
regulation of microtubule-based process	4.33E-08	1.35E-05	4.45
regulation of metabolic process	4.78E-08	1.45E-05	1.3
chromatin modification	5.42E-08	1.61E-05	2.46
regulation of microtubule cytoskeleton organization	6.24E-08	1.81E-05	4.84
chromatin organization	6.49E-08	1.84E-05	2.28
centrosome organization	7.51E-08	2.08E-05	6.38
regulation of protein kinase activity	7.58E-08	2.05E-05	2.15
mitotic cell cycle checkpoint	1.02E-07	2.69E-05	4.69
chromosome segregation	1.18E-07	3.06E-05	4.93
regulation of transferase activity	1.82E-07	4.62E-05	1.99
microtubule organizing center organization	1.86E-07	4.64E-05	5.94
positive regulation of cellular metabolic process	1.91E-07	4.67E-05	1.55
single-organism process	2.12E-07	5.09E-05	1.16
spindle assembly checkpoint	2.32E-07	5.46E-05	8.03
mitotic cell cycle phase transition	2.47E-07	5.69E-05	2.86
positive regulation of metabolic process	2.71E-07	6.14E-05	1.52
nucleic acid metabolic process	2.93E-07	6.51E-05	1.39
regulation of mitotic metaphase/anaphase transition	3.02E-07	6.59E-05	6.94
cell cycle phase transition	3.11E-07	6.69E-05	2.83
regulation of metaphase/anaphase transition of cell cycle	3.92E-07	8.26E-05	6.77
DNA replication	3.95E-07	8.19E-05	3.35
covalent chromatin modification	4.91E-07	1.00E-04	2.77
regulation of kinase activity	5.10E-07	1.03E-04	2.03
microtubule cytoskeleton organization	5.39E-07	1.07E-04	3.02
regulation of mitotic cell cycle phase transition	5.50E-07	1.07E-04	2.94
phosphorylation	5.63E-07	1.08E-04	1.87
positive regulation of cell cycle	6.53E-07	1.23E-04	3.94
cellular macromolecule biosynthetic process	7.64E-07	1.42E-04	1.45
positive regulation of protein modification process	8.02E-07	1.47E-04	1.93
protein metabolic process	1.12E-06	2.02E-04	1.38
regulation of cell cycle phase transition	1.13E-06	2.01E-04	2.84
sister chromatid segregation	1.18E-06	2.06E-04	9.21
histone modification	1.23E-06	2.13E-04	2.7

Table O.1. GO enrichment analysis (Biological Process) for IRF4-activated genes in common ($q<10^{-3}$).

Description	P-value	FDR q-value	Enrichment
cell cycle checkpoint	1.31E-06	2.24E-04	3.46
regulation of cell division	1.33E-06	2.23E-04	2.96
protein phosphorylation	1.55E-06	2.57E-04	2.02
nucleobase-containing compound metabolic process	1.65E-06	2.70E-04	1.32
negative regulation of mitotic cell cycle phase transition	1.65E-06	2.67E-04	3.18
regulation of mitosis	1.72E-06	2.75E-04	4.07
macromolecule biosynthetic process	1.88E-06	2.97E-04	1.41
mitotic spindle assembly checkpoint	1.90E-06	2.96E-04	7.45
positive regulation of cellular protein metabolic process	2.10E-06	3.23E-04	1.83
cytoskeleton organization	2.23E-06	3.39E-04	2.08
negative regulation of cell cycle phase transition	2.84E-06	4.26E-04	3.08
nuclear envelope organization	3.02E-06	4.47E-04	5.6
negative regulation of mitotic metaphase/anaphase transition	3.32E-06	4.87E-04	7.01
regulation of macromolecule biosynthetic process	3.57E-06	5.16E-04	1.35
regulation of protein metabolic process	3.79E-06	5.42E-04	1.53
negative regulation of cell cycle process	4.31E-06	6.10E-04	2.77
negative regulation of metaphase/anaphase transition of cell cycle	4.33E-06	6.05E-04	6.81
regulation of RNA biosynthetic process	4.38E-06	6.06E-04	1.37
positive regulation of cellular process	4.40E-06	6.02E-04	1.35
regulation of protein phosphorylation	4.86E-06	6.58E-04	1.79
regulation of transcription, DNA-templated	4.98E-06	6.67E-04	1.37
regulation of cyclin-dependent protein serine/threonine kinase activity	5.08E-06	6.73E-04	4.21
regulation of transcription from RNA polymerase II promoter	5.30E-06	6.95E-04	1.61
negative regulation of microtubule depolymerization	5.35E-06	6.94E-04	9.27
mitotic sister chromatid segregation	5.35E-06	6.87E-04	9.27
cellular response to DNA damage stimulus	5.54E-06	7.04E-04	1.99
positive regulation of catalytic activity	5.92E-06	7.45E-04	1.69
positive regulation of protein metabolic process	6.09E-06	7.59E-04	1.74
negative regulation of macromolecule metabolic process	6.26E-06	7.72E-04	1.58
histone H4 acetylation	6.56E-06	8.01E-04	5.76
cell cycle G2/M phase transition	6.83E-06	8.26E-04	3.36
G2/M transition of mitotic cell cycle	6.83E-06	8.18E-04	3.36
mitotic nuclear envelope disassembly	7.12E-06	8.45E-04	6.44
cellular aromatic compound metabolic process	7.26E-06	8.53E-04	1.29
regulation of catalytic activity	7.99E-06	9.29E-04	1.49
heterocycle metabolic process	8.43E-06	9.73E-04	1.29
cytokinesis	8.66E-06	9.89E-04	4.3
positive regulation of transferase activity	8.69E-06	9.83E-04	2.03
regulation of RNA metabolic process	8.78E-06	9.85E-04	1.35
regulation of molecular function	8.80E-06	9.79E-04	1.44

APPENDIX P: ENRICHED GENE ONTOLOGY (BIOLOGICAL PROCESS) TERMS IN IRF4-REPRESSED GENE LIST SHARED BETWEEN SKMEL-5 AND SKMEL-28

Table P.1. GO enrichment analysis (Biological Process) for IRF4-repressed genes in common ($q<10^{-3}$).

Description	P-value	FDR q-value	Enrichment
lipid biosynthetic process	5.01E-11	6.24E-07	3
single-organism biosynthetic process	1.17E-10	7.26E-07	2.19
sterol biosynthetic process	1.72E-09	7.14E-06	9.67
lipid metabolic process	1.91E-09	5.95E-06	2.11
cholesterol biosynthetic process	6.50E-08	1.62E-04	9.24
membrane lipid metabolic process	2.46E-07	5.12E-04	4.03
steroid biosynthetic process	2.68E-07	4.76E-04	4.7
glycolipid metabolic process	5.15E-07	8.02E-04	5.11
cellular lipid metabolic process	6.79E-07	9.39E-04	2.04
alcohol biosynthetic process	6.91E-07	8.60E-04	4.67

APPENDIX Q: MITF LEVELS UPON IRF4 KNOCK-DOWN IN SKMEL-5 AND SKMEL-28 CELL LINES

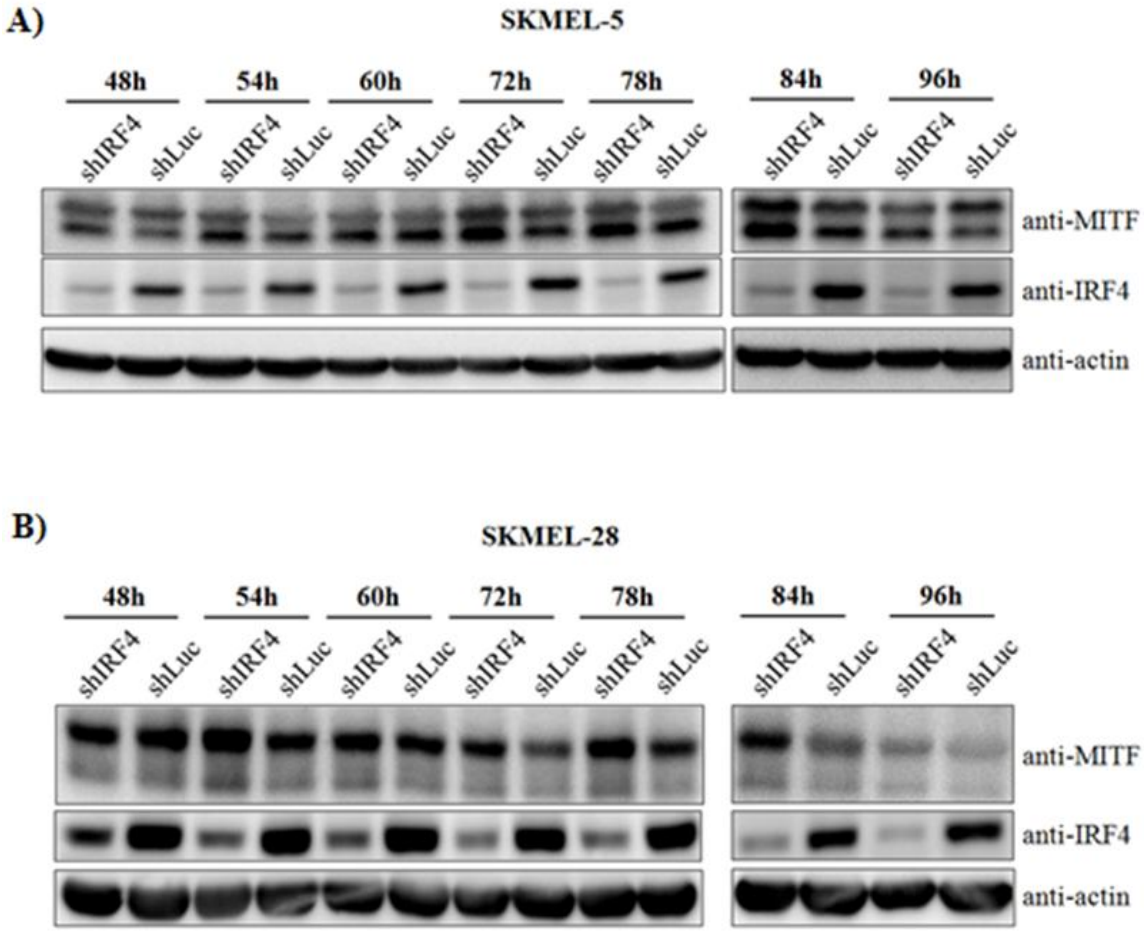

Figure Q.1. Repeat experiments showing MITF protein levels upon IRF4 knock-down in A) SKMEL-5 and B) SKMEL-28 cell lines.

APPENDIX R: MITF AND P-AKT LEVELS UPON IRF4 KNOCK-DOWN IN A2058 AND G-361 CELL LINES

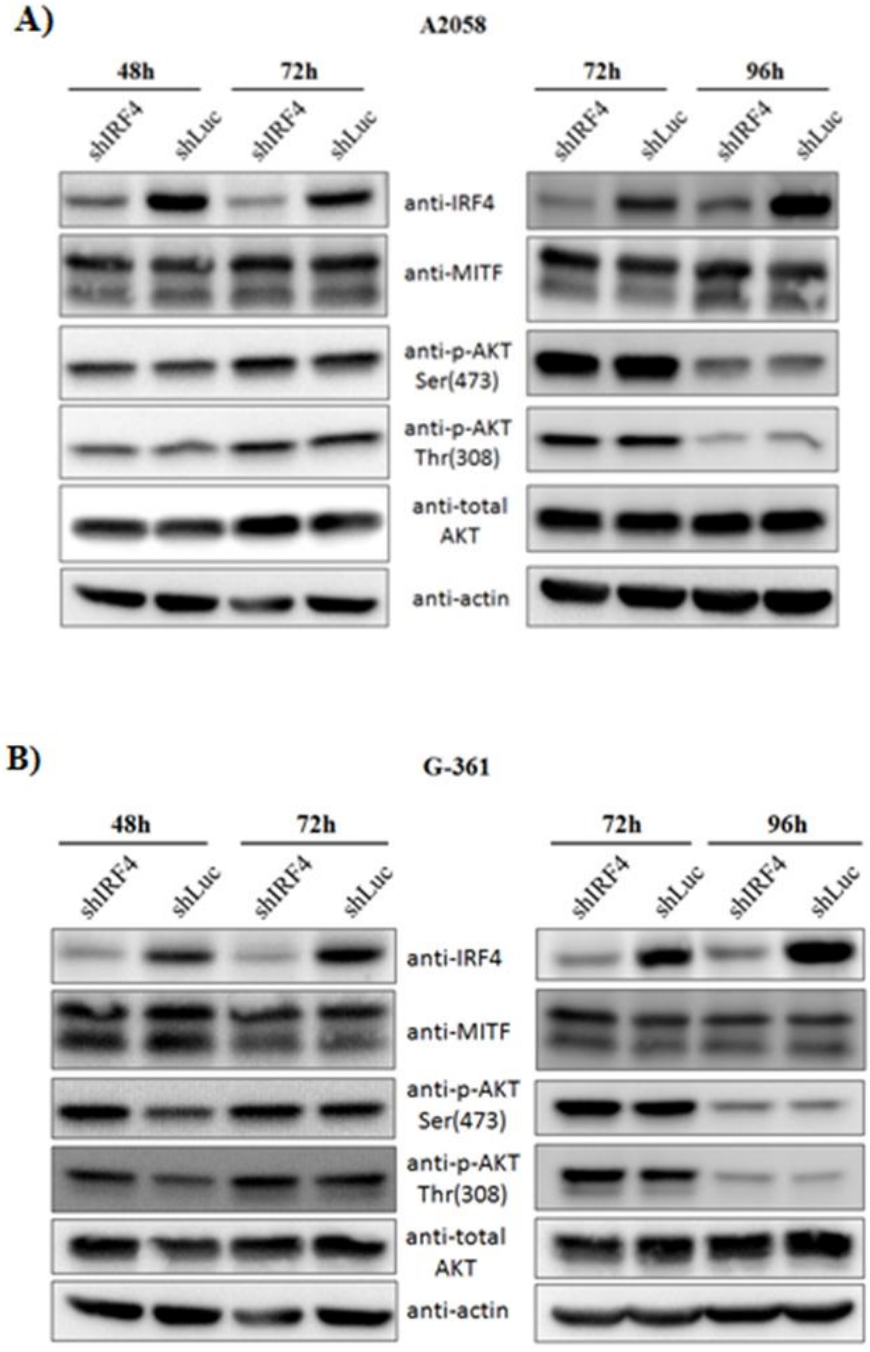

Figure R.1. MITF and AKT phosphorylation levels upon IRF4 down-regulation in A) A2058 and B) G-361 cell lines.

APPENDIX S: MITF PROTEIN LEVELS IN IRF4 OVER-EXPRESSED SKMEL-28 CELL LINE

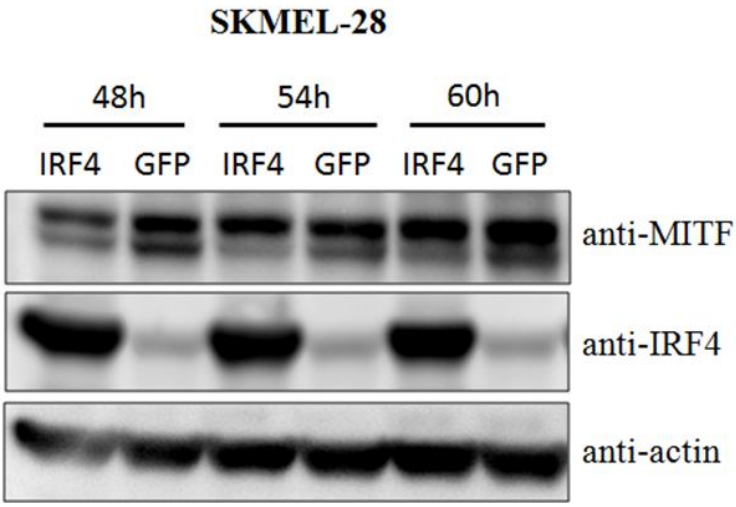

Figure S.1. Repeat experiment showing MITF levels upon IRF4 over-expression in SKMEL-28 cell line.

APPENDIX T: p-ERK1/2 LEVELS UPON IRF4 KNOCK-DOWN IN SKMEL-5 AND SKMEL-28 CELL LINES

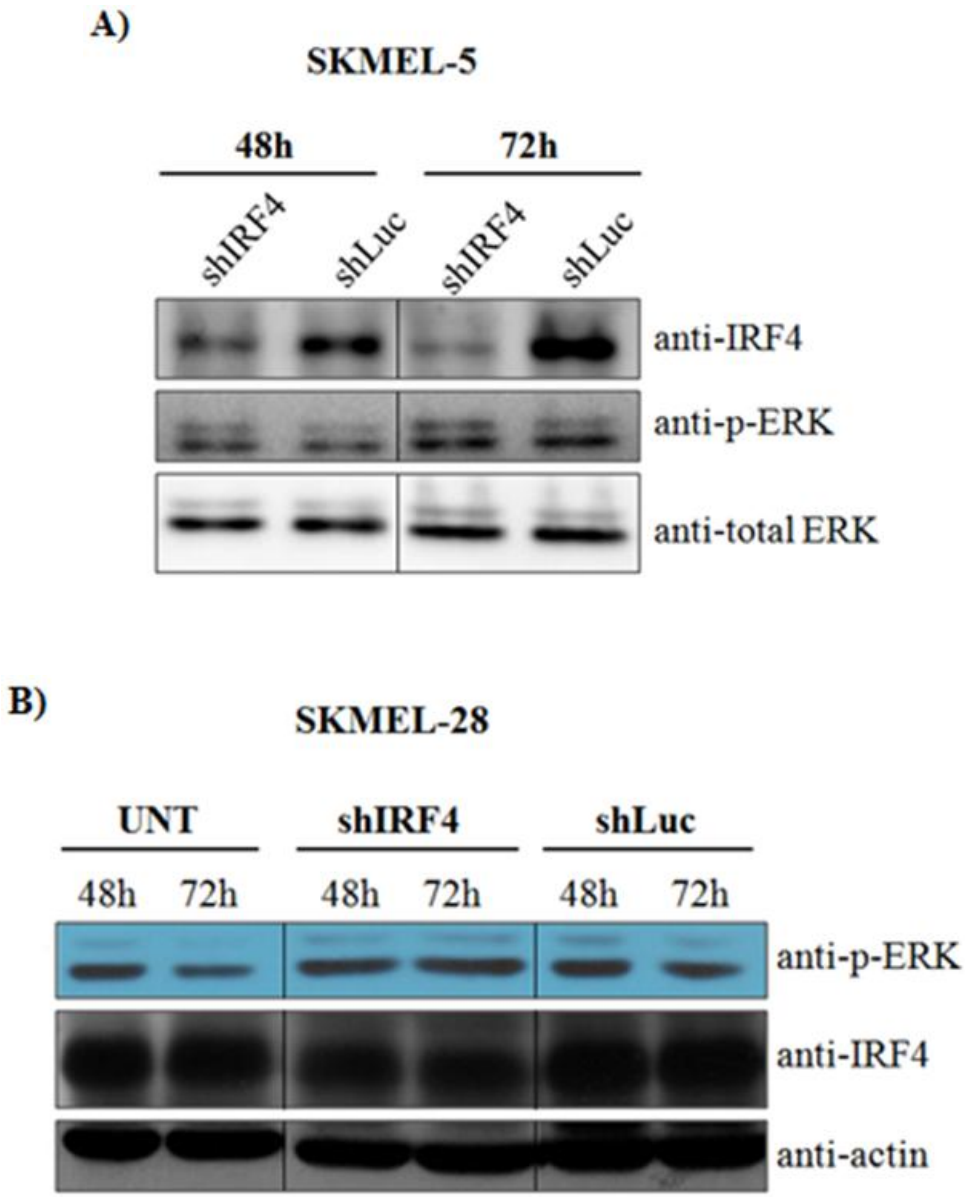

Figure T.1. Repeat experiments showing p-ERK1/2 levels upon IRF4 down-regulation in A) SKMEL-5 and B) SKMEL-28 cell lines. Figure B lacks immunoblotting for total-ERK.

APPENDIX U: p-AKT LEVELS UPON IRF4 KNOCK-DOWN IN SKMEL-5 AND SKMEL-28 CELL LINES

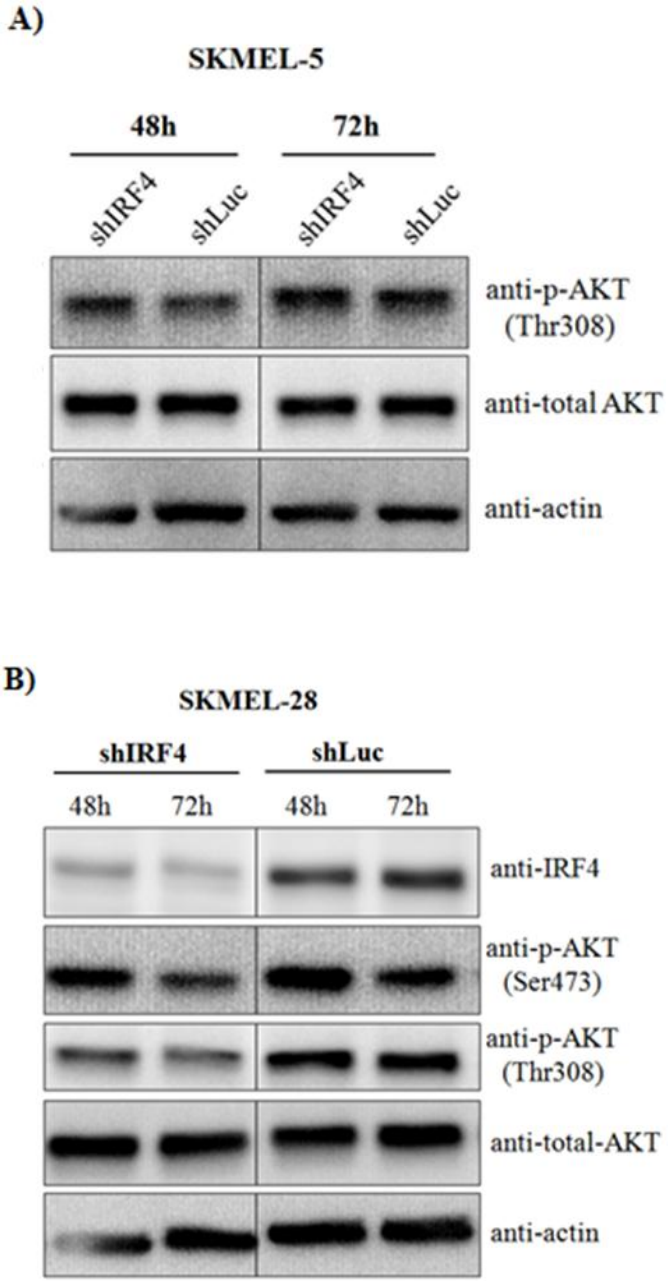

Figure U.1. Repeat experiments showing p-AKT levels upon IRF4 down-regulation in A) SKMEL-5 and B) SKMEL-28 cell lines.

APPENDIX V: p-AKT LEVELS IN IRF4 OVER-EXPRESSED SKMEL-28 AND MEL-ST CELL LINES

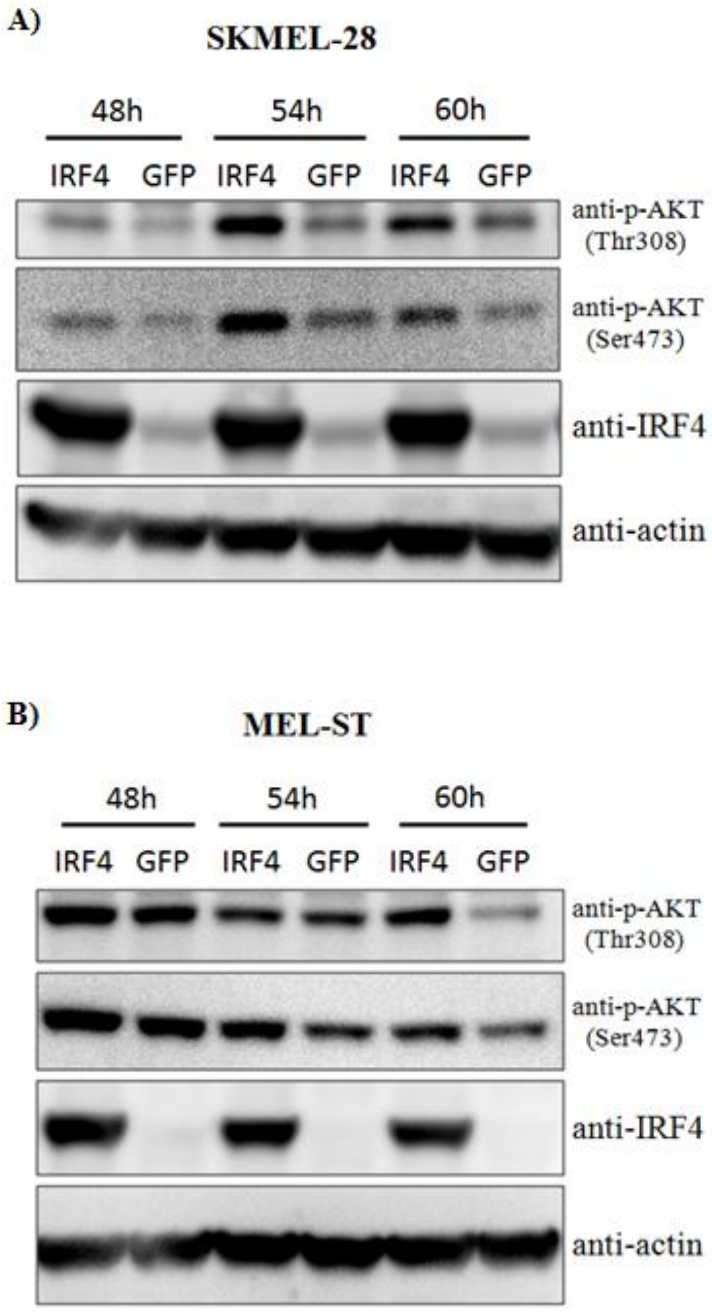

Figure V.1. Western blottings showing p-AKT levels upon IRF4 over-expression in A) SKMEL-28 and B) MEL-ST cell lines.

REFERENCES

Ackermann, J., M. Frutschi, K. Kaloulis, T. McKee, A. Trumpp and F. Beermann, 2005, "Metastasizing Melanoma Formation Caused by Expression of Activated N-Rasq61k on an Ink4a-Deficient Background", *Cancer Research*, Vol. 65, No. 10, pp. 4005-4011.

Acquaviva, J., X. Chen and R. Ren, 2008, "Irf-4 Functions as a Tumor Suppressor in Early B-Cell Development", *Blood*, Vol. 112, No. 9, pp. 3798-3806.

Adams, J.M. and S. Cory, 2007, "Bcl-2-Regulated Apoptosis: Mechanism and Therapeutic Potential", *Current Opinion in Immunology*, Vol. 19, No. 5, pp. 488-496.

Agarwal, A.K., R.P. Gude and R.D. Kalraiya, 2014, "Regulation of Melanoma Metastasis to Lungs by Cell Surface Lysosome Associated Membrane Protein-1 (Lamp1) Via Galectin-3", *Biochemical and Biophysical Research Communications*, Vol. 449, No. 3, pp. 332-337.

Alain, T., M. Morita, B.D. Fonseca, A. Yanagiya, N. Siddiqui, M. Bhat, D. Zammit, V. Marcus, P. Metrakos, L.A. Voyer, V. Gandin, Y. Liu, I. Topisirovic and N. Sonenberg, 2012, "Eif4e/4e-Bp Ratio Predicts the Efficacy of Mtor Targeted Therapies", *Cancer Research*, Vol. 72, No. 24, pp. 6468-6476.

Anders, S. and W. Huber, 2010, "Differential Expression Analysis for Sequence Count Data", *Genome Biology*, Vol. 11, No. 10, pp. 106.

Ayhan, M.C., 2014, "Characterization of Irf4 in Melanoma Cell Lines", M.Sc. Thesis, Bogazici University

Balch, C.M., J.E. Gershenwald, S.j. Soong, J.F. Thompson, M.B. Atkins, D.R. Byrd, A.C. Buzaid, A.J. Cochran, D.G. Coit, S. Ding, A.M. Eggermont, K.T. Flaherty, P.A. Gimotty, J.M. Kirkwood, K.M. McMasters, M.C. Mihm, D.L. Morton, M.I. Ross,

A.J. Sober and V.K. Sondak, 2009, "Final Version of 2009 Ajcc Melanoma Staging and Classification", *Journal of Clinical Oncology*, Vol. 27, No. 36, pp. 6199-6206.

Barretina, J., G. Caponigro, N. Stransky, K. Venkatesan, A.A. Margolin, S. Kim, C.J. Wilson, J. Lehar, G.V. Kryukov, D. Sonkin, A. Reddy, M. Liu, L. Murray, M.F. Berger, J.E. Monahan, P. Morais, J. Meltzer, A. Korejwa, J. Jane-Valbuena, F.A. Mapa, J. Thibault, E. Bric-Furlong, P. Raman, A. Shipway, I.H. Engels, J. Cheng, G.K. Yu, J. Yu, P. Aspesi, Jr., M. de Silva, K. Jagtap, M.D. Jones, L. Wang, C. Hatton, E. Palescandolo, S. Gupta, S. Mahan, C. Sougnez, R.C. Onofrio, T. Liefeld, L. MacConaill, W. Winckler, M. Reich, N. Li, J.P. Mesirov, S.B. Gabriel, G. Getz, K. Ardlie, V. Chan, V.E. Myer, B.L. Weber, J. Porter, M. Warmuth, P. Finan, J.L. Harris, M. Meyerson, T.R. Golub, M.P. Morrissey, W.R. Sellers, R. Schlegel and L.A. Garraway, 2012, "The Cancer Cell Line Encyclopedia Enables Predictive Modelling of Anticancer Drug Sensitivity", *Nature*, Vol. 483, No. 7391, pp. 603-607.

Bernstein, B.E., J.A. Stamatoyannopoulos, J.F. Costello, B. Ren, A. Milosavljevic, A. Meissner, M. Kellis, M.A. Marra, A.L. Beaudet, J.R. Ecker, P.J. Farnham, M. Hirst, E.S. Lander, T.S. Mikkelsen and J.A. Thomson, 2010, "The Nih Roadmap Epigenomics Mapping Consortium", *Nature Biotechnology*, Vol. 28, No. 10, pp. 1045-1048.

Bertolotto, C., 2013, "Melanoma: From Melanocyte to Genetic Alterations and Clinical Options", *Scientifica (Cairo)*, Vol. 2013, pp. 635203.

Berx, G. and F. van Roy, 2009, "Involvement of Members of the Cadherin Superfamily in Cancer", *Cold Spring Harbor Perspectives in Biology*, Vol. 1, No. 6, pp. a003129.

Bogunovic, D., D.W. O'Neill, I. Belitskaya-Levy, V. Vacic, Y.L. Yu, S. Adams, F. Darvishian, R. Berman, R. Shapiro, A.C. Pavlick, S. Lonardi, J. Zavadil, I. Osman and N. Bhardwaj, 2009, "Immune Profile and Mitotic Index of Metastatic Melanoma Lesions Enhance Clinical Staging in Predicting Patient Survival", *Proceedings of the National Academy of Sciences of the United States of America*, Vol. 106, No. 48, pp. 20429-20434.

Boyle, G.M., S.L. Woods, V.F. Bonazzi, M.S. Stark, E. Hacker, L.G. Aoude, K. Dutton-Regester, A.L. Cook, R.A. Sturm and N.K. Hayward, 2011, "Melanoma Cell Invasiveness Is Regulated by Mir-211 Suppression of the Brn2 Transcription Factor", *Pigment Cell Melanoma Research*, Vol. 24, No. 3, pp. 525-537.

Brass, A.L., E. Kehrli, C.F. Eisenbeis, U. Storb and H. Singh, 1996, "Pip, a Lymphoid-Restricted Irf, Contains a Regulatory Domain That Is Important for Autoinhibition and Ternary Complex Formation with the Ets Factor Pu.1", *Genes Development*, Vol. 10, No. 18, pp. 2335-2347.

Brustle, A., S. Heink, M. Huber, C. Rosenplanter, C. Stadelmann, P. Yu, E. Arpaia, T.W. Mak, T. Kamradt and M. Lohoff, 2007, "The Development of Inflammatory T(H)-17 Cells Requires Interferon-Regulatory Factor 4", *Nature Immunology*, Vol. 8, No. 9, pp. 958-966.

Byrne, A.M., D.J. Bouchier-Hayes and J.H. Harmey, 2005, "Angiogenic and Cell Survival Functions of Vascular Endothelial Growth Factor (Vegf)", *Journal of Cellular and Molecular Medicine*, Vol. 9, No. 4, pp. 777-794.

Calipel, A., G. Lefevre, C. Pouponnot, F. Mouriaux, A. Eychene and F. Mascarelli, 2003, "Mutation of B-Raf in Human Choroidal Melanoma Cells Mediates Cell Proliferation and Transformation through the Mek/Erk Pathway", *Journal of Biological Chemistry*, Vol. 278, No. 43, pp. 42409-42418.

Carmeliet, P., 2005, "Vegf as a Key Mediator of Angiogenesis in Cancer", *Oncology*, Vol. 69 Suppl 3, pp. 4-10.

Carreira, S., J. Goodall, L. Denat, M. Rodriguez, P. Nuciforo, K.S. Hoek, A. Testori, L. Larue and C.R. Goding, 2006, "Mitf Regulation of Dia1 Controls Melanoma Proliferation and Invasiveness", *Genes Development*, Vol. 20, No. 24, pp. 3426-3439.

Castellano, E. and J. Downward, 2011, "Ras Interaction with Pi3k: More Than Just Another Effector Pathway", *Genes Cancer*, Vol. 2, No. 3, pp. 261-274.

Chalhoub, N. and S.J. Baker, 2009, "Pten and the Pi3-Kinase Pathway in Cancer", *Annual Review Pathology*, Vol. 4, pp. 127-150.

Chambard, J.C., R. Lefloch, J. Pouyssegur and P. Lenormand, 2007, "Erk Implication in Cell Cycle Regulation", *Biochimica et Biophysica Acta*, Vol. 1773, No. 8, pp. 1299-1310.

Cheli, Y., M. Ohanna, R. Ballotti and C. Bertolotto, 2010, "Fifteen-Year Quest for Microphthalmia-Associated Transcription Factor Target Genes", *Pigment Cell Melanoma Research*, Vol. 23, No. 1, pp. 27-40.

Clarke, J., H.C. Wu, L. Jayasinghe, A. Patel, S. Reid and H. Bayley, 2009, "Continuous Base Identification for Single-Molecule Nanopore DNA Sequencing", *Nature Nanotechnology*, Vol. 4, No. 4, pp. 265-270.

Costin, G.E. and V.J. Hearing, 2007, "Human Skin Pigmentation: Melanocytes Modulate Skin Color in Response to Stress", *FASEB Journal*, Vol. 21, No. 4, pp. 976-994.

Dahl, C. and P. Guldberg, 2007, "The Genome and Epigenome of Malignant Melanoma", *APMIS*, Vol. 115, No. 10, pp. 1161-1176.

Davies, H., G.R. Bignell, C. Cox, P. Stephens, S. Edkins, S. Clegg, J. Teague, H. Woffendin, M.J. Garnett, W. Bottomley, N. Davis, E. Dicks, R. Ewing, Y. Floyd, K. Gray, S. Hall, R. Hawes, J. Hughes, V. Kosmidou, A. Menzies, C. Mould, A. Parker, C. Stevens, S. Watt, S. Hooper, R. Wilson, H. Jayatilake, B.A. Gusterson, C. Cooper, J. Shipley, D. Hargrave, K. Pritchard-Jones, N. Maitland, G. Chenevix-Trench, G.J. Riggins, D.D. Bigner, G. Palmieri, A. Cossu, A. Flanagan, A. Nicholson, J.W. Ho, S.Y. Leung, S.T. Yuen, B.L. Weber, H.F. Seigler, T.L. Darrow, H. Paterson, R. Marais, C.J. Marshall, R. Wooster, M.R. Stratton and P.A. Futreal, 2002, "Mutations of the Braf Gene in Human Cancer", *Nature*, Vol. 417, No. 6892, pp. 949-954.

De Silva, N.S., G. Simonetti, N. Heise and U. Klein, 2012, "The Diverse Roles of Irf4 in Late Germinal Center B-Cell Differentiation", *Immunological Reviews*, Vol. 247, No. 1, pp. 73-92.

Duffy, D.L., M.M. Iles, D. Glass, G. Zhu, J.H. Barrett, V. Hoiom, Z.Z. Zhao, R.A. Sturm, N. Soranzo, C. Hammond, M. Kvaskoff, D.C. Whiteman, M. Mangino, J. Hansson, J.A. Newton-Bishop, GenoMel, V. Bataille, N.K. Hayward, N.G. Martin, D.T. Bishop, T.D. Spector and G.W. Montgomery, 2010, "Irf4 Variants Have Age-Specific Effects on Nevus Count and Predispose to Melanoma", *American Journal of Human Genetics*, Vol. 87, No. 1, pp. 6-16.

Duronio, R.J. and Y. Xiong, 2013, "Signaling Pathways That Control Cell Proliferation", *Cold Spring Harbor Perspectives in Biology*, Vol. 5, No. 3, pp. a008904.

Easty, D.J., S.G. Gray, K.J. O'Byrne, D. O'Donnell and D.C. Bennett, 2011, "Receptor Tyrosine Kinases and Their Activation in Melanoma", *Pigment Cell Melanoma Research*, Vol. 24, No. 3, pp. 446-461.

Eden, E., R. Navon, I. Steinfeld, D. Lipson and Z. Yakhini, 2009, "Gorilla: A Tool for Discovery and Visualization of Enriched Go Terms in Ranked Gene Lists", *BMC Bioinformatics*, Vol. 10, pp. 48.

Edgar, R., M. Domrachev and A.E. Lash, 2002, "Gene Expression Omnibus: Ncbi Gene Expression and Hybridization Array Data Repository", *Nucleic Acids Research*, Vol. 30, No. 1, pp. 207-210.

Eguchi, J., Q.W. Yan, D.E. Schones, M. Kamal, C.H. Hsu, M.Q. Zhang, G.E. Crawford and E.D. Rosen, 2008, "Interferon Regulatory Factors Are Transcriptional Regulators of Adipogenesis", *Cell Metabolism*, Vol. 7, No. 1, pp. 86-94.

Eid, J., A. Fehr, J. Gray, K. Luong, J. Lyle, G. Otto, P. Peluso, D. Rank, P. Baybayan, B. Bettman, A. Bibillo, K. Bjornson, B. Chaudhuri, F. Christians, R. Cicero, S. Clark, R. Dalal, A. Dewinter, J. Dixon, M. Foquet, A. Gaertner, P. Hardenbol, C. Heiner, K. Hester, D. Holden, G. Kearns, X. Kong, R. Kuse, Y. Lacroix, S. Lin, P.

Lundquist, C. Ma, P. Marks, M. Maxham, D. Murphy, I. Park, T. Pham, M. Phillips, J. Roy, R. Sebra, G. Shen, J. Sorenson, A. Tomaney, K. Travers, M. Trulson, J. Vieceli, J. Wegener, D. Wu, A. Yang, D. Zaccarin, P. Zhao, F. Zhong, J. Korlach and S. Turner, 2009, "Real-Time DNA Sequencing from Single Polymerase Molecules", *Science*, Vol. 323, No. 5910, pp. 133-138.

Eisenbeis, C.F., H. Singh and U. Storb, 1995, "Pip, a Novel Irf Family Member, Is a Lymphoid-Specific, Pu.1-Dependent Transcriptional Activator", *Genes Development*, Vol. 9, No. 11, pp. 1377-1387.

Ekedahl, H., H. Cirenajwis, K. Harbst, A. Carneiro, K. Nielsen, H. Olsson, L. Lundgren, C. Ingvar and G. Jonsson, 2013, "The Clinical Significance of Braf and Nras Mutations in a Clinic-Based Metastatic Melanoma Cohort", *British Journal of Dermatology*, Vol. 169, No. 5, pp. 1049-1055.

Escalante, C.R., J. Yie, D. Thanos and A.K. Aggarwal, 1998, "Structure of Irf-1 with Bound DNA Reveals Determinants of Interferon Regulation", *Nature*, Vol. 391, No. 6662, pp. 103-106.

Ewing, B., L. Hillier, M.C. Wendl and P. Green, 1998, "Base-Calling of Automated Sequencer Traces Using Phred. I. Accuracy Assessment", *Genome Research*, Vol. 8, No. 3, pp. 175-185.

Fang, Z. and X. Cui, 2011, "Design and Validation Issues in Rna-Seq Experiments", *Briefings in Bioinformatics*, Vol. 12, No. 3, pp. 280-287.

Garraway, L.A., H.R. Widlund, M.A. Rubin, G. Getz, A.J. Berger, S. Ramaswamy, R. Beroukhim, D.A. Milner, S.R. Granter, J. Du, C. Lee, S.N. Wagner, C. Li, T.R. Golub, D.L. Rimm, M.L. Meyerson, D.E. Fisher and W.R. Sellers, 2005, "Integrative Genomic Analyses Identify Mitf as a Lineage Survival Oncogene Amplified in Malignant Melanoma", *Nature*, Vol. 436, No. 7047, pp. 117-122.

Gene Ontology, C., 2008, "The Gene Ontology Project in 2008", *Nucleic Acids Research*, Vol. 36, pp. D440-444.

Georgopoulou, N., C. Hurel, P.K. Politis, M. Gaitanou, R. Matsas and D. Thomaidou, 2006, "Bm88 Is a Dual Function Molecule Inducing Cell Cycle Exit and Neuronal Differentiation of Neuroblastoma Cells Via Cyclin D1 Down-Regulation and Retinoblastoma Protein Hypophosphorylation", *The Journal of Biological Chemistry*, Vol. 281, No. 44, pp. 33606-33620.

Ghebranious, N. and L.A. Donehower, 1998, "Mouse Models in Tumor Suppression", *Oncogene*, Vol. 17, No. 25, pp. 3385-3400.

Goodall, J., S. Carreira, L. Denat, D. Kobi, I. Davidson, P. Nuciforo, R.A. Sturm, L. Larue and C.R. Goding, 2008, "Brn-2 Represses Microphthalmia-Associated Transcription Factor Expression and Marks a Distinct Subpopulation of Microphthalmia-Associated Transcription Factor-Negative Melanoma Cells", *Cancer Research*, Vol. 68, No. 19, pp. 7788-7794.

Grada, A. and K. Weinbrecht, 2013, "Next-Generation Sequencing: Methodology and Application", *Journal of Investigative Dermatology*, Vol. 133, No. 8, pp. e11.

Graham, F.L. and A.J. van der Eb, 1973, "A New Technique for the Assay of Infectivity of Human Adenovirus 5 DNA", *Virology*, Vol. 52, No. 2, pp. 456-467.

Gray-Schopfer, V., C. Wellbrock and R. Marais, 2007, "Melanoma Biology and New Targeted Therapy", *Nature*, Vol. 445, No. 7130, pp. 851-857.

Gray-Schopfer, V.C., S. da Rocha Dias and R. Marais, 2005, "The Role of B-Raf in Melanoma", *Cancer and Metastasis Reviews*, Vol. 24, No. 1, pp. 165-183.

Guo, S., Z.Z. Li, D.S. Jiang, Y.Y. Lu, Y. Liu, L. Gao, S.M. Zhang, H. Lei, L.H. Zhu, X.D. Zhang, D.P. Liu and H. Li, 2014, "Irf4 Is a Novel Mediator for Neuronal Survival in Ischaemic Stroke", *Cell Death Differentiation*, Vol. 21, pp. 888-903.

Halaban, R., E. Cheng, Y. Smicun and J. Germino, 2000, "Deregulated E2f Transcriptional Activity in Autonomously Growing Melanoma Cells", *The Journal of Experimental Medicine*, Vol. 191, No. 6, pp. 1005-1016.

Han, J., P. Kraft, H. Nan, Q. Guo, C. Chen, A. Qureshi, S.E. Hankinson, F.B. Hu, D.L. Duffy, Z.Z. Zhao, N.G. Martin, G.W. Montgomery, N.K. Hayward, G. Thomas, R.N. Hoover, S. Chanock and D.J. Hunter, 2008, "A Genome-Wide Association Study Identifies Novel Alleles Associated with Hair Color and Skin Pigmentation", *PLoS Genetics*, Vol. 4, No. 5, pp. e1000074.

Han, J., A.A. Qureshi, H. Nan, J. Zhang, Y. Song, Q. Guo and D.J. Hunter, 2011, "A Germline Variant in the Interferon Regulatory Factor 4 Gene as a Novel Skin Cancer Risk Locus", *Cancer Research*, Vol. 71, No. 5, pp. 1533-1539.

Hanahan, D. and R.A. Weinberg, 2011, "Hallmarks of Cancer: The Next Generation", *Cell*, Vol. 144, No. 5, pp. 646-674.

Heintel, D., N. Zojer, M. Schreder, K. Strasser-Weippl, B. Kainz, M. Vesely, H. Gisslinger, J. Drach, A. Gaiger, U. Jager and H. Ludwig, 2008, "Expression of Mum1/Irf4 Mrna as a Prognostic Marker in Patients with Multiple Myeloma", *Leukemia*, Vol. 22, No. 2, pp. 441-445.

Hoek, K., D.L. Rimm, K.R. Williams, H. Zhao, S. Ariyan, A. Lin, H.M. Kluger, A.J. Berger, E. Cheng, E.S. Trombetta, T. Wu, M. Niinobe, K. Yoshikawa, G.E. Hannigan and R. Halaban, 2004, "Expression Profiling Reveals Novel Pathways in the Transformation of Melanocytes to Melanomas", *Cancer Research*, Vol. 64, No. 15, pp. 5270-5282.

Hoek, K.S., O.M. Eichhoff, N.C. Schlegel, U. Dobbeling, N. Kobert, L. Schaerer, S. Hemmi and R. Dummer, 2008a, "In Vivo Switching of Human Melanoma Cells between Proliferative and Invasive States", *Cancer Research*, Vol. 68, No. 3, pp. 650-656.

Hoek, K.S., N.C. Schlegel, O.M. Eichhoff, D.S. Widmer, C. Praetorius, S.O. Einarsson, S. Valgeirsdottir, K. Bergsteinsdottir, A. Schepsky, R. Dummer and E. Steingrimsson, 2008b, "Novel Mitf Targets Identified Using a Two-Step DNA Microarray Strategy", *Pigment Cell Melanoma Research*, Vol. 21, No. 6, pp. 665-676.

Honma, K., D. Kimura, N. Tominaga, M. Miyakoda, T. Matsuyama and K. Yui, 2008, "Interferon Regulatory Factor 4 Differentially Regulates the Production of Th2 Cytokines in Naive Vs. Effector/Memory Cd4+ T Cells", *Proceedings of the National Academy of Sciences of the United States of America*, Vol. 105, No. 41, pp. 15890-15895.

Huang da, W., B.T. Sherman and R.A. Lempicki, 2009, "Systematic and Integrative Analysis of Large Gene Lists Using David Bioinformatics Resources", *Nature Protocols*, Vol. 4, No. 1, pp. 44-57.

Iida, S., P.H. Rao, M. Butler, P. Corradini, M. Boccadoro, B. Klein, R.S. Chaganti and R. Dalla-Favera, 1997, "Deregulation of Mum1/Irf4 by Chromosomal Translocation in Multiple Myeloma", *Nature Genetics*, Vol. 17, No. 2, pp. 226-230.

Inazu, M., T. Yamada, N. Kubota and T. Yamanaka, 2013, "Functional Expression of Choline Transporter-Like Protein 1 (Ctl1) in Small Cell Lung Carcinoma Cells: A Target Molecule for Lung Cancer Therapy", *Pharmacological Research*, Vol. 76, pp. 119-131.

Ji, X.D., G. Li, Y.X. Feng, J.S. Zhao, J.J. Li, Z.J. Sun, S. Shi, Y.Z. Deng, J.F. Xu, Y.Q. Zhu, H.P. Koeffler, X.J. Tong and D. Xie, 2011, "Ephb3 Is Overexpressed in Non-Small-Cell Lung Cancer and Promotes Tumor Metastasis by Enhancing Cell Survival and Migration", *Cancer Research*, Vol. 71, No. 3, pp. 1156-1166.

Jiang, D.S., Z.Y. Bian, Y. Zhang, S.M. Zhang, Y. Liu, R. Zhang, Y. Chen, Q. Yang, X.D. Zhang, G.C. Fan and H. Li, 2013, "Role of Interferon Regulatory Factor 4 in the Regulation of Pathological Cardiac Hypertrophy", *Hypertension*, Vol. 61, No. 6, pp. 1193-1202.

Jonsson, G., C. Busch, S. Knappskog, J. Geisler, H. Miletic, M. Ringner, J.R. Lillehaug, A. Borg and P.E. Lonning, 2010, "Gene Expression Profiling-Based Identification of Molecular Subtypes in Stage Iv Melanomas with Different Clinical Outcome", *Clinical Cancer Research*, Vol. 16, No. 13, pp. 3356-3367.

Journe, F., H. Id Boufker, L. Van Kempen, M.D. Galibert, M. Wiedig, F. Sales, A. Theunis, D. Nonclercq, A. Frau, G. Laurent, A. Awada and G. Ghanem, 2011, "Tyrp1 Mrna Expression in Melanoma Metastases Correlates with Clinical Outcome", *British Journal of Cancer*, Vol. 105, No. 11, pp. 1726-1732.

Kamijo, T., J.D. Weber, G. Zambetti, F. Zindy, M.F. Roussel and C.J. Sherr, 1998, "Functional and Physical Interactions of the Arf Tumor Suppressor with P53 and Mdm2", *Proceedings of the National Academy of Sciences of the United States of America*, Vol. 95, No. 14, pp. 8292-8297.

Kim, D., G. Pertea, C. Trapnell, H. Pimentel, R. Kelley and S.L. Salzberg, 2013, "Tophat2: Accurate Alignment of Transcriptomes in the Presence of Insertions, Deletions and Gene Fusions", *Genome Biology*, Vol. 14, No. 4, pp. R36.

Langmead, B., C. Trapnell, M. Pop and S.L. Salzberg, 2009, "Ultrafast and Memory-Efficient Alignment of Short DNA Sequences to the Human Genome", *Genome Biology*, Vol. 10, No. 3, pp. R25.

Lazaris-Karatzas, A., K.S. Montine and N. Sonenberg, 1990, "Malignant Transformation by a Eukaryotic Initiation Factor Subunit That Binds to Mrna 5' Cap", *Nature*, Vol. 345, No. 6275, pp. 544-547.

Lehtonen, A., V. Veckman, T. Nikula, R. Lahesmaa, L. Kinnunen, S. Matikainen and I. Julkunen, 2005, "Differential Expression of Ifn Regulatory Factor 4 Gene in Human Monocyte-Derived Dendritic Cells and Macrophages", *Journal of Immunology*, Vol. 175, No. 10, pp. 6570-6579.

Levy, C., M. Khaled and D.E. Fisher, 2006, "Mitf: Master Regulator of Melanocyte Development and Melanoma Oncogene", *Trends in Molecular Medicine*, Vol. 12, No. 9, pp. 406-414.

Li, H., B. Handsaker, A. Wysoker, T. Fennell, J. Ruan, N. Homer, G. Marth, G. Abecasis, R. Durbin and S. Genome Project Data Processing, 2009, "The Sequence

Alignment/Map Format and Samtools", *Bioinformatics*, Vol. 25, No. 16, pp. 2078-2079.

Lin, C.Y., H.J. Chen, C.C. Huang, L.C. Lai, T.P. Lu, G.C. Tseng, T.T. Kuo, Q.Y. Kuok, J.L. Hsu, S.Y. Sung, M.C. Hung and Y.P. Sher, 2014, "Adam9 Promotes Lung Cancer Metastases to Brain by a Plasminogen Activator-Based Pathway", *Cancer Research*, Vol. 74, pp. 5229-5243.

Loman, N.J., R.V. Misra, T.J. Dallman, C. Constantinidou, S.E. Gharbia, J. Wain and M.J. Pallen, 2012, "Performance Comparison of Benchtop High-Throughput Sequencing Platforms", *Nature Biotechnology*, Vol. 30, No. 5, pp. 434-439.

Lopez-Girona, A., D. Heintel, L.H. Zhang, D. Mendy, S. Gaidarova, H. Brady, J.B. Bartlett, P.H. Schafer, M. Schreder, A. Bolomsky, B. Hilgarth, N. Zojer, H. Gisslinger, H. Ludwig, T. Daniel, U. Jager and R. Chopra, 2011, "Lenalidomide Downregulates the Cell Survival Factor, Interferon Regulatory Factor-4, Providing a Potential Mechanistic Link for Predicting Response", *British Journal of Haematology*, Vol. 154, No. 3, pp. 325-336.

Ma, S., S. Pathak, L. Trinh and R. Lu, 2008, "Interferon Regulatory Factors 4 and 8 Induce the Expression of Ikaros and Aiolos to Down-Regulate Pre-B-Cell Receptor and Promote Cell-Cycle Withdrawal in Pre-B-Cell Development", *Blood*, Vol. 111, No. 3, pp. 1396-1403.

Macheda, M.L., S. Rogers and J.D. Best, 2005, "Molecular and Cellular Regulation of Glucose Transporter (Glut) Proteins in Cancer", *Journal of Cellular Physiology*, Vol. 202, No. 3, pp. 654-662.

Martineau, Y., R. Azar, C. Bousquet and S. Pyronnet, 2013, "Anti-Oncogenic Potential of the Eif4e-Binding Proteins", *Oncogene*, Vol. 32, No. 6, pp. 671-677.

Masgrau, R., C. Hurel, F. Papastefanaki, N. Georgopoulou, D. Thomaidou and R. Matsas, 2009, "Bm88/Cend1 Regulates Stimuli-Induced Intracellular Calcium Mobilization", *Neuropharmacology*, Vol. 56, No. 3, pp. 598-609.

Metzker, M.L., 2010, "Sequencing Technologies - the Next Generation", *Nature Reviews Genetics*, Vol. 11, No. 1, pp. 31-46.

Mittrucker, H.W., T. Matsuyama, A. Grossman, T.M. Kundig, J. Potter, A. Shahinian, A. Wakeham, B. Patterson, P.S. Ohashi and T.W. Mak, 1997, "Requirement for the Transcription Factor Lsirf/Irf4 for Mature B and T Lymphocyte Function", *Science*, Vol. 275, No. 5299, pp. 540-543.

Morlan, J.D., K. Qu and D.V. Sinicropi, 2012, "Selective Depletion of Rrna Enables Whole Transcriptome Profiling of Archival Fixed Tissue", *PLoS One*, Vol. 7, No. 8, pp. e42882.

Morozova, O. and M.A. Marra, 2008, "Applications of Next-Generation Sequencing Technologies in Functional Genomics", *Genomics*, Vol. 92, No. 5, pp. 255-264.

Nagalakshmi, U., K. Waern and M. Snyder, 2010, "Rna-Seq: A Method for Comprehensive Transcriptome Analysis", *Current Protocols in Molecular Biology*, Vol. Chapter 4, pp. Unit 4 11 11-13.

Natkunam, Y., R.A. Warnke, K. Montgomery, B. Falini and M. van De Rijn, 2001, "Analysis of Mum1/Irf4 Protein Expression Using Tissue Microarrays and Immunohistochemistry", *Modern Pathology*, Vol. 14, No. 7, pp. 686-694.

Negishi, H., Y. Ohba, H. Yanai, A. Takaoka, K. Honma, K. Yui, T. Matsuyama, T. Taniguchi and K. Honda, 2005, "Negative Regulation of Toll-Like-Receptor Signaling by Irf-4", *Proceedings of the National Academy of Sciences of the United States of America*, Vol. 102, No. 44, pp. 15989-15994.

Ng, P.C. and E.F. Kirkness, 2010, "Whole Genome Sequencing", *Methods in Molecular Biology*, Vol. 628, pp. 215-226.

Nikolaou, V.A., A.J. Stratigos, K.T. Flaherty and H. Tsao, 2012, "Melanoma: New Insights and New Therapies", *Journal of Investigative Dermatology*, Vol. 132, No. 3 Pt 2, pp. 854-863.

Panka, D.J., M.B. Atkins and J.W. Mier, 2006, "Targeting the Mitogen-Activated Protein Kinase Pathway in the Treatment of Malignant Melanoma", *Clinical Cancer Research*, Vol. 12, No. 7 Pt 2, pp. 2371-2375.

Pathak, S., S. Ma, L. Trinh, J. Eudy, K.U. Wagner, S.S. Joshi and R. Lu, 2011, "Irf4 Is a Suppressor of C-Myc Induced B Cell Leukemia", *PLoS One*, Vol. 6, No. 7, pp. e22628.

Pena-Chilet, M., M. Blanquer-Maceiras, M. Ibarrola-Villava, C. Martinez-Cadenas, M. Martin-Gonzalez, C. Gomez-Fernandez, M. Mayor, J.A. Aviles, A. Lluch and G. Ribas, 2013, "Genetic Variants in Parp1 (Rs3219090) and Irf4 (Rs12203592) Genes Associated with Melanoma Susceptibility in a Spanish Population", *BMC Cancer*, Vol. 13, pp. 160.

Pennisi, E., 2012, "Genome Sequencing. Search for Pore-Fection", *Science*, Vol. 336, No. 6081, pp. 534-537.

Politis, A.D., J. Sivo, P.H. Driggers, K. Ozato and S.N. Vogel, 1992, "Modulation of Interferon Consensus Sequence Binding Protein Mrna in Murine Peritoneal Macrophages. Induction by Ifn-Gamma and Down-Regulation by Ifn-Alpha, Dexamethasone, and Protein Kinase Inhibitors", *Journal of Immunology*, Vol. 148, No. 3, pp. 801-807.

Pollock, P.M., U.L. Harper, K.S. Hansen, L.M. Yudt, M. Stark, C.M. Robbins, T.Y. Moses, G. Hostetter, U. Wagner, J. Kakareka, G. Salem, T. Pohida, P. Heenan, P. Duray, O. Kallioniemi, N.K. Hayward, J.M. Trent and P.S. Meltzer, 2003, "High Frequency of Braf Mutations in Nevi", *Nature Genetics*, Vol. 33, No. 1, pp. 19-20.

Praetorius, C., C. Grill, S.N. Stacey, A.M. Metcalf, D.U. Gorkin, K.C. Robinson, E. Van Otterloo, R.S. Kim, K. Bergsteinsdottir, M.H. Ogmundsdottir, E. Magnusdottir, P.J. Mishra, S.R. Davis, T. Guo, M.R. Zaidi, A.S. Helgason, M.I. Sigurdsson, P.S. Meltzer, G. Merlino, V. Petit, L. Larue, S.K. Loftus, D.R. Adams, U. Sobhiafshar, N.C. Emre, W.J. Pavan, R. Cornell, A.G. Smith, A.S. McCallion, D.E. Fisher, K. Stefansson, R.A. Sturm and E. Steingrimsson, 2013, "A Polymorphism in Irf4

Affects Human Pigmentation through a Tyrosinase-Dependent Mitf/Tfap2a Pathway", *Cell*, Vol. 155, No. 5, pp. 1022-1033.

Rhodes, D.R., J. Yu, K. Shanker, N. Deshpande, R. Varambally, D. Ghosh, T. Barrette, A. Pandey and A.M. Chinnaiyan, 2004, "Oncomine: A Cancer Microarray Database and Integrated Data-Mining Platform", *Neoplasia*, Vol. 6, No. 1, pp. 1-6.

Robinson, M.D., D.J. McCarthy and G.K. Smyth, 2010, "Edger: A Bioconductor Package for Differential Expression Analysis of Digital Gene Expression Data", *Bioinformatics*, Vol. 26, No. 1, pp. 139-140.

Rothberg, J.M., W. Hinz, T.M. Rearick, J. Schultz, W. Mileski, M. Davey, J.H. Leamon, K. Johnson, M.J. Milgrew, M. Edwards, J. Hoon, J.F. Simons, D. Marran, J.W. Myers, J.F. Davidson, A. Branting, J.R. Nobile, B.P. Puc, D. Light, T.A. Clark, M. Huber, J.T. Branciforte, I.B. Stoner, S.E. Cawley, M. Lyons, Y. Fu, N. Homer, M. Sedova, X. Miao, B. Reed, J. Sabina, E. Feierstein, M. Schorn, M. Alanjary, E. Dimalanta, D. Dressman, R. Kasinskas, T. Sokolsky, J.A. Fidanza, E. Namsaraev, K.J. McKernan, A. Williams, G.T. Roth and J. Bustillo, 2011, "An Integrated Semiconductor Device Enabling Non-Optical Genome Sequencing", *Nature*, Vol. 475, No. 7356, pp. 348-352.

Rui, L., R. Schmitz, M. Ceribelli and L.M. Staudt, 2011, "Malignant Pirates of the Immune System", *Nature Immunology*, Vol. 12, No. 10, pp. 933-940.

Saito, M., J. Gao, K. Basso, Y. Kitagawa, P.M. Smith, G. Bhagat, A. Pernis, L. Pasqualucci and R. Dalla-Favera, 2007, "A Signaling Pathway Mediating Downregulation of Bcl6 in Germinal Center B Cells Is Blocked by Bcl6 Gene Alterations in B Cell Lymphoma", *Cancer Cell*, Vol. 12, No. 3, pp. 280-292.

Saito, T., T. Yamagata, T. Takahashi, H. Honda and H. Hirai, 1999, "Icsat Overexpression Is Not Sufficient to Cause Adult T-Cell Leukemia or Multiple Myeloma", *Biochemical and Biophysical Research Communications*, Vol. 260, No. 2, pp. 329-331.

Sanger, F., S. Nicklen and A.R. Coulson, 1977, "DNA Sequencing with Chain-Terminating Inhibitors", *Proceedings of the National Academy of Sciences of the United States of America*, Vol. 74, No. 12, pp. 5463-5467.

Sciammas, R., A.L. Shaffer, J.H. Schatz, H. Zhao, L.M. Staudt and H. Singh, 2006, "Graded Expression of Interferon Regulatory Factor-4 Coordinates Isotype Switching with Plasma Cell Differentiation", *Immunity*, Vol. 25, No. 2, pp. 225-236.

Seyednasrollah, F., A. Laiho and L.L. Elo, 2013, "Comparison of Software Packages for Detecting Differential Expression in Rna-Seq Studies", *Briefings in Bioinformics*

Shaffer, A.L., N.C. Emre, L. Lamy, V.N. Ngo, G. Wright, W. Xiao, J. Powell, S. Dave, X. Yu, H. Zhao, Y. Zeng, B. Chen, J. Epstein and L.M. Staudt, 2008, "Irf4 Addiction in Multiple Myeloma", *Nature*, Vol. 454, No. 7201, pp. 226-231.

Shaffer, A.L., N.C. Emre, P.B. Romesser and L.M. Staudt, 2009, "Irf4: Immunity. Malignancy! Therapy?", *Clinical Cancer Research*, Vol. 15, No. 9, pp. 2954-2961.

Shah, R., P. Smith, C. Purdie, P. Quinlan, L. Baker, P. Aman, A.M. Thompson and T. Crook, 2009, "The Prolyl 3-Hydroxylases P3h2 and P3h3 Are Novel Targets for Epigenetic Silencing in Breast Cancer", *British Journal of Cancer*, Vol. 100, No. 10, pp. 1687-1696.

Sharma, A., N.R. Trivedi, M.A. Zimmerman, D.A. Tuveson, C.D. Smith and G.P. Robertson, 2005, "Mutant V599eb-Raf Regulates Growth and Vascular Development of Malignant Melanoma Tumors", *Cancer Research*, Vol. 65, No. 6, pp. 2412-2421.

Siegel, R., J. Ma, Z. Zou and A. Jemal, 2014, "Cancer Statistics, 2014", *A Cancer Journal for Clinicians*, Vol. 64, No. 1, pp. 9-29.

Sigurgeirsson, B., O. Emanuelsson and J. Lundeberg, 2014, "Sequencing Degraded Rna Addressed by 3' Tag Counting", *PLoS One*, Vol. 9, No. 3, pp. e91851.

Smith, L.M., J.Z. Sanders, R.J. Kaiser, P. Hughes, C. Dodd, C.R. Connell, C. Heiner, S.B. Kent and L.E. Hood, 1986, "Fluorescence Detection in Automated DNA Sequence Analysis", *Nature*, Vol. 321, No. 6071, pp. 674-679.

Smollich, M., M. Gotte, G.W. Yip, E.S. Yong, C. Kersting, J. Fischgrabe, I. Radke, L. Kiesel and P. Wulfing, 2007, "On the Role of Endothelin-Converting Enzyme-1 (Ece-1) and Neprilysin in Human Breast Cancer", *Breast Cancer Research and Treatment*, Vol. 106, No. 3, pp. 361-369.

Soltani, M.H., R. Pichardo, Z. Song, N. Sangha, F. Camacho, K. Satyamoorthy, O.P. Sangueza and V. Setaluri, 2005, "Microtubule-Associated Protein 2, a Marker of Neuronal Differentiation, Induces Mitotic Defects, Inhibits Growth of Melanoma Cells, and Predicts Metastatic Potential of Cutaneous Melanoma", *American Journal of Pathology*, Vol. 166, No. 6, pp. 1841-1850.

Song, Z., C.D. He, C. Sun, Y. Xu, X. Jin, Y. Zhang, T. Xiao, Y. Wang, P. Lu, Y. Jiang, H. Wei and H.D. Chen, 2010, "Increased Expression of Map2 Inhibits Melanoma Cell Proliferation, Invasion and Tumor Growth in Vitro and in Vivo", *Experimental Dermatology*, Vol. 19, No. 11, pp. 958-964.

Stahl, J.M., A. Sharma, M. Cheung, M. Zimmerman, J.Q. Cheng, M.W. Bosenberg, M. Kester, L. Sandirasegarane and G.P. Robertson, 2004, "Deregulated Akt3 Activity Promotes Development of Malignant Melanoma", *Cancer Research*, Vol. 64, No. 19, pp. 7002-7010.

Subramanian, A., P. Tamayo, V.K. Mootha, S. Mukherjee, B.L. Ebert, M.A. Gillette, A. Paulovich, S.L. Pomeroy, T.R. Golub, E.S. Lander and J.P. Mesirov, 2005, "Gene Set Enrichment Analysis: A Knowledge-Based Approach for Interpreting Genome-Wide Expression Profiles", *Proceedings of the National Academy of Sciences of the United States of America*, Vol. 102, No. 43, pp. 15545-15550.

Sulem, P., D.F. Gudbjartsson, S.N. Stacey, A. Helgason, T. Rafnar, K.P. Magnusson, A. Manolescu, A. Karason, A. Palsson, G. Thorleifsson, M. Jakobsdottir, S. Steinberg, S. Palsson, F. Jonasson, B. Sigurgeirsson, K. Thorisdottir, R. Ragnarsson, K.R.

Benediktsdottir, K.K. Aben, L.A. Kiemeney, J.H. Olafsson, J. Gulcher, A. Kong, U. Thorsteinsdottir and K. Stefansson, 2007, "Genetic Determinants of Hair, Eye and Skin Pigmentation in Europeans", *Nature Genetics*, Vol. 39, No. 12, pp. 1443-1452.

Sundram, U., J.D. Harvell, R.V. Rouse and Y. Natkunam, 2003, "Expression of the B-Cell Proliferation Marker Mum1 by Melanocytic Lesions and Comparison with S100, Gp100 (Hmb45), and Melana", *Modern Pathology*, Vol. 16, No. 8, pp. 802-810.

Suzuki, S., K. Honma, T. Matsuyama, K. Suzuki, K. Toriyama, I. Akitoyo, K. Yamamoto, T. Suematsu, M. Nakamura, K. Yui and A. Kumatori, 2004, "Critical Roles of Interferon Regulatory Factor 4 in Cd11bhighcd8alpha- Dendritic Cell Development", *Proceedings of the National Academy of Sciences of the United States of America*, Vol. 101, No. 24, pp. 8981-8986.

Talmadge, J.E. and I.J. Fidler, 2010, "Aacr Centennial Series: The Biology of Cancer Metastasis: Historical Perspective", *Cancer Research*, Vol. 70, No. 14, pp. 5649-5669.

Tariq, M.A., H.J. Kim, O. Jejelowo and N. Pourmand, 2011, "Whole-Transcriptome Rnaseq Analysis from Minute Amount of Total Rna", *Nucleic Acids Research*, Vol. 39, No. 18, pp. 120.

Teng, Y., Y. Takahashi, M. Yamada, T. Kurosu, T. Koyama, O. Miura and T. Miki, 2007, "Irf4 Negatively Regulates Proliferation of Germinal Center B Cell-Derived Burkitt's Lymphoma Cell Lines and Induces Differentiation toward Plasma Cells", *European Journal of Cell Biology*, Vol. 86, No. 10, pp. 581-589.

Thorvaldsdottir, H., J.T. Robinson and J.P. Mesirov, 2013, "Integrative Genomics Viewer (Igv): High-Performance Genomics Data Visualization and Exploration", *Briefings in Bioinformics*, Vol. 14, No. 2, pp. 178-192.

Tondera, D., A. Santel, R. Schwarzer, S. Dames, K. Giese, A. Klippel and J. Kaufmann, 2004, "Knockdown of Mtp18, a Novel Phosphatidylinositol 3-Kinase-Dependent

Protein, Affects Mitochondrial Morphology and Induces Apoptosis", *The Journal of Biological Chemistry*, Vol. 279, No. 30, pp. 31544-31555.

Trapnell, C., L. Pachter and S.L. Salzberg, 2009, "Tophat: Discovering Splice Junctions with Rna-Seq", *Bioinformatics*, Vol. 25, No. 9, pp. 1105-1111.

Trapnell, C., A. Roberts, L. Goff, G. Pertea, D. Kim, D.R. Kelley, H. Pimentel, S.L. Salzberg, J.L. Rinn and L. Pachter, 2012, "Differential Gene and Transcript Expression Analysis of Rna-Seq Experiments with Tophat and Cufflinks", *Nature Protocols*, Vol. 7, No. 3, pp. 562-578.

Trapnell, C., B.A. Williams, G. Pertea, A. Mortazavi, G. Kwan, M.J. van Baren, S.L. Salzberg, B.J. Wold and L. Pachter, 2010, "Transcript Assembly and Quantification by Rna-Seq Reveals Unannotated Transcripts and Isoform Switching During Cell Differentiation", *Nature Biotechnology*, Vol. 28, No. 5, pp. 511-515.

Tsao, H., V. Goel, H. Wu, G. Yang and F.G. Haluska, 2004, "Genetic Interaction between Nras and Braf Mutations and Pten/Mmac1 Inactivation in Melanoma", *Journal of Investigative Dermatology*, Vol. 122, No. 2, pp. 337-341.

Tsioras, K., F. Papastefanaki, P.K. Politis, R. Matsas and M. Gaitanou, 2013, "Functional Interactions between Bm88/Cend1, Ran-Binding Protein M and Dyrk1b Kinase Affect Cyclin D1 Levels and Cell Cycle Progression/Exit in Mouse Neuroblastoma Cells", *PLoS One*, Vol. 8, No. 11, pp. e82172.

Udayakumar, D., G. Zhang, Z. Ji, C.N. Njauw, P. Mroz and H. Tsao, 2011, "Epha2 Is a Critical Oncogene in Melanoma", *Oncogene*, Vol. 30, No. 50, pp. 4921-4929.

van Oijen, M.G. and P.J. Slootweg, 2000, "Gain-of-Function Mutations in the Tumor Suppressor Gene P53", *Clinical Cancer Research*, Vol. 6, No. 6, pp. 2138-2145.

Vultur, A. and M. Herlyn, 2013, "Snapshot: Melanoma", *Cancer Cell*, Vol. 23, No. 5, pp. 706-706 e701.

Wang, B., 2011, "Cancer Cells Exploit the Eph-Ephrin System to Promote Invasion and Metastasis: Tales of Unwitting Partners", *Science Signaling*, Vol. 4, No. 175, pp. pe28.

Wang, J., X. Xu, Z. Liu, X. Wei, R. Zhuang, D. Lu, L. Zhou, H. Xie and S. Zheng, 2013, "Leprel1 Expression in Human Hepatocellular Carcinoma and Its Suppressor Role on Cell Proliferation", *Gastroenterology Research and Practice*, Vol. 2013, pp. 109759.

Wang, Z., M. Gerstein and M. Snyder, 2009, "Rna-Seq: A Revolutionary Tool for Transcriptomics", *Nature Reviews Genetics*, Vol. 10, No. 1, pp. 57-63.

Whyteside, A.R., E.E. Hinsley, L.A. Lambert, P.J. McDermott and A.J. Turner, 2010, "Ece-1 Influences Prostate Cancer Cell Invasion Via Et-1-Mediated Fak Phosphorylation and Et-1-Independent Mechanisms", *Canadian Journal of Physiology and Pharmacology*, Vol. 88, No. 8, pp. 850-854.

Willmore-Payne, C., J.A. Holden, S. Tripp and L.J. Layfield, 2005, "Human Malignant Melanoma: Detection of Braf- and C-Kit-Activating Mutations by High-Resolution Amplicon Melting Analysis", *Human Pathology*, Vol. 36, No. 5, pp. 486-493.

Witte, I., S. Altenhofer, P. Wilgenbus, J. Amort, A.M. Clement, A. Pautz, H. Li, U. Forstermann and S. Horke, 2011, "Beyond Reduction of Atherosclerosis: Pon2 Provides Apoptosis Resistance and Stabilizes Tumor Cells", *Cell Death Disease*, Vol. 2, pp. e112.

Wu, H., V. Goel and F.G. Haluska, 2003, "Pten Signaling Pathways in Melanoma", *Oncogene*, Vol. 22, No. 20, pp. 3113-3122.

Xie, X., E.P. White and J.M. Mehnert, 2013, "Coordinate Autophagy and Mtor Pathway Inhibition Enhances Cell Death in Melanoma", *PLoS One*, Vol. 8, No. 1, pp. e55096.

Yamagata, T., J. Nishida, S. Tanaka, R. Sakai, K. Mitani, M. Yoshida, T. Taniguchi, Y. Yazaki and H. Hirai, 1996, "A Novel Interferon Regulatory Factor Family Transcription Factor, Icsat/Pip/Lsirf, That Negatively Regulates the Activity of Interferon-Regulated Genes", *Molecular and Cellular Biology*, Vol. 16, No. 4, pp. 1283-1294.

Yamaguchi, S., K. Hong, R. Liu, A. Inoue, L. Shen, K. Zhang and Y. Zhang, 2013, "Dynamics of 5-Methylcytosine and 5-Hydroxymethylcytosine During Germ Cell Reprogramming", *Cell Research*, Vol. 23, No. 3, pp. 329-339.

Yang, Y., A.L. Shaffer, N.C. Emre, M. Ceribelli, M. Zhang, G. Wright, W. Xiao, J. Powell, J. Platig, H. Kohlhammer, R.M. Young, H. Zhao, Y. Yang, W. Xu, J.J. Buggy, S. Balasubramanian, L.A. Mathews, P. Shinn, R. Guha, M. Ferrer, C. Thomas, T.A. Waldmann and L.M. Staudt, 2012, "Exploiting Synthetic Lethality for the Therapy of Abc Diffuse Large B Cell Lymphoma", *Cancer Cell*, Vol. 21, No. 6, pp. 723-737.

Zhao, S., W.P. Fung-Leung, A. Bittner, K. Ngo and X. Liu, 2014, "Comparison of Rna-Seq and Microarray in Transcriptome Profiling of Activated T Cells", *PLoS One*, Vol. 9, No. 1, pp. e78644.

Zhao, Y. and R. Simon, 2008, "Brb-Arraytools Data Archive for Human Cancer Gene Expression: A Unique and Efficient Data Sharing Resource", *Cancer Information*, Vol. 6, No. pp. 9-15.